A N-ary Sorting System Using an

Integrated Droplet-Digital Microfluidics (ID2M)

Fatemeh Ahmadi

A Thesis

In the Department of

Electrical and Computer Engineering

Presented in Partial Fulfillment of the Requirements

For the Degree of

Master's in Applied Science (Electrical and Computer Engineering) at

Concordia University

Montreal, Québec, Canada

September 2018

CONCORDIA UNIVERSITY
SCHOOL OF GRADUATE STUDIES

This is to certify that the thesis prepared

By: Fatemeh Ahmadi

Entitled: A N-ary Sorting System Using An Integrated Droplet-Digital Microfluidics
            (ID2M)

and submitted in partial fulfillment of the requirements for the degree of

Master of Applied Science (Electrical and Computer Engineering)

complies with the regulations of this University and meets the accepted standards with respect to
originality and quality.

Signed by the final examining committee:

_____ Chair
            Dr. D. Qiu

_____ External Examiner
            Dr. A. De Visscher (CME)

_____ Internal Examiner
            Dr. H. Benali

_____ Supervisor
            Dr. S. Shih

Approved by: _____
            Dr. W.E. Lynch, Chair
            Department of Electrical and Computer Engineering

_____ 20___   _____
                                            Dr. Amir Asif, Dean,
                                    Faculty of Engineering and Computer Science

ABSTRACT

A N-ary sorting system using an Integrated Droplet-Digital Microfluidics (ID2M)

Fatemeh Ahmadi

Droplet microfluidics has the ability to compartmentalize reactions in sub nano-liter (or pico) volumes that can potentially enable millions of distinct biological assays to be performed on individual cells. Typically, there are two main droplet operations that can be performed with these platforms: cell encapsulation and sorting. Droplet sorting has been a means to select a subset of reactions or activities that can be used for further manipulation and it has been used for single cell analysis and directed evolution. But one of the challenges with these techniques is that these are typically binary sorters – i.e. only relying on two sorting channels. This can limit the range of detecting rare events and to sort based on multiple conditions (i.e. more than two conditions). To alleviate this challenge, we have integrated droplet microfluidics with digital microfluidics to enable n-ary sorting techniques, which we call 'Integrated Droplet-Digital Microfluidics' (ID2M). Furthermore, our 'ID2M' microfluidic technique also allow on-demand droplet creation and droplet mixing which are two other operations that are difficult to perform in current droplet microfluidic platforms. ID2M is integrated to an automation system for on-demand manipulation of droplets and a spectrometer to detect droplet of interest. The ID2M platform has been validated as a robust on-demand screening system by sorting fluorescein droplets of different concentration with an efficiency of $\sim 96 \%$. The device is further demonstrated for sorting tolerant wild-type and yeast mutants to ionic liquid. We propose that this system has the potential to be used for screening different types of cells and for performing directed evolution on chip.

"This thesis is dedicated to my beloved parents & family,

Nader, Jamileh, Zohreh, and Zahra,

For their love, endless support, encouragement & sacrifices!"

Acknowledgements

First and foremost, praises and thanks to the God, the Almighty, for His showers of blessings throughout my work to complete the research successfully.

Next, I would like to express my deep and sincere gratitude to my research supervisor, Dr. Steve Shih for the trust he deposited in my work and for this unique opportunity he gave me to follow my passion, do research, and develop myself as a researcher in the best possible way. I am so grateful for the freedom you have given me to find my own path and the guidance and support you offered when needed. Your dynamism, vision, sincerity and motivation have always inspired me.

To all my friends and research colleagues in our lab, I express my appreciation for their help and support throughout my journey toward this degree. Special thanks go to Kenza Samlali for all her kind assistance. Her mix of straightforward criticism combined with heart-warming support have always given me great confidence and a better insight into my research experience. She was a true friend ever since we began to collaborate on our projects and I truly hope that we will be given the opportunity to work even closer together in the future. A special acknowledgement goes to my office mates Hugo Sinha and James Perry. Thank you for putting smile on my face every day we worked together and for all your feedbacks and encouragements. I always enjoyed our brain storming and discussions. Thank you to Philippe Vo and Mathieu Husser for their great work as exemplary undergrads. Working with you was a great pleasure for me and I learned a lot.

I thank the ECE department for their FRS funding and for creating such an invaluable space for me to gain experience and achieve my goal. I would also like to thank the entire Martin Lab who have been so helpful and cooperative in giving their support at all times. I also thank the

Martin Lab and the Centre for Applied Synthetic Biology for their resources and making the working environment so pleasant.

I would also like to thank my committee members, Dr. Alex De Visscher and Dr. Habib Benali, as well as my chair, Dr. Dongyu Qiu, for reading, reviewing and accommodating my thesis.

My acknowledgement would be incomplete without thanking my adorable parents. Words fail to express how grateful I am to you, whose love and support has been the biggest source of my strength. Thank you for believing in me and for inspiring me to follow my dreams. This would not have been possible without your unwavering and unselfish love and support given to me at all times. Thank you for all your prayer, caring, and sacrifices you have done for educating and preparing me for my future. Also, I express my thanks to my lovely sisters, who never let things get boring, have made a tremendous contribution in helping me reach this stage in my life. Finally, thank you Mohammad, my dearest friend, for making me stand my ground and ensuring that the fire keeps burning and being there at all those tough times when I required motivation.

Overview of Chapters

This thesis describes the project I conducted and completed for my Master's in Applied Science in Dr. Steve Shih's research group at Concordia University. In this work, I aimed to develop an integrated droplet-digital microfluidic platform tailored to perform automated screening of library of biofuel organisms such as yeasts through on-demand mixing and sorting of droplets. This thesis provides a literature review on the history of miniaturization and microfluidic paradigms, an in-depth review of droplet, digital, and hybrid microfluidic platforms and their advantages and disadvantages, and finally a commentary on the state of biofuel production and its challenges. While assessing the technological challenges in screening libraries of microorganism in terms of lack of individual addressability in the existing platforms, I will then get into the core of my research, reporting the methodology utilized for the development of an integrated microfluidic platform, and validating the platform with experimental results.

Chapter 1 will introduce microfluidics in the bigger realm of miniaturization, discuss its progress over time and its future market, and describe the three dominant paradigms. Then we elaborate on the two paradigms that my project is focused on and discuss their physics, applications, and challenges.

Chapter 2 will introduce hybrid microfluidics and describe its superiority over the other paradigms owing to its combinatorial characteristics. Then, the novelty of the hybrid device fabricated in this project as well as the integrated automation system will be highlighted.

Chapter 3 reviews the biological stakes that we will be addressing with our platform, presenting microfluidics screening techniques for analyzing biofuel microorganism with a special focus on the tolerance of yeast Saccharomyces cerevisiae cell in Imidazolium-Based Ionic Liquids in the

context of biofuel production. This commentary will lead to the presentation of my thesis objectives.

Chapter 4 *describes my methodology for integrating the processes needed for n-ary sorting of biofuel organisms on the ID2M platform. Device fabrication, assembly, operation with the automation system, syringe pump and the flame spectroscopy will be described before reviewing the method for generating an on-chip calibration curve for fluorescein. Finally, the macro-scale experiments that were done for generating ionic liquid tolerant yeast cells and the work flow for on-chip sorting of the generated mutants will be presented.*

Chapter 5 *describes my results in validating the n-ary sorting system. Device characterization and optimization, proof-of-concept work by constructing a fluorescein calibration curve on chip, and applying our platform for studying the ionic liquid tolerance of two yeast mutants will be discussed.*

Chapter 6 *provides concluding remarks regarding my work and its potential in screening library of microorganism. We will also evaluate future perspectives for ID2M platform and its potential application in directed evolution.*

Overview of Author Contributions

This work described in my thesis was made possible with the help of colleagues from the Shih Lab. Here, I outline the contributions that each author made to the work.

The project was thought out and designed by Dr. Steve Shih and myself and the research article relevant to this work was written and edited by Dr. Steve Shih and myself.

All experiments were conducted by myself, and I collected and analyzed all the data relevant to my thesis. The resulting figures were revised and approved by Dr. Steve Shih.

Yeast mutagenesis and mutant culture work (cell passaging, maintenance) was performed with the help of Kenza Samlali.

The code for the automation system was written, optimized and troubleshooted by Philippe Vo. The hardware for the automation system was designed and optimized by Amin Firouzeh and Philippe Vo.

Table of Contents

List of Figures

List of Tables

List of Equations

List of Abbreviations

1. Alternating Current (**AC**)
2. Digital microfluidics (**DMF**)
3. Optical Density (**OD**)
4. MicroElectroMechanical Systems (**MEMS**)
5. labs-on-a-chip (**LOC**)
6. Reynolds Number (**Re**)
7. Polydimethylsiloxane (**PDMS**)
8. Dielectrophoresis (**DEP**)
9. Computer-Aided Design (**CAD**)
10. Deoxyribonucleic Acid (**DNA**)
11. Indium Tin Oxide (**ITO**)
12. Electrowetting-on-Dielectric (**EWOD**)
13. Positron emission tomography (**PET**)
14. Integrated Digital-Droplet Microfluidics (**ID2M**)
15. Graphical user interface (**GUI**)
16. Printed Circuit Board (**PCB**)
1. High-Throughput Screening (**HTS**)
2. Ionic liquids (**IL**)
3. Imidazolium ionic liquids (**IILs**)
4. Ethyl methanesulfonate (**EMS**)
5. Wild type (**WT**)
6. Deionized (**DI**)
7. Bovine serum albumin (**BSA**)
8. Isopropanol (**IPA**)
9. Direct Current (**DC**)
10. SubMiniature version A (**SMA**)
11. Phosphate Buffer Saline (**PBS**)
12. Sodium phosphate buffer (**SPB**)
13. Sodium thiosulfate (**STS**)
14. Bovine serum albumin (**BSA**)
15. (3-Aminopropyl)triethoxysilane (**APTES**)

List of Foundations and Funding Sources

List of Co-Authored Publications

Image-based Feedback and Analysis System for Digital Microfluidics

Philippe Q.N. Vo [1,2], Mathieu C. Husser, [2,3] Fatemeh Ahmadi [1,3], Hugo Sinha[1,3], Steve C.C. Shih[1-3]

[1]Department of Electrical and Computer Engineering, Concordia University, Montréal, Québec, Canada
[2]Centre for Applied Synthetic Biology, Concordia University, Montréal, Québec, Canada
[3] Department of Biology, Concordia University, Montréal, Québec, Canada

Abstract

Digital microfluidics (DMF) is a technology that provides a means of manipulating nL-µL volumes of liquids on an array of electrodes. By applying an electric potential to an electrode, these discrete droplets can be controlled in parallel which can be transported, mixed, reacted, and analyzed. Typically, an automation system is interfaced with a DMF device uses a standard set of basic instructions written by the user to execute droplet operations. Here, we present the first feedback method for DMF that relies on imaging techniques that will allow online detection of droplets without the need to reactivate all destination electrodes while minimizing the biofouling within a given experiment. Our system consists of integrating open-source electronics with a CMOS camera with a zoom lens for acquisition of the droplet movements on the device. We also created an algorithm that uses a Hough transform to detect a variety of droplet sizes and to detect singular droplet dispensing and movement failures on the device. As a first test, we applied this feedback system to testing the droplet movement of a variety of liquids used in cell-based assays and implemented a colorimetric cellulase assay to determine enzymes suitable for breaking down biomass for biofuel production. We believe using our approach of integrating imaging and feedback with DMF can provide a platform for automating biological assays with high-fidelity.

An Automated Induction Microfluidics System (AIMS) for Synthetic Biology

Mathieu C. Husser[1, 2], Philippe Q. N. Vo[3], Hugo Sinha[2, 3], Fatemeh Ahmadi[2,3], Steve C.C. Shih[1-3]

[1]Department of Biology, Concordia University, Montréal, Québec, Canada
[2]Centre for Applied Synthetic Biology, Concordia University, Montréal, Québec, Canada
[3]Department of Electrical and Computer Engineering, Concordia University, Montréal, Québec, Canada

Abstract

The expression of a recombinant gene in a host organism through induction can be an extensively manual procedure. Several methods have been developed to simplify the protocol, but none has fully replaced the traditional IPTG-based induction. To simplify this process, we describe the development of an auto-induction platform based on digital microfluidics. This system consists of a 600 nm LED and a light sensor to enable the real-time monitoring of samples optical density (OD) coordinated with the semi-continuous mixing of a bacterial culture. A hand-held device was designed as a micro-bioreactor to culture cells and to measure the OD of the bacterial culture. In addition, it serves as a platform for the analysis of regulated protein expression in *E.coli* without the requirement of standardized well-plates or pipetting-based platforms. Here, we report for the first time, a system that offers great convenience without the user to physically monitor the culture or to manually add inducer at specific times. We characterized our system by looking at several parameters (electrode designs, gap height, and growth rates) required for an auto-inducible system. As a first step, we carried out an automated induction assay on a RFP reporter gene to identify conditions suitable for our system. Next, we used our system to identify active thermophilic β-glucosidase enzymes which may be suitable candidates for biomass hydrolysis. Overall, we believe that this platform may be useful for synthetic biology applications that require regulating and analyzing expression of heterologous genes.

Chapter 1.   Lab on a chip: A Miniaturized World

In this section, we will introduce microfluidics in the bigger realm of miniaturization, discuss its progress over time and its future market, and describe the three dominant paradigms. Then we elaborate on the two paradigms that my project is focused on and discuss their physics, applications, and challenges.

1.1   Miniaturization technologies: Past, Present, and Future

The origin of microfluidics devices goes back to hundreds of years ago where scientists were interested to study body fluids and behavior of liquids confined in small diameters. They had not micro devices, but they have been able to investigate some diseases. Later, in the 17th century, the famous Hagen–Poiseuille law for calculating the pressure drop in an incompressible and Newtonian fluid was established by studying a laminar flow through a long cylindrical pipe of constant cross section.

Advancement towards microfluidics technology as we know it today, however, is intrinsically linked to the development of microelectromechanical systems (MEMS) and synthesis of new materials in the end of 1960s; when the primitive micro devices in capillary format were developed for micro-analytical studies like gas chromatography (GPC) at Stanford University and later for ink jet printer nozzles at IBM. [1, 2]

Another research field that has been a motivational force for the development of microfluidics system is the molecular biology and the genomics revolution in the 1980s. Frequent transfer and/or dispensing of a small volume of liquid bio-samples (micro- or nanoliter level) between containers of varying sizes and onto substrates of varying types is the basis of most

biotechnological lab tests. This liquid handling, conventionally done by manual micro-pipetting[2-4], is needed for experiments like gene sequencing, protein crystallization, antibody testing, and drug screening. A need for analytical methods with much greater throughput and higher sensitivity and resolution, increased the demand for miniaturization and automation

Although many integrated robotic workstations have been developed to automate liquid handling,[4] the cost of the workstation, and the consumption of consumables (reagents, tips, plates, etc.) made microfluidics an interesting alternative technology to be used. Consequently, microfluidics has rapidly grown in popularity over the last few years, as indicated by the skyrocketing numbers of publications featuring microfluidic applications. Although in the early stage around 2000, most of the publications were focused on ''synthetic chemistry'', they later shifted toward cell-based analysis and more generally ''biochemical experimentation'' due to the microscale nature of these applications. Several labs-on-a-chip have been commercialized for some key applications such as glucose monitoring, breast cancer detection, HIV screening or heart attack diagnostics, and as laboratory hardware for procedures like single-cell analysis. According to the latest report published by Credence Research, Inc. Lab-on-a-Chip Market was valued at USD 4.16 Bn in 2015, and is expected to reach USD 9.06 Bn by 2025, expanding at a CAGR* of 8.9% from 2017 to 2025. [5, 6]

Microfluidic system, also known as "labs-on-a-chip" (LOC) technology, is a devices capable of scaling a single or multiple laboratory functions down to a tiny hand-held chip. Microfluidics devices are capable of manipulating small (10^{-9} to 10^{-18} liters) volumes of fluids using channels with dimensions ranging from hundreds of nanometers to hundreds of micrometers or arrays of electrodes.[2, 7] Reduction of sample/reagent consumption, shorter experiments time,

---

* The compound annual growth rate (CAGR) is a useful measure of growth over multiple time periods.

improvement of the precision of experiments, smaller device footprint, lower limits of detection, superior analytical performance, integration capacity, portability, and low costs are some of the salient advantages of microfluidics technology over conventional platforms.[2, 8, 9]

There are three paradigms of lab-on-a-chip technologies (Figure 1-1) that are frequently used by researchers: 1) Continuous Flow microfluidics that enables manipulation of liquid flow through fabricated microchannels without breaking continuity.[10, 11] 2) Droplet-based microfluidics that manipulates only discrete volumes of fluids in a second continuous phase (gas or liquid) and each droplet serves as an individual microvessels.[12, 13] 3) Digital microfluidics in which discrete droplets are manipulated electrostatically on an open array of electrodes.[14-16]
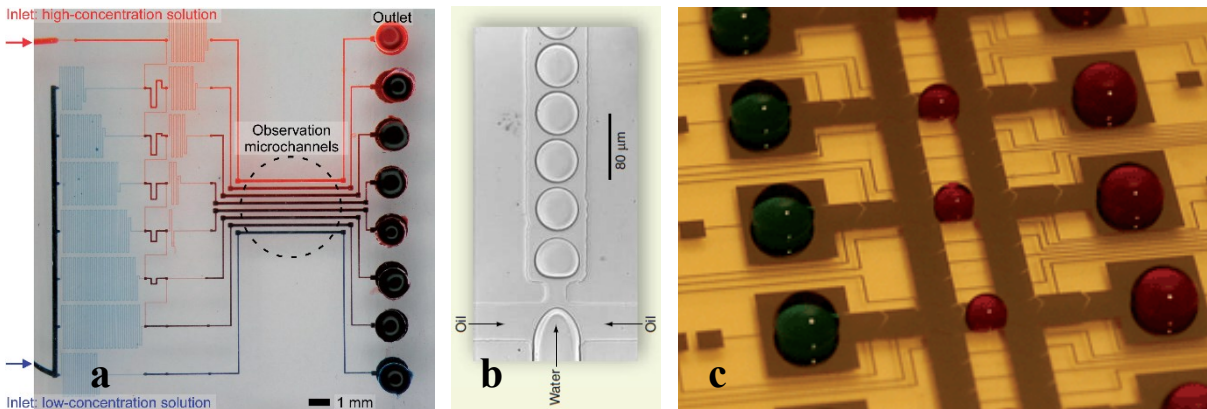
Figure 1-1– Microfluidic Paradigms.

(a) Microchannels. Adapted from K. Hattori et al, 2009. [17]
(b) Droplets-in-channel. Adapted from M. Joanicot et al, 2005. [18]
(c) Digital Microfluidics. Adapted from D. Bogojevic et al, 2012. [19]

1.2 Continuous Flow Microfluidics

Continuous flow microfluidics are based on the manipulation of continuous liquid flow through micro-fabricated channels. Samples and reagents are injected into the chip inlet either batch-wise or in continuous mode and the fluid flow is established by pressure gradients from

external sources such as micro-pumps (e.g., peristaltic or syringe pumps) or internal mechanisms such as electric, magnetic or capillary forces.[20, 21]

Channel microfluidics gained more popularity after 1998, when professor George Whitesides, one of the leaders in the field of lab-on-a-chip, presented the rapid prototyping of microfluidic systems in polydimethylsiloxane (PDMS) and fabrication procedure became much easier for researchers. [22] Since then, this platform has been widely used for many well-defined biochemical applications such as chemical separations,[23] single cell/molecule analysis,[24] and simple reactions with high surface area/volume ratio.[25] Integration of microchannel microfluidics with different types of actuators, micro-valves, micro-pumps, and flow sensors has made these devices popular among high-throughput systems.[10, 26-28]

A significant advantage of microchannels is the effective heat and mass transfer due to the higher surface area/volume ratio that has made these systems a potential platform for applications involving exothermic and endothermic reactions. Moreover, the ability to fabricate multilayer microchannels has led to the integration of microvalves relying on flexible membranes and pneumatic control layers that consequently increases the throughput of the system.[10, 26-28] This compartmentalization enables multiplexing, by which $\sim 10^6$ independent compartments are formed; each containing volumes in the range of 10-100 picoliters.[26] However, there is a trade-off between the throughput and simplicity of the system, because each compartment requires at least one valve. As the number of microvalves increases, fabrication procedures become more complex and precise alignment techniques are required to make a functional device. Besides, the more number of chambers and channels in device corresponds to more number of inlets and outlets as well as external pressure sources such as syringe pumps for fluid control that increases the complexity of the fabrication, manual intervention, expertise, and costs.

In microchannels, as dimensions shrink, the surface to volume ratio (S/V) increases and macro-scale forces such as inertia that keep liquid in motion become insignificant. However, viscous forces that are responsible for resistance of the body of liquid to deformations become extremely important in micro scale due to decrease in fluid mass. Dominance of each of these forces would change the regime of the flow. The dimensionless Reynolds number that relates the ratio of inertial to viscous forces is used to determine the type of flow expected in the system:

Equation 1-1: Reynolds Number

$$Re = \frac{Net\ Inertial\ Forces}{Net\ Viscous\ Forces} = \frac{\rho v L}{v}$$

Where ρ stands for fluid density (kg/m^3), v for the mean velocity (m/s), L for the characteristic length of the system, and v for the kinematic viscosity (m^2/s). Table 1.1 shows the nature of flow for different Reynolds number.[29]

Table 1.1. Fluid Flow on the basis of Reynolds Number

Range of Reynolds Number (Re)	Nature of fluid flow
Re < 2303	Laminar Flow
2300 < Re < 4000	Transient Flow
Re > 4000	Turbulent Flow

One of the consequences of laminar flow in microchannels is that mixing requires quite a different approach, since there is no whirls or eddies of a turbulent flow. Therefore, liquids blend only by diffusion, which is very slow and needs optimization. Since mixing is an essential step in most lab-on-a-chip platforms, and reagents preparation is required for a variety of biological and chemical assays, alternative strategies have been developed to satisfy the recent demand for rapid and homogeneous mixing.[30, 31] Generally, there are two types of mixing that can be induced in

channels: passive and active. Passive mixing is built up through specific geometry of the

microchannels and it enhances mixing by increasing the contact area and contact time between

multiple samples. In other words, passive mixing only relies on diffusion or chaotic advection. It

requires no moving parts or energy input other than the pressure that is used for fluid flows.

Lamination, intersecting channels, zigzag channels, 3D serpentine structure, embedded barriers,

slanted wells, twisted channels, and grooved staggered herringbone are some of the major

configurations that have been developed for passive microfluidic mixing schemes (Figure 1-2). [32-38]
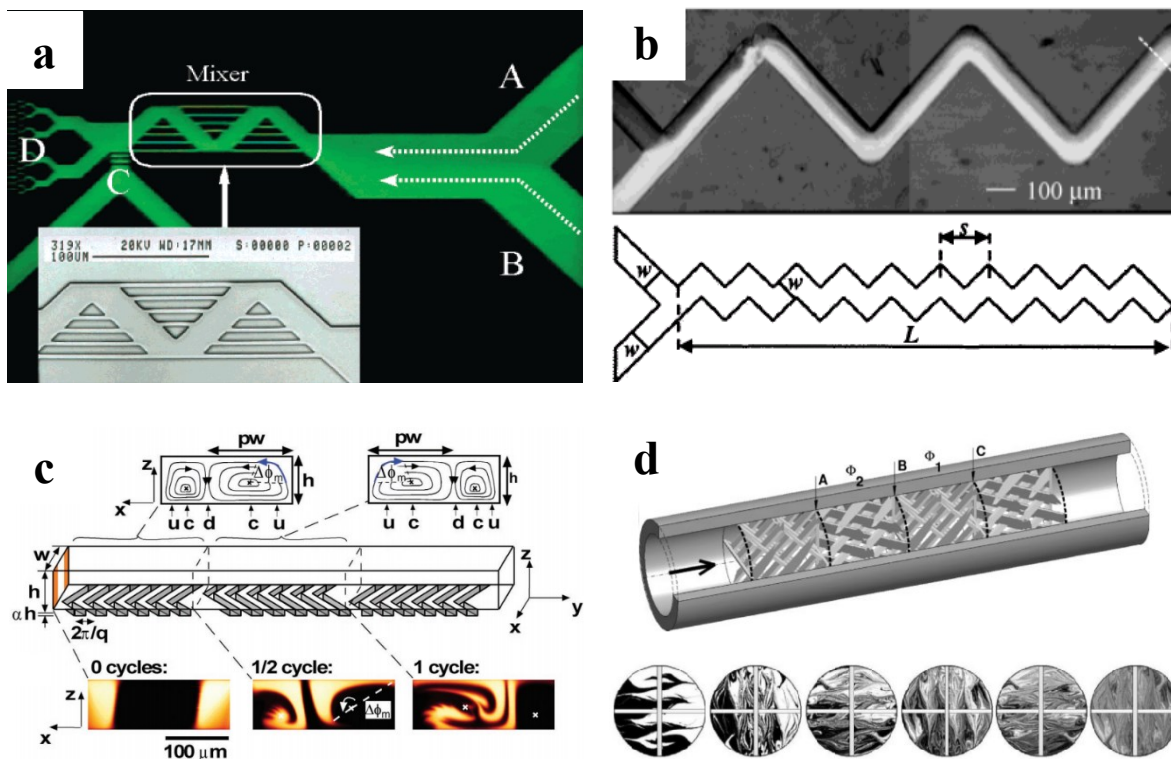
Figure 1-2. Passive mixing in microchannels.

(a) Intersecting Channels: Photomicrograph of picoliter-volume mixer. Adapted from B. He et al. 2001. [39] (b) Zigzag Channels: White-light microscopy image of a zigzag microchannel. Adapted from V. Mengeaud et al. 2002. [35] (c) Three-Dimensional Serpentine Structures: Staggered herringbone mixer (SHM).Adapted from A.D Stroock et al. 2002. [40] (d) Embedded Barriers: Schematic diagrams of static mixer with qualitative mixing profiles. Adapted from M.K. Singh et al 2009. [41]

Although utilizing complex geometries for chaotic advection is not an expensive method, but these schemes have a lower mixing efficiency and one needs to design longer mixing channel to achieve a satisfactory mixing result for high throughput systems. Hence, the other type of mixing strategies known as active mixing has been designed that employs external energy sources to create disturbances and speed up the diffusion process, such as acoustic/ultrasonic,[42-44] electrokinetic time-pulse,[45-47] dielectrophoretic,[48-50] electro-hydrodynamic,[51] magnetic,[52-54] or thermal[55, 56] techniques (Figure 1-3). Nevertheless, active micro-mixing is still expensive and challenging due to the required external actuations and the complicated fabrication process. Furthermore, the integration of active mixers in a microfluidic system is often complex. Another debatable feature in this paradigm is the essence of continuity that comes with laminar flow and limits the applications. There is no individual addressability for all the functions including mixing and sorting and samples are studied in series in microchannel channels.
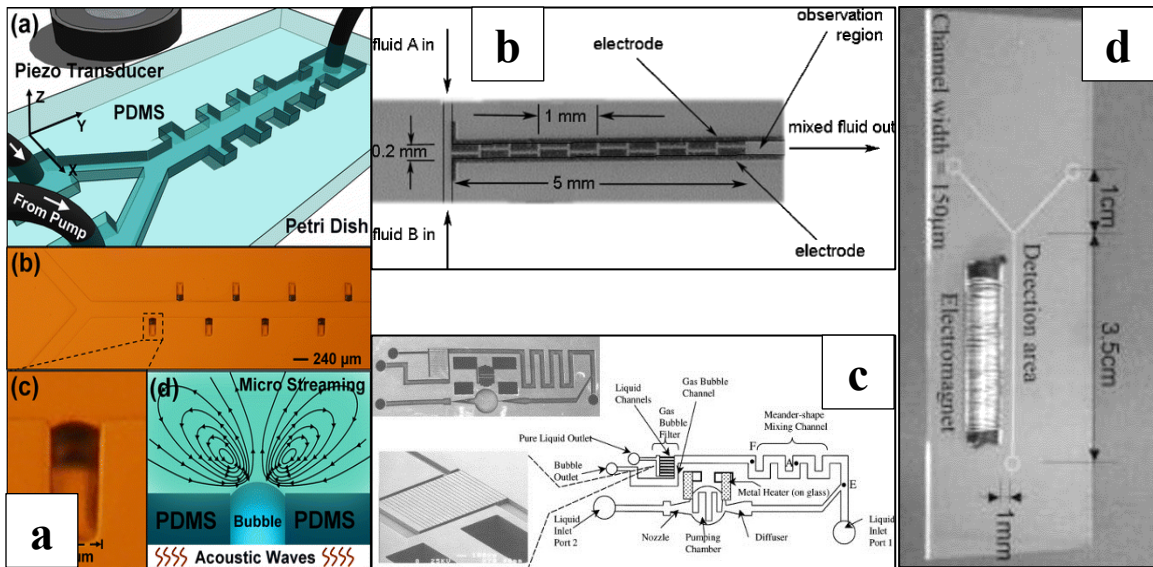
Figure 1-3. Active Mixing in microchannels.

(a) Acoustic Mixing: through utilizing piezo transducer. Adapted from D. Ahmed et al. 2009.[42] (b) Electro-kinetic mixing: through micro-electrodes actuation on the substrate layer. Adapted from M. Campisi et al. 2009. [48](c) Thermal mixers: a thermal bubble actuated nozzle-diffuser micro-pump. Adapted from J. Tsai et al. 2002. [56] (d) Magnetic mixer: utilizing AC electromagnetic field. Adapted from C.Y Wen et al. 2009. [53]

1.3   Droplets-in-Channel Microfluidics

Unlike continuous flow microfluidics, droplet based microfluidics manipulates only discrete volumes of fluids. The laminar flow of two immiscible liquid or gas-liquid in microchannels with certain geometries enables the generation of monodisperse droplets usually at rates in the thousands of droplets per second and these micro-droplets can serve as isolated micro-reactors. Indeed, droplet-based microsystems enable miniaturization of reactions by confining reagents in droplets of femtoliter to microliter volumes. Droplets can be generated,[57] mixed,[57] sorted,[58-60] split,[61] and merged with other droplets [62, 63] on chip. Confining reagents in droplets and the singularity of each droplet, brings various benefits and adds more functional features to the system including eliminating the risk of cross-contamination, rapid mixing of reagents, control of the timing of reactions and the ability to manipulate reagents with high throughput (10-100 kHz). Moreover, samples can be stored and incubated in liquid droplets over a long period of time without evaporation.[12, 64] These advantages make droplets-base microfluidics a suitable platform for chemical and biochemical screening, protein crystallization,[65] magnetic bead based assays,[66] chemical synthesis,[67] single cell high-throughput analysis,[68-70] enzymatic kinetics,[71-73] and assays[74, 75]. Furthermore, such a high throughput system with multiphase-fluid flow opened a new horizon of possibility in other applications such as emulsions for nano-particle synthesis,[76] cell-based drug delivery[77, 78] etc.

To increase the functionality of droplet-based platforms for a wider range of application and to have more control over droplets, many functional components have been developed including in-channel guiding and sorting using rails,[79-81] laser forcing,[82] or electrostatic charging[83-85].

While the use of micro-droplets can bypass certain limitations (i.e. like throughput, and analytical efficiency) that exist in conventional process conditions, there are still some disadvantages that makes less number of researchers to adopt microfluidics in their daily workflow. For instance, connections to external equipment such as pumps, tubing are complex and it even becomes more complicated for experiments running with multiple reagents. Although, many of the functions required for biological and chemical reactions like mixing, sorting, and splitting are done in droplet-based microfluidics, but for multiple reagents (i.e. more than three) there are still challenges. Moreover, in the field of biological application, the high speed manipulation of droplets has made the individual addressability a challenge. In multi-step long-term processes for example, reagent addition, staining, and media exchange is complicated.

1.3.1   Fabrication of the Droplet-based Microfluidics

Droplet microfluidic devices are mostly fabricated by soft lithography techniques [22] in an elastomeric material called poly(dimethylsiloxane) (PDMS). The fabrication procedure of PDMS-based microfluidics starts by designing the network of the microfluidic channels in a CAD software. The design is printed as a mask with transparent features with a very high resolution. Using this transparency mask and a silicon wafer coated with a negative resist, a master mold is fabricated by standard photolithography procedures that can be used several times for soft lithography. The PDMS polymer is mixed following standard procedures,[22] and then poured over this mold, and left to cure, after which the polymer can be peeled off and diced. To seal the microchannels, the surface of the PDMS is oxidized in an oxygen plasma and is irreversibly bonded to a flat substrates like a slab of PDMS, glass, silicon, silicon oxide, or oxidized polystyrene. Although PDMS is inherently hydrophobic, in order to have a smooth flow of the fluorinated oil in the channels and form stabilized water-in-oil emulsions, various surfactants have

been developed to wet the microchannel walls of the PDMS such as Aquapel® that contains fluorinated silane and improves the surface hydrophobicity of PDMS. [22, 86] One of advantages of using PDMS is the materials permeability to O2 and CO2, which allows live cells to be encapsulated within the channel. PDMS-based microfluidic chips are well established and are being vastly used by researchers; nevertheless, accurate alignment of structure features on different PDMS layers is still an issue in multilayer microfluidic structures.

However, there have been also other methods being developed that use other materials such as fused silica,[87] thiolene resin,[88] poly(methyl methacrylate) (PMMA)[89, 90], polystyrene (PS),[91] and fluorinated thermoplastic polymers[92].
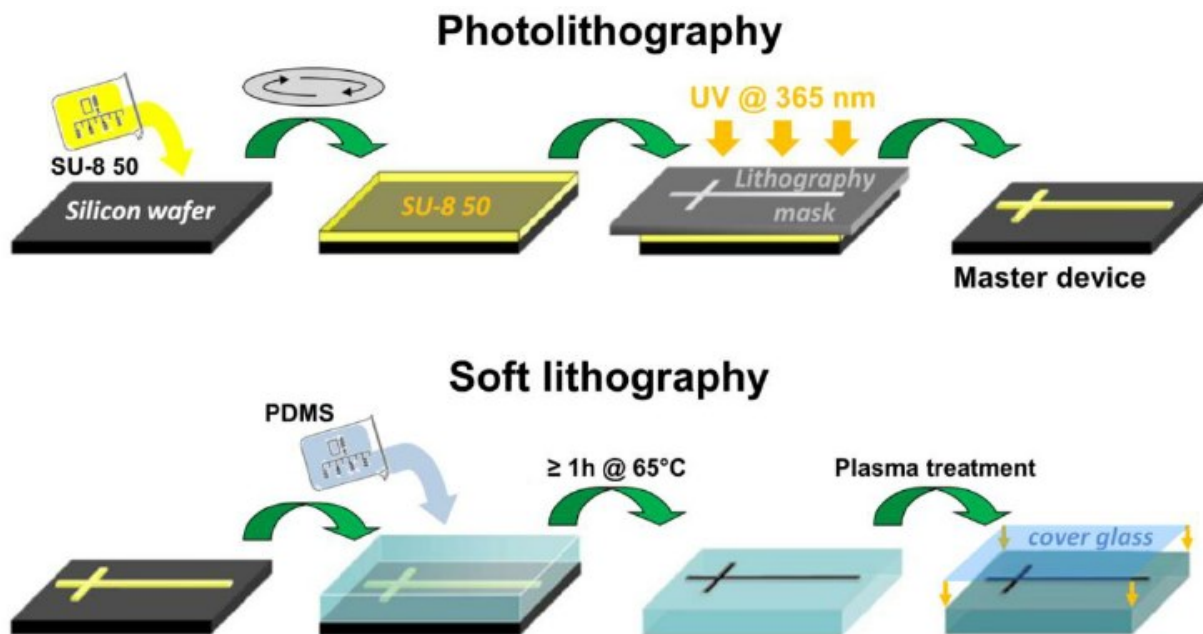
Figure 1-4. PDMS-based microfluidic device fabrication by photo- and soft lithography.

Adapted from Y. Ma et al, 2014. [93]

10

1.3.2   Droplet formation: Active and Passive

For many of the applications, the potency of droplet-based microfluidic systems lies in the formation of uniform droplets and particles, thus fine control over the size and shape of droplets is of the utmost importance. To achieve this objective, a variety of techniques have been developed for droplet generation. In general, droplet generation originates from flow instabilities between two immiscible liquids. The developed methods to create this instability inside channels are either passive or active. Passive methods are mostly used and these methods do not require any moving parts or external actuation. There are three main strategies for this continuous pressure-driven generation of droplets and they are characterized by the nature of the flow field near pinch-off (Shown in Figure 1-5): (1) breakup in co-flowing streams, (2) breakup in cross-flowing streams and (3) breakup in elongational or stretching dominated flows (mostly known as T-junction).[94]
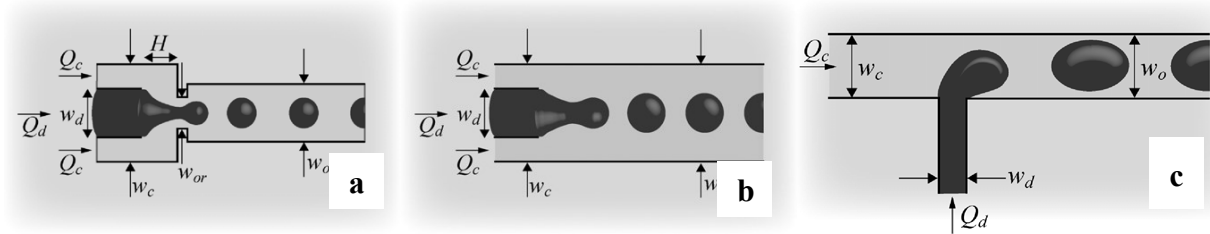
Figure 1-5. Schematic of the three microchannel geometries used for droplet generation.

(a) Flow focusing streams, (b) Co-flowing streams, and (c) cross flowing streams in a T-shaped junction. Reproduced with permission from Applied Physics.[95]

In general, two immiscible fluids are driven into microchannels by a pressure-driven flow and these two streams meet at a junction in such a way that the dispersed phase liquid extends to form a "finger" or "jet" due to the shear forces generated by the continuous phase. The head of the finger-shaped liquid elongates until the neck of the dispersed phase thins and eventually, a droplet pinches off from the dispersed phase finger by a free surface instability. Droplet formation and the liquids flow is controlled either by the volume flow rate or the applied pressure. In addition to the

geometry of the junction and the volumetric flow rates of the two fluids, surface/interfacial chemistry also plays an important role in droplet generation. Many fluorosurfactants have been reported to decrease interfacial forces and help droplet generation.[94, 95]

Active methods, in comparison with passive techniques, use external elements and have an active control on droplet formation with a fast response time. This feature brings higher flexibility to the system in terms of controlling droplet size and production rate and expands droplet microfluidics application for some extreme situations such as utilizing highly viscous liquids as dispersed phase and for on-demand droplet generation for deterministic cell-in-droplet encapsulation.

Generally, droplet formation is a result of liquids instability and force imbalance on the interface. Forces that affect droplet formation are either intrinsic including inertial, viscous, and capillary or external like electrical, magnetic, centrifugal, optical, thermal, and mechanical. Active control is modifying or applying any of the aforementioned intrinsic or external forces respectively. Intrinsic forces can be modified by manipulating the dynamic velocity and material properties, including viscosity, interfacial tension, channel wettability, and fluid density.[94]

For both methods, to avoid coalescence and cross-contamination of the generated droplets two strategies have been employed; first, using fluorocarbon oils as the continuous phase instead of hydrocarbon oils, as these oils are hydrophobic and lipophobic thus have low solubility for the biological components of the dispersed phase. They also prevent molecular diffusion between droplets. Fluorocarbon oils result in less swelling of PDMS and due to their good solubility for gases, they allow sufficient gas exchanges to maintain cell viability for extended periods of time. Second, several biocompatible fluorosurfactants have been developed to help stabilizing the water-in-oil droplets.[96, 97]

1.3.3　　Droplet manipulation

　　　　Various methods of manipulating droplets have been developed by researchers. Droplets can be mixed, split, fused, coded and sorted on chip either in active or passive mode. To perform such manipulations, passive methods employ various channel geometries while active methods use external resources such as electrohydrodynamic, and magnetic forces to manipulate droplets. I will specifically explain mixing and sorting operations which are the two developed functions in this project.

(i)　Mixing, Droplet Coalescence, and Picoinjection

　　　　Mixing of multiple reagents is an essential step for carrying out and studying the kinetics of biological and chemical reactions. There are generally three schemes of mixing in droplet-based microfluidics. One is mixing various reagents confined within a droplet. Droplets are formed by using multiple streams of reagents introduced to the device individually from distinct branches. Because the droplet's diameter is greater than the microchannel's width, the droplet forms a plug that has contact with the channel's wall (Figure 1-6). This interface with the channel's wall makes a double recirculating flow pattern within the droplet, which acts like a turbulent flow and enhances the rate of mixing inside the plug. This recirculating flow actually, is the result of shear forces from either the continuous phase fluid or the channel wall. Using winding channels configuration, uneven shear forces are made on sides of the plugs leading to a phenomenon known as "stretching and folding" that consequently results in a faster mixing droplet contents. Varying the relative flow rates of the reagents varies the concentration of the reagents within the plug.[12, 64, 98] This method however, is not suitable for multistep reactions that needs reagents to be added in a certain time one after another.
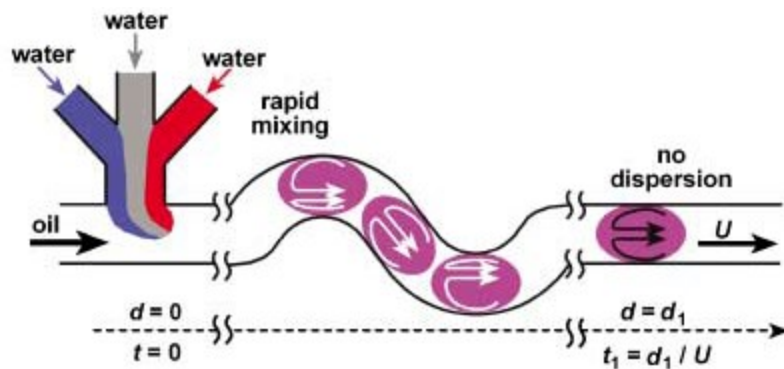
Figure 1-6. Mixing multiple reagents confined within a single droplet.

Generating uniform plugs out of multiple reagents streams – Adapted from H .Song et al, 2003.[64]

The second scheme of mixing is merging two droplets with different contents. As with previous fluidic operations, mixing schemes can also be categorized as either "passive", where novel channel configurations have been implemented to enhance rapid internal mixing, or "active", where an external energy force such as hydrodynamic and magnetic is applied to make disturbance inside microchannels. In both strategies, to initiate droplet coalescence of surfactant-stabilized droplets, two conditions are required to be satisfied: bringing droplets into close contact by draining the continuous phase separating the two droplets and disrupting their stabilizing surfactant layer by causing an imbalance in their surface tension.[61, 98, 99]

To fulfill these pre-requisites, passive methods mostly rely on the precise control over the individual droplets velocity and channel geometries to cause relative motion of two droplets. Two droplets thus gradually come close to each other and eventually coalesce. Incorporation of an expanded portion[100] and pillar structures [62] inside the microchannels are two of the most common geometry modifications for passive mixing (Figure 1-7Figure 1-7a, b).

Although passive mixers have simpler designs, less possibility of inter-droplet contamination and are more biocompatible in comparison with active techniques, they are limited by their mixing rate and have much lower throughput. [101, 102]

For surfactant stabilized droplets, active fusion methods are employed, as it is normally not possible to fuse those droplets using passive techniques. Active methods usually use electric fields to merge droplets. Electrocoalescence, dielectrophoresis (DEP), and optical tweezers are some of the prevalent strategies for active mixing. Priest et al. demonstrated a device for electrocoalescence of tightly packed droplets with a very low voltage of 1 V DC. They placed two electrodes parallel to the microchannel and applied a range of AC and DC voltages to rapture the surfactant layer between droplets and fuse them together (Figure 1-7c).[103] Another approach is to induce coalescence of droplets without using electrodes and by imposing an opposite electrical charge on different groups of droplets once they are generated. Then, in the presence of an electric field, oppositely charged droplets become fused together. The main disadvantage of this method is in applications with multiple mixing steps which requires recharging the neutral mixed droplets (Figure 1-7d).[83] Applying DEP forces on differently-sized droplets is another strategy for active mixing. In this method, droplets of different sizes are generated and once they are in the main channel, the smaller droplets run faster in comparison with the larger ones and pair with them. These paired droplets become fused when passing through a microchannel surrounded by two parallel electrodes. Precise timing and flow rate is challenging in this method (Figure 1-7e).[104] Another DEP mixing protocol, is trapping droplets in a side chamber adjoining the main fluidic channel by applying a DC voltage and inducing DEP force on the desired droplets to move in a specific direction. Once a second type of droplet containing a different reagent is passing by the chamber, a DC voltage is again applied which brings the trapped droplet in contact with the passing droplet resulting in their fusion. In general, DEP can be used to manipulate droplets that are dielectrically distinct from the continuous phase composition. For example, dielectric permittivity of water is much higher than that of oil ($\varepsilon_{H2O} \approx 81$, $\varepsilon_{oil} \approx 2.5$).[61, 105]
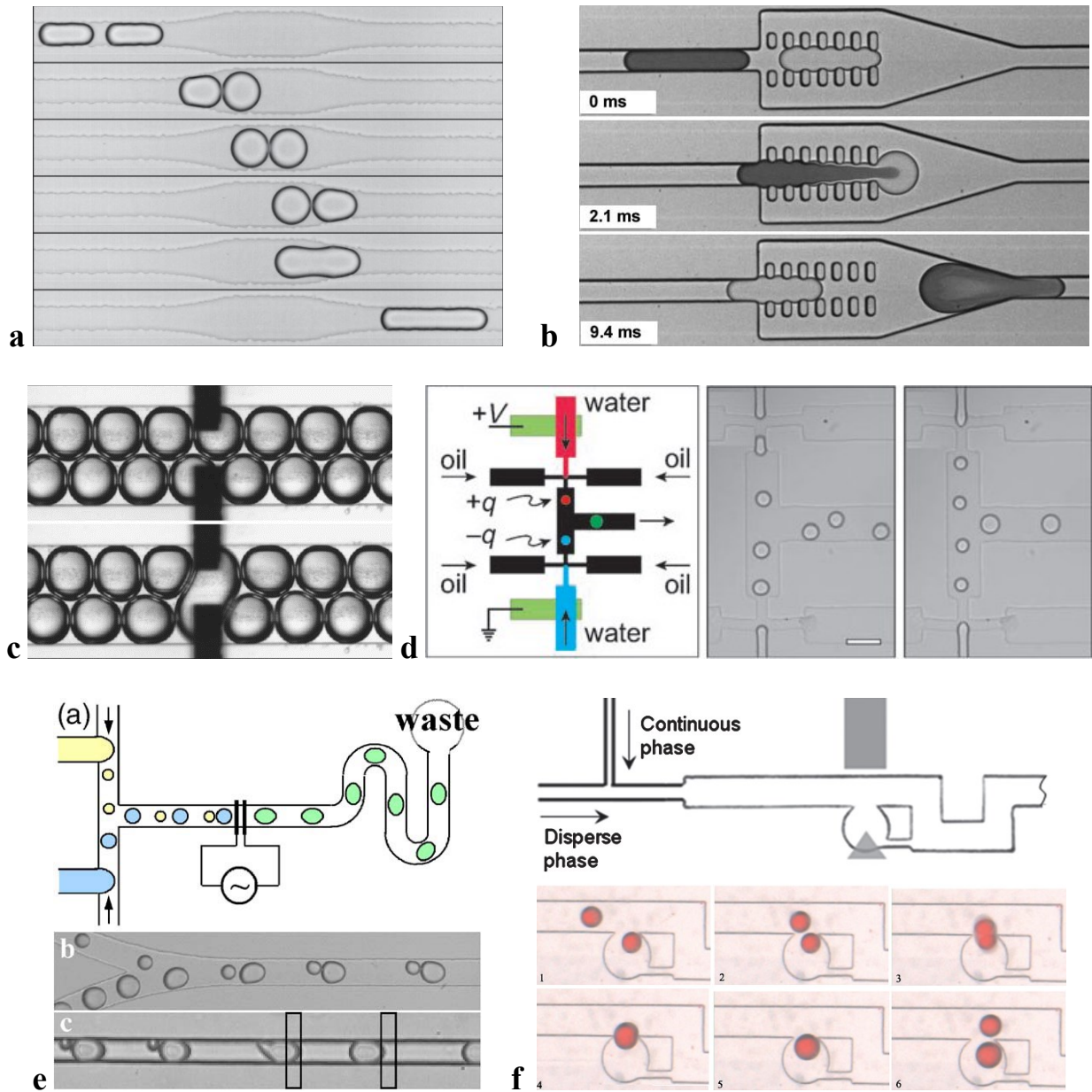
Figure 1-7. Passive and active droplet coalescence.

(a) Droplet fusion through channel geometry modification – Adapted from N. Bremond et al, 2008.
[100](b) Passive droplet fusion by destabilizing the liquid flow using pillar structures inside microchannels – Adapted from X. Niu et al, 2008. [62] (c) Controlled electrocoalescence of tightly packed droplets within 100 μs with voltage as low as 1 V DC – Adapted from Priest et al, 2006.
[103] (d) Coalescence of electrically charged droplets in presence of an electric field – Adapted from D. Link et al. 2006. [83](e) Active droplet fusion using DEP force on differently sized droplets– Adapted from K. Ahn et al. 2006. [104] (f) On-demand mixing of two droplets using trapping mechanism and DEP –Adapted from W. Wang et al, 2009. [105]

16

In addition to the higher efficiency of these active mixers, on-demand mixing of certain droplet pairs upon an upstream detection, is one of the main benefits of electrically controlled fusion which also helps automating the system. Integrating the external electronic elements required for on-demand control, however, adds to the complexity of the system operation and its fabrication process. Moreover, due to electrode actuation and possible deposition of droplets' contents on the electrodes, cross contamination between droplets becomes a concern. Furthermore, biocompatibility of the high voltage applied in some of the active methods on biological components such as DNA or proteins is still debatable. [98, 99]

Some other protocols for droplet mixing have also been exploited including different combinations of hydrodynamic stress and electric field,[106-108] thermocapillary,[109, 110] magnetism[111] and acoustics[112]. In spite of all the considerable advantages of these on-demand mixing methods, it is still difficult to perform multiple additions, since several streams of droplet should be synchronized.

An alternative to mixing droplets of different contents, is adding reagents into passing droplets (Figure 1-8). In this technique, several narrow hydrophilic T-junction channels are designed to introduce new reagents to the passing droplets in the main channel.[113] This method however, has several disadvantages including significant possibility for contamination due to direct contact of droplets with the reagents stream, and less control over the volumes of the reagents added to a passing droplet. Moreover, this technique is not applicable for surfactant stabilized droplets, as the surfactant layer on the droplet surface prevents reagents addition to the droplet. To address this issue, Abate et al. reported an electric field controlled addition of a defined volume by direct injection into a passing droplet. In this method passing droplets pass by the reagents stream without coalescing to it due to the presence of surfactant on all interfaces.

Switching on the electric field disrupts this stabilized layer and the liquid from the adjoining channel is injected into the passing droplet.[114] Nevertheless, this techniques needs precise control over the flow rate of the aqueous phase and timing of the interval between droplets.
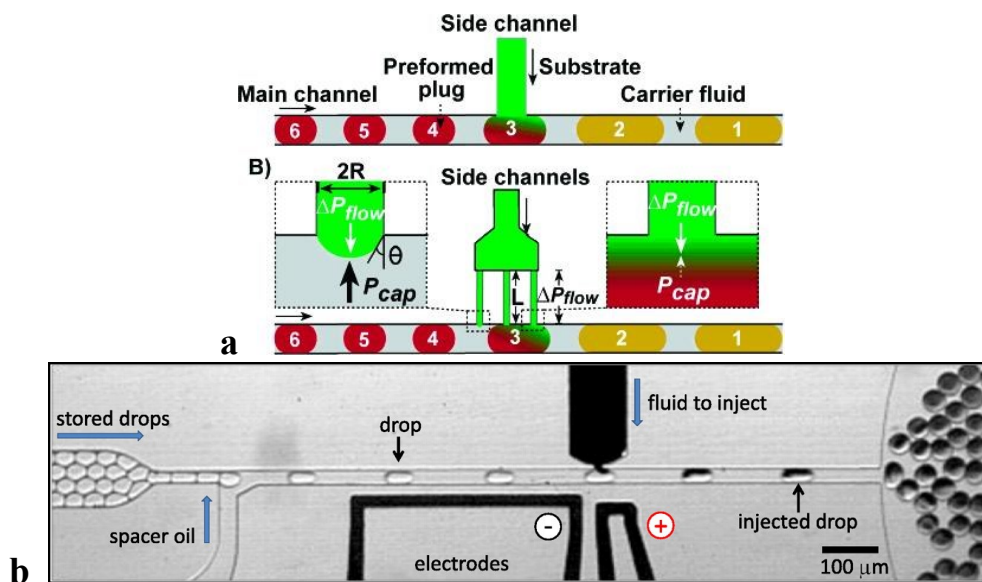
Figure 1-8. Adding Reagents into Passing Droplets.

(a) Passive injection of reagents into droplets – Adapted from L. Li, 2007 [113] (b) Pico-injection of reagents by electric actuation – Adapted from A. Abate et al, 2010. [114]

(ii) Sorting

Sorting is another important operation for isolating droplets of particular interest and purifying samples for further analysis and has many application in cell studies such as circulating tumor cells and drug screening. Droplet sorting and distinguishing different subsets of droplets is based on a characteristic of the droplet or droplet's content. Similar to other on-chip function, sorting can also be done either in passive or active mode. While passive sorting mechanisms mostly rely on channel geometries and gravity and uses droplet size as the discriminating characteristic, active sorting, employs various types of labels in droplets to differentiate groups of droplets.[99, 115]

An example of size-based sorting using channel geometry is the setup demonstrated by Griffiths et al (2009) (Figure 1-9a). In this setup, droplets with larger and smaller dimensions are

generated and collected to flow together in a main channel that its depth is set to be between the sizes of two droplets. The larger droplets flow slowly and smaller droplets are trapped in between the larger ones. Downstream, the main channel branches into two narrowing side channels and a widening channel in center. The smaller droplets that are not constrained by the walls of the device and flow near the wall of the channel, enter the side channels while the larger droplets move along the wider central channel.[116] Huh et al (2007) developed a gravity driven microfluidic droplet separation system to purify perfluorocarbon droplets from a polydispersed emulsion (Figure 1-9b). The theory of this mechanism is that the sedimentation velocity of larger particles is greater than that of smaller particles at a given density. Therefore, larger droplets move toward the bottom channel. Asymmetrical design of the daughter channel enhances the droplet separation[117]. Although the implementation of passive sorting is simple, this technology is limited with its fixed geometry. Using a single device, only a certain range of droplet sizes and speeds are amenable for sorting. Moreover, this size-dependent sorting is not applicable for categorizing droplets of similar size. Their efficiency is also not comparable to active methods due to a weak control over droplets movements.
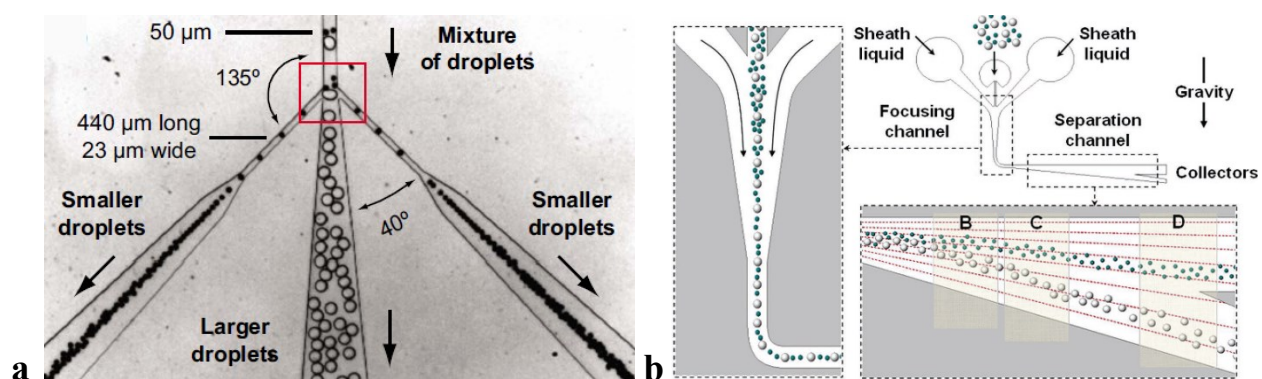
Figure 1-9. Passive sorting methods.

(a) Size-based sorting using channel geometry – Adapted from L. Mazutis et al, 2009. [116]
(b) Gravity-driven size-based sorting – Adapted from D. Huh et al, 2007. [117]

In active sorting techniques, prior to the controlled separation, the target group of droplets are required to be detected with an external source such as a photomultiplier tube (PMT) and optical fibers. For droplets to be detected they are usually labeled with a marker like fluorescent and magnet beads, or their encapsulated cells contain fluorescent proteins as a biomarker. [61, 98]

One of the first developed and popular active sorting strategy is through using DEP forces. When an AC electric field is applied across the electrodes that are placed either beneath the microfluidic channels or adjacent to the sorting junction, droplets are deflected to the desired pathway. Baret et al. demonstrated a fluorescence activated droplet sorting system based on enzymatic activity and achieved sorting rates of around 300 droplets per second with false positive error rates of 1 in 104 droplets. [60] To surpass throughputs of a few kilohertz, Sciambi et al, presented a new geometry of the collection channels that replaces the hard divider separating the outlets with a gapped divider. With this new geometry they could accurately sort droplets at 30 kHz with > 99% accuracy. [118] Using DEP, Gielen et al, has also reported an ultrahigh-throughput (300 droplets per second or >1 million droplets per hour) absorbance-activated droplet sorting with a false-positive rates of below 5%[119]. In addition to DEP based sorting, other methods have also been demonstrated by various groups such as surface acoustic wave actuated sorting,[120] pneumatic valve actuated sorting,[121] pressure actuation sorting using a solenoid valve,[122] magnetic particle sorting,[123] and electrostatic droplet charging and sorting based on the polarity of the charged droplets. [85] In spite of the very high throughput and efficient sorting of the developed methods, they all lack some important features like the ability to do multiple sorting that is required in some applications like directed evolution or single cell studies. Moreover, all of the mentioned protocol can only analyze droplets in series and individual addressability is not possible.
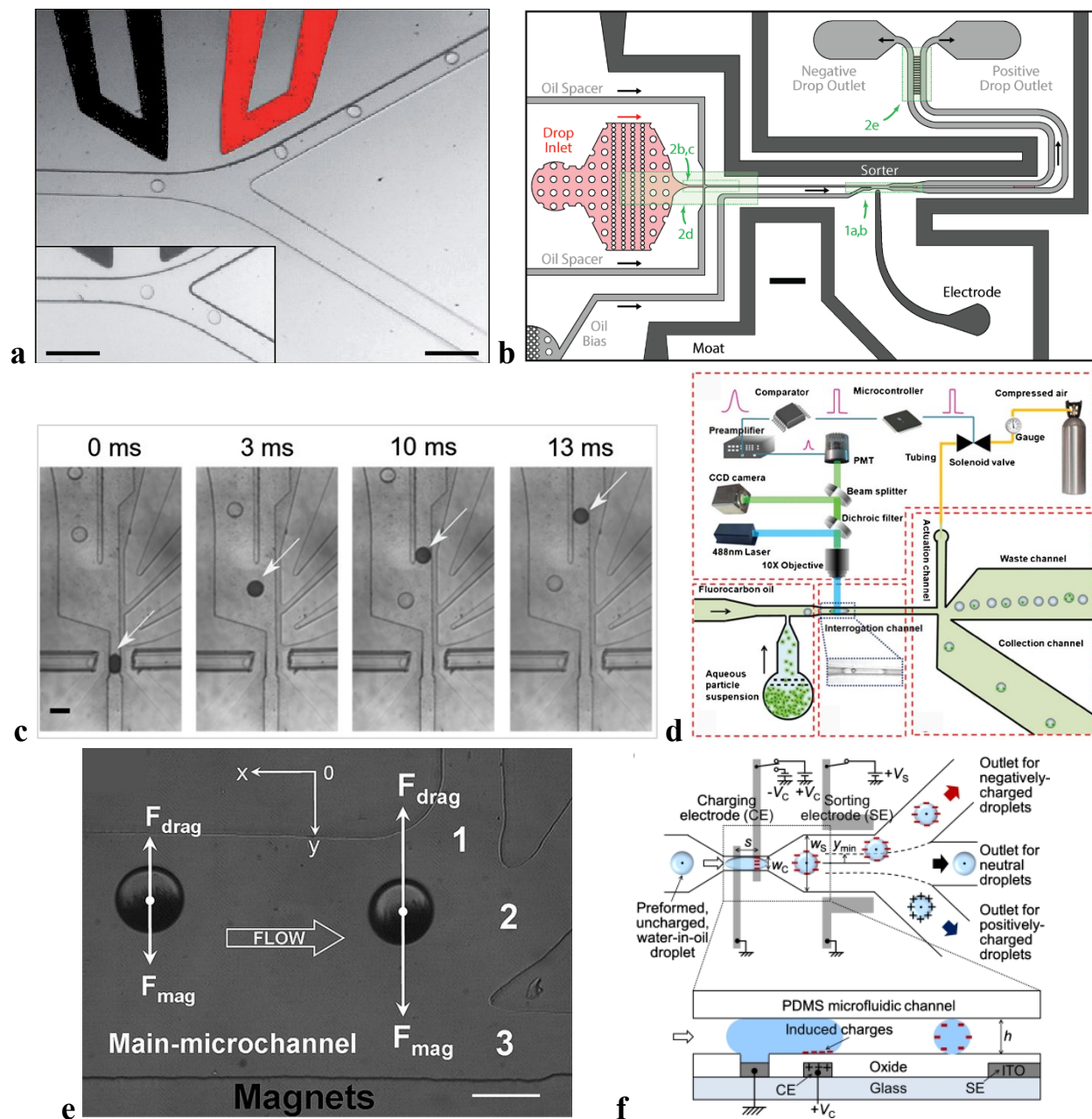
Figure 1-10. Active sorting mechanisms.

(a) Fluorescence-activated DEP-based sorting – Adapted from J. Baret et al, 2009. [60](b) Geometry modification for enhancing DEP-based droplet sorting – Adapted from A. Sciambi et al, 2015. [118] (c) absorbance-activated droplet sorting – Adapted from F. Gielena et al, 2016. [119] (d) Pressure actuation sorting using solenoid valve – Adapted from Z. Cao et al, 2013. [122] (e) Magnetic sorting – Adapted from K. Zhang, 2009. [123](f) Electrostatically sorting of charged droplets based on their polarity – Adapted from B. Ahn et al, 2011.[85]

1.3.4   Droplet-Based Microfluidics for single cell studies

Compartmentalizing reactions by isolating single molecules and cells into droplets have been investigated since 1950s, but the idea did not come true until the advent of droplet microfluidics. The highly reproducible and on-demand fabrication of microfluidic devices allows for analyzing different reaction conditions. Moreover, droplet-based microfluidic enables fast sensitive (qualitative and quantitative) detection of secreted biomolecules from cells inside droplets through integration with the modern analysis systems. In comparison with bulk experiments, droplets act as tiny reactor containers, in which the concentration of cell-produced or excreted compounds, is much higher and thus easier to analyze. Furthermore, the multi-parallel and high-throughput platform is promising for studying libraries of biological component like enzymes or cells.[98]

In addition, single cell encapsulation in droplets, enables studying the potentially important heterogeneity of individual cells and analysis of rare cells by separating them from the whole population. Gene expression, phenotypic variation, quorum sensing and screening of protein libraries for in vivo directed evolution, and drug screening of cancer cell lines have been demonstrated in micro droplets at single cell level using stochastic confinement. [98, 124-126]

In order to make the most use of droplet microfluidics for cell analysis, encapsulation of cells in droplets with control over cell occupancy and droplet size is crucial. Various methods have been demonstrated to control the number of cells in droplets such as stochastic loading at low cell density,[127] optical trapping,[128] bio-electrospraying,[129] and inertial focusing [130]. The number of cells in each droplet follows the non-uniform Poisson distribution (Figure 1-11), meaning each droplet might contain one, two, three, or no cells, stochastically. The Poisson distribution is given by:

Equation 1-2: Poisson distribution

$$p(k, \lambda) = \frac{\lambda^k e^{-\lambda}}{k!}$$

where k is the number of cells in a droplet and λ is the average number of cells per droplet volume.

For a given oil-water flow rates and system geometry, where the average cell and droplet volume

$\bar{V_c}$ and $\bar{V_d}$ are constant, λ can be defined as the ratio between the volume fraction of cells in the pre-

encapsulation solution ϕ_s and that of a droplet containing one cell, defined as: $\phi_d = \frac{\bar{V_c}}{\bar{V_d}}$. Thus, λ

can also be expressed as:

Equation 1-3: Lambda λ value for a given fluids flow and channel geometry

$$\lambda = \frac{\phi_s}{\phi_d}$$
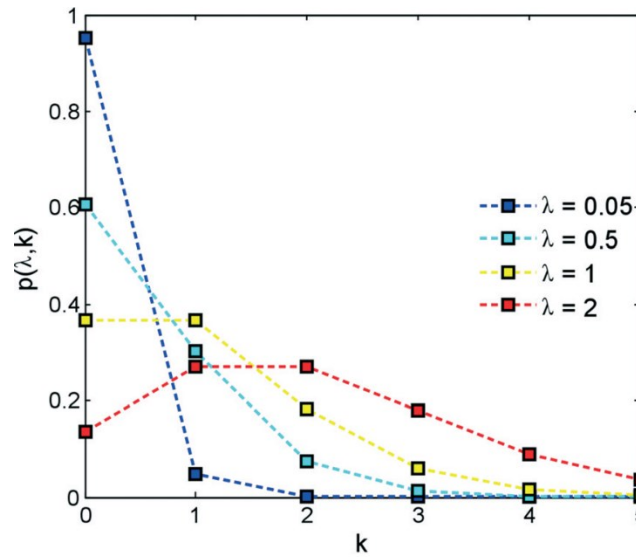
Figure 1-11. The Poisson distribution.

The proportion of droplets p(λ, k) containing a given number of cells k is shown for different discrete values of λ. Adapted from D. Collins et al, 2015 [127]

1.4 Digital Microfluidics

During the last decade, a new microfluidics technology has emerged called digital microfluidics (DMF), although in the early stages, it literally has the greatest potential to make lab-on-a-chip slogan truly possible and brings all laboratory instruments and components onto a hand-held device. This idea was first introduced in the late 1990s and was inspired by digital microelectronics for timed motion of fluids, with accurate control, representing an alternative to the conventional paradigm of transporting fluids in enclosed channels. [131, 132]

In digital microfluidics, picoliter–microliter sized droplets are manipulated on arrays of electrodes by the controlled application of voltages.[15, 16, 133] Through sequential actuation of electrodes, droplets can be individually made to merge, mix, split, and dispense from reservoirs.
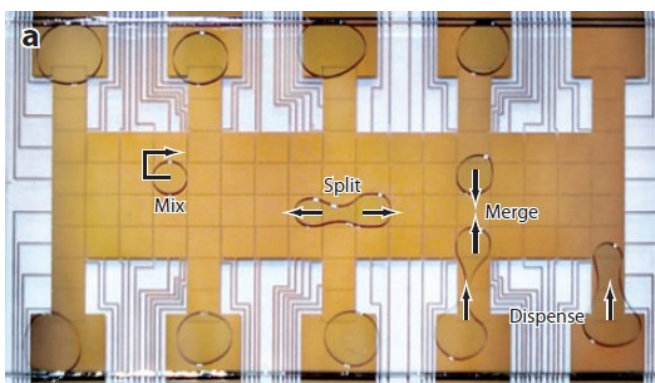
Figure 1-12. Droplet Manipulation on DMF.

Adapted from K. Choi et al, 2012[134]

This technology gives the big advantage of fluid motion and control without pumps and valves, and eliminate the clogging problem that is an issue in enclosed channels. The principal difference is that in digital microfluidics, droplets are addressed individually, whereas in channels, they are controlled in series. Digital microfluidics is well fit with a wide diversity of biomedical applications that can be parsed into manageable components given its advantages of being

programmable, reconfigurable, reusable, and its ability to speed up the process through massive parallelization.[7, 133]

Two configurations of DMF devices have been developed: single-plate (open), and two-plate (closed) devices (Figure 1-13). In the two-plate DMF, droplets are sandwiched between two substrates: bottom plate bearing arrays of actuation electrodes and top plate acting as a continuous ground electrode which is usually made of a by a transparent, conductive indium tin oxide (ITO) layer. In open configuration, however, both actuation and ground electrodes are patterned on the bottom plate. In both types of DMF, a layer of insulating dielectric such as Parylene C is coated on bottom plates and a layer of hydrophobic coating like Teflon covers all the surfaces in touch with droplets. Both types of DMF are widely used for a wide range of application. Nevertheless, the one-plate configuration is less popular, as it is not capable of splitting and dispensing due to a weaker electric field.[134]
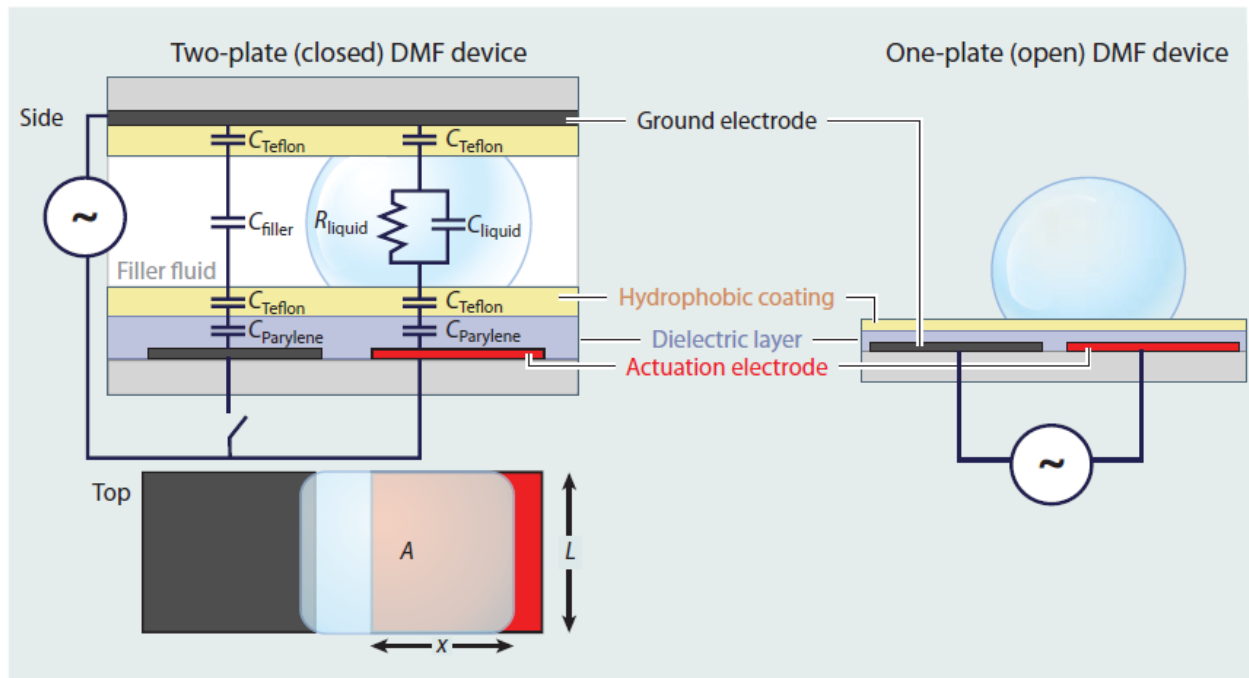
Figure 1-13. Single-plate and two-plate configurations for DMF.

Adapted from Choi et al.[134]

1.4.1   Digital Microfluidic Theory

In the broad field of biomimicry, scientists have been fascinated by the way nature has engineered "self-cleaning" lotus leaves or "fog-collecting" Stenocara beetle for a long time and there have been many researches in developing artificial mimics with similar properties to control the surface wettability by fluids.[135] One of the strategies for tuning the surface's wettability found to be applying pulses of electric potential which later was explained by a phenomenon known as "electrowetting".[136-138] Electrowetting-on-dielectric (EWOD) is a phenomenon can be applied to control aqueous liquids. EWOD utilizes the change in contact angle of a droplet sitting on a substrate when charge is accumulated on the dielectric layer separating the liquid and the conducting substrate by means of an electric field.[138]

When properly sequenced, this change in contact angle can motivates transporting a droplet from one charged region to another. This phenomenon has been used as tool for modulating fluid position in digital microfluidics by placing droplets on an array of electrodes coated with an insulator and sequentially applying electrical potential to adjacent electrodes on a path, thus enabling on-demand movements of droplets.[135]

In the earliest theoretical attempt for estimating the driving forces in EWOD, there was a thermodynamic approach using the Young-Lippmann equation:

Equation 1-4: Young-Lippmann Equation

$$\cos \theta_w = \cos \theta_0 + \frac{\varepsilon_0 \varepsilon_r V^2}{2\gamma_{LG} t}$$

Where θ_w and θ_0 are the wetted and static contact angles, respectively; ε_0 and ε_r are the permittivities of free space and of the dielectric, respectively; V is the applied voltage; γ is the liquid/filler media surface tension (air or oil); and t is the dielectric thickness. In this model, droplet

movement is assumed to be due to capillary pressure resulting from asymmetric contact angles across the droplet.

To adopt a dynamic model of the droplet motion after deformation from Equation 1-4 (as this equation only accounts the static contact angles), the driving force F in this model can be expressed as:

Equation 1-5: Driving force using Young-Lippmann

$$\mathbf{F} = \mathbf{L}\boldsymbol{\gamma}_{LG}(\cos\boldsymbol{\theta}_w - \cos\boldsymbol{\theta}_0) = \frac{\varepsilon_0\varepsilon_r LV^2}{2t}$$

Where F is the driving force and L is the length of the contact line overlapping the actuated electrode. This driving force is often referred to as the "EWOD force". [134]

However, it has been shown that for a liquid with a certain conductivity and dielectric constant, the electric field in the contact line (i.e, between liquid and dielectric layer) at certain frequencies can potentially change the contact angle, but this phenomenon is not necessary for liquid motion. Droplets of chloroform or toluene for example, can be moved on electrodes without any apparent change in their contact angle. [139, 140] Upon discovery of the fact that the theory behind electrowetting does not apply to dielectric liquids [141] and fluids with low surface tension, [139] the term "Digital Microfluidics" emerged. Moreover, the thermodynamic approach fails in explaining contact angle saturation (i.e. there is a limit on contact angle change when increasing the applied potential), and liquid-dielectrophoretic force, which is predominant at high frequencies. [14]

In fact, the EWOD force itself is a purely electrostatic phenomenon that applies equally to conducting solids and fluids. This being said, electrostatic fields have two observable effects upon the hydrostatics of liquids. First, in presence of a nonuniform electric field, a net force is applied on the liquid and second, the contact angle of the liquid on a dielectric surface changes. For the

case of arrays of electrode coated with micron-thick dielectric in DMF both of these effects are mostly assumed to be electromechanical, however, depending on the conditions, they can also occur in independently.

Considering the wetting as a result of the exerted forces on the droplet, the most accurate way to estimate the forces on the droplet in DMF is adopting an electromechanical approach and using a circuit diagram. The amount of energy stored in this system is calculated as a function of the applied voltage frequency and droplet position along the direction of translation. [142] Here is the Equation 1-6 representing the amount of energy, E, of the system:

Equation 1-6: Energy equation using electromechanical model

$$E(f,x) = \frac{L}{2}\left(x\sum_i \frac{\varepsilon_0\varepsilon_{ri,liquid}V_{i,liquid}^2(j2\pi f)}{d_i} + (L-x)\sum_i \frac{\varepsilon_0\varepsilon_{ri,filler}V_{i,filler}^2(j2\pi f)}{d_i}\right)$$

where L is the dimension of the droplet (estimated by the cross-section of the drop), $\varepsilon_{ri,liquid}$, $V_{i,liquid}$ and $\varepsilon_{ri,filler}$, $V_{i,filler}$ are the relative permittivity and voltage drop for the liquid and filler fluid portions of the electrode, respectively, and d_i is the thickness of layer i (corresponds to the dielectric, hydrophobic, liquid or filler layers). Differentiating the energy calculated in Equation 1-6 with respect to x yields the driving force as a function of frequency:

Equation 1-7: Force equation using electromechanical model

$$F(f) = \frac{\partial E(f,x)}{\partial x} = \frac{L}{2}\left(\sum_i \frac{\varepsilon_0\varepsilon_{ri,liquid}V_{i,liquid}^2(j2\pi f)}{d_i} - \sum_i \frac{\varepsilon_0\varepsilon_{ri,filler}V_{i,filler}^2(j2\pi f)}{d_i}\right)$$

The key advantage of the electromechanical model is that it takes into account the frequency of the applied voltage on droplets across each layer and portion of the device – it represents the stored energy that results in an applied force.

28

From this, we can calculate a critical frequency (f_c) for each device geometry and the liquids being operated.[142] Below the critical frequency, the voltage drop occurs across the dielectric layer and we can apply the equations relative to the EWOD model. The force that is driving the droplet at low frequencies comes from charges accumulation near the three-phase contact line, which are being pulled toward the actuated electrode electrostatically. The magnitude of this force depends on the capacitive energy stored within the dielectric. When we apply frequencies above f_c, the liquid is purely insulating and an electric field gradient is generated across the droplet, generating a liquid-dielectrophoretic force (DEP) to pull the droplet toward the activated electrode. Here, the magnitude depends on the difference in permittivity between the liquid and filler medium (air, in our case). In DMF, droplets are manipulated by AC frequencies in the order of kHz and the majority of the voltage drops across the dielectric. [142] When inserting this range of frequencies in Equation 1-7, we obtain an estimation of DMF forces with magnitudes in the range of μN, which can be applied to a wide range of fluids using driving voltages of 100-300 V_{RMS}.

The driving electrostatic forces acting on the drop compete with counteracting forces. The first is the shear force between the droplet and the plates, [143, 144] which is highly dependent on local surface smoothness and heterogeneity, dictated by the quality of dielectric and hydrophobic coating and resulting nano- and micro- scale roughness of the hydrophobic surface. The second factor impeding droplet movement is the viscous drag force resulting from displacement of the filler fluid during droplet translation.[144] As soon as the driving force is greater than both the shear and viscous drag forces, droplet movement can be observed. Overcoming such movement limitations is critical in enhancing droplet movement, and the optimization lies in surface characterization, use of surfactants, device design and the device hydrophobicity. For most DMF systems, the forces calculated by electrowetting and electromechanical models reach consensus.

1.4.2   Applications and Challenges

Given the versatility of digital microfluidics (DMF) and its unique features, it has been applied to a variety of applications that were performed conventionally in macroscale such as chemical synthesis,[145, 146] enzymatic reactions,[147, 148] immunoassays,[149, 150] DNA-based and proteomics analysis,[151-153] cell-based applications,[19, 154, 155] clinical diagnostics,[156, 157] and studies of multicellular organisms[158, 159].

Considering the precise metering of reactants through dispensing droplets from individually addressable micro-reactors that DMF is capable of, chemical synthesis and reactions have been widely implemented on DMF for synthesizing new compound, analyzing substances of interest, and studying reaction kinetics. Jebrail et al (2010), reported a DMF for synthesizing cyclic macro-molecules from aminoacids with similar properties to the products made by conventional methods proving the potential of DMF platform for efficient and automated synthesis of compounds for drug discovery.[146] Another group presented an integrated two-plate DMF device with four concentric heaters for synthesizing a radiotracer (2-[18F]-fluoro-2-deoxy-D-glucose) that is widely used in positron emission tomography (PET) scan for in-vivo imaging of living organism. Using their developed DMF, they could produce radiotracers with high and reliable radio-fluorination efficiency (85%).[145]

As mentioned above, another popular target for digital microfluidics has been cell-based assays as the reagents and other materials used in conventional methods are often prohibitively expensive. Moving droplets without the need of valves and pumps or any other movable parts, and with the great controllability provided by the integrated automation system, has made DMF a perfect platform for a variety of cell-based assays, cell sorting and cell culture.[131]

Barbulovic-Nad et al. (2008) demonstrated the first cell-based assay implemented by DMF. They were able to actuate high density cell suspensions (6×10^7 cells mL^{-1}) on electrodes using a Pluronics additive. Moreover, they reported that the electric field resulting electrode actuation has no significant effect on cell viability.[154]

To be able to explore a wider range of application, other techniques have been integrated with DMF to manipulate cells inside droplets using electrical, optical, or magnetic forces. For concentrating a specific cell populations, for instance, Shah et al. (2010), purified a specific type of lymphocyte cells from a cell suspension using antibody-conjugated magnetic beads inside droplets and an external magnet.[160]

However, there are still challenges for implementing cell-based studies in DMF. For cells to be viable, there must be gas exchange between cells and the atmosphere. Therefore, oil-filed DMF are usually not compatible with this application. In addition, DMF is limited by a major problem known as surface biofouling that is nonspecific adsorption of cells and protein to device surfaces. Due to this problem, DMF usually requires addition of extra chemical reagents such as Pluronic to the droplet or its surroundings that could potentially affect droplet content.[134] Furthermore, throughput of DMF is limited by the amount of reservoirs, the size of the reservoir (that cannot not be replenished), and the amount of electrodes available, while channel can produce droplets by 30 KHz [125] and this is impossible with the existing DMF technology. Therefore, more optimization is needed to be implemented on DMF for high-throughput screening (HTS).

Chapter 2. Hybrid Microfluidics:

Toward a True Lab-on-a-chip

This chapter will introduce hybrid microfluidics and describe its superiority over the other paradigms owing to its combinatorial characteristics. Then, the novelty of the hybrid device fabricated in this project as well as the integrated automation system will be highlighted.

2.1 Overview

The idea of integrating DMF with other microfluidic paradigms is an exciting innovation as it combines advantages of both systems while minimizing the disadvantages of the individual systems. Hybrid microfluidics has been emerging over the past decade for a variety of applications such as single cell assays and synthetic biology applications. [161-168] In most of these studies, DMF was integrated with microchannels and is used to control bulk fluid flow or for pre-separation of chemical reactions. Aside from integration with microchannels, there are two groups (to our best knowledge) that have implemented DMF with droplets-in-channel microfluidics. Shih et al. (2015),[163] have created two separate devices and used the droplet microfluidic device for encapsulation of single cells and the DMF device for generating ionic liquid concentrations and analysing their effects on single cells. However, a disadvantage with this system is the configuration of two devices as it is prone to droplet breakup between the interfaces of the droplet microfluidic device with the DMF. In another study by Shih et al.,[168] the DMF is used to mix different DNA parts together to initiate the process of DNA assembly and this mixed droplet was suctioned into the droplet microfluidic region for incubation and transformation. However, the integration of valves has resulted in complicated fabrication and control infrastructure and has

limited the number of droplets that can be stored and analyzed. In Gu et al. (2008),[165] they have implemented electrowetting with microfluidics to control the size and frequency of drop formation while in another study[167] they have implemented a guiding and sorting system of drops. Although both studies are exciting innovations, they do not show multiple sorting or on-demand droplet generation or mixing on the same device.

Moreover, the ideal result of automating functions in DMF is that every set of instructions would equate to a droplet movement (e.g., mix, dispense, split) towards the energized electrode. However, in a DMF device, due to surface heterogeneity or roughness or the contents of the droplet, every application of a potential does not easily translate to a movement on the device. This issue points to the other advantage of hybrid microfluidics over DMF which is limiting DMF applications for any study that includes cells and protein manipulation, as they tend to stick to the surface. This behavior is exacerbated when the droplet constituents contains cells, proteins or other cellular debris, and is known as biofouling.[169, 170]

In the method presented here, we integrated, droplet-in-channel and single-plate DMF configuration for droplet generation, mixing, incubation, and n-ary sorting of droplets.

2.2   ID2M Novelty

In this study, a new multilayer droplet-digital microfluidic method is introduced in which a droplet microfluidic device is mated to a digital microfluidic device below, which we call integrated digital-droplet microfluidics (ID2M). This new configuration has several substantial new developments – (1) there is only one device that does not depend on side-on configurations thereby eliminating the need for vacuum or valve-based techniques for droplet manipulation at the interface. (2) This device enables on-demand droplet mixing enabling control and creation of

different concentration of droplets. Typical droplet-in-channel techniques have depended on fusion[99] or picoinjection[171] methods for mixing but these techniques only allow one reagent addition to an existing droplet and require exquisite control over flow rates, timing, and fluidic resistance. Our device can create a range of different concentrations with multiple additions of reagent droplets by application of an electric potential without any consideration for other parameters. (3) Single plate DMF devices are usually prone to droplet evaporation. This device integration limits evaporation since droplets are in fluorinated oil (commonly used in droplet microfluidics) and are covered with a top-layer PDMS. (4) Droplets are sorted through n different channels (not just two channels) which allow for a range of droplets to be analyzed. In the following, I describe the implementation of this platform and discuss its application in determining the effects of ionic liquid on single yeast cells. This is an important step in the field of digital and droplet microfluidics as this can possibly enable more control for droplet microfluidic devices while increase droplet throughput for digital microfluidic devices.

2.3   Hybrid Microfluidics and Automation

Similar to DMF, hybrid microfluidics also benefits from the amenability to integrating automation systems [172, 173] and coupling the platform to external detectors (or internal in-line detectors [174, 175]) for real-time or downstream biological analysis [176, 177] that is inheriting from its DMF part. The core of automation systems interfaces with a hybrid device which enables droplet manipulation with a standard set of basic instructions written by the user. The user will interact with the graphical user interface (GUI) to program a set of instructions to generate, merge, mix, and sort droplets for analysis. Such automation gives hybrid microfluidics the capacity to control droplets individually and operate in parallel on a single device.

Typically, DMF automation systems rely on an array of relay switches, each of which is responsible for one individual electrode on the device and relays AC or DC voltages to it when instructed. The state of the switches is controlled through a computer and microcontroller. Here in this project, I have exploited a similar automation setup and a graphical user interface (GUI) to what has been previously developed in our lab[178]. This automation system consists of a MATLAB program that is used to control an Arduino Uno microcontroller. Driving input potentials of 130-270 V_{RMS} are generated by amplification of a sine wave output from a function generator operating at 15 kHz by an amplifier and delivered to the PCB control board. The Arduino controls the state of high-voltage relays that are soldered onto the PCB control board. The logic state of an individual solid-state switch is controlled through an I^2C communication protocol by an I/O expander. This control board is mated to a pogo pin interface (104 pins), where each switch delivers a high-voltage potential (or ground) signal to a contact pad on the DMF device. See our GitHub registry (https://github.com/shihmicrolab/Automation) to assemble the hardware and to install the open-source software program to execute the automation system.

In addition to the setup reported in our previous publication,[178] a modular low pressure syringe pump for controlling droplets flow and a flame spectrometer for optical detection are integrated with the system (Figure 2-1). Moreover, to be able to actuate different sequences of electrodes in parallel and with the minimum delay possible, the GUI interface was upgraded to a new version capable of defining multiple sequences with different times of electrode actuation (Figure 2-2). However, the syringe pump and the flame spectrometer have separate user interface and were controlled manually. A detailed description of the automation is presented in the following chapter.
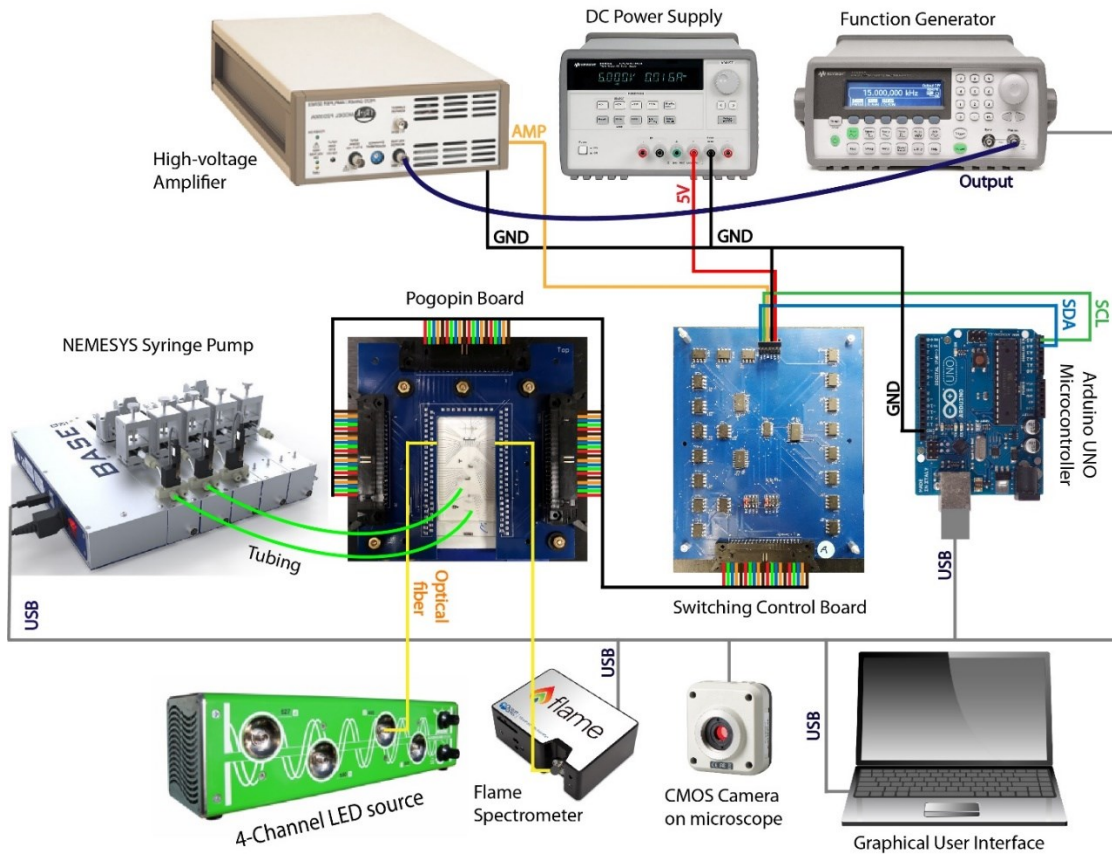
Figure 2-1. ID2M Automation Setup.
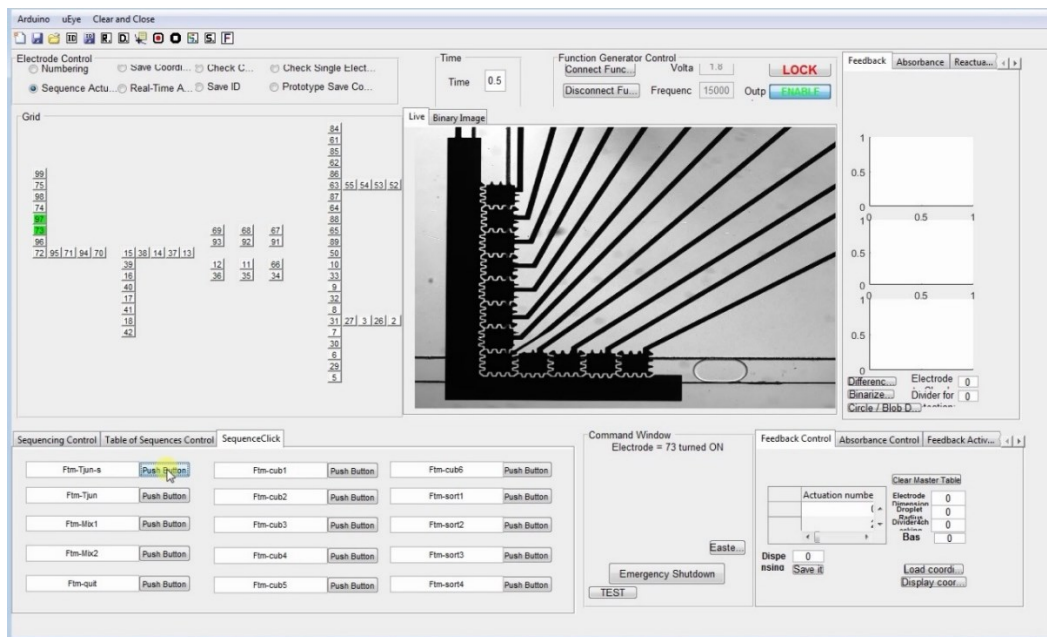
Figure 2-2. Graphical User Interface.

Chapter 3.   Biofuel Production and Thesis Objectives

Here, we review the biological stakes that we will be addressing with our platform, presenting microfluidics screening techniques for analyzing biofuel organism with a special focus on the tolerance of yeast Saccharomyces cerevisiae cells in Imidazolium-Based Ionic Liquids in the context of biofuel production. This commentary will lead to the presentation of my thesis objectives.

3.1   Biofuel Production: Opportunities and Challenges

Over the past two decades, there has been a growing demand for petroleum-derived fuels and the oil supply cannot meet the demand at prices to which the global economy was accustomed (Figure 3-1).[179] Given that other exhaustible sources such as tar sands, shale oil, shale gas, natural gas, and coal have limited reserves and problems with large green-house gas emissions associated with their conversion process, they cannot replace conventional oil. Therefore, there have been many researches demonstrated to investigate the possibility of using biofuels as alternatives. However, replacement of conventional petroleum-derived fuels with biofuels requires production of compounds that have a large capacity and energy density which is the biggest disadvantage in other alternative technologies (e.g. fuel cells, hydrogen, and electricity).[180-182]

Amongst first generation biofuel, ethanol is currently most widely used and is produced from sugar cane, corn or wheat. But it has not fully expanded as an alternative to fossil fuel, because its feedstock is competing with food production and it has contributed to higher food prices and deforestation. Moreover, its low energy content and incompatibility with existing fuel distribution and storage infrastructure has led to a replacement of 1st generation biofuels by 2nd

generation biofuels that are derived from cellulosic biomass. Production of the second generation

biofuels from renewable materials has recently attracted much attention and are expected to

address energy security and climate change concerns, as cellulose is the most abundant and

renewable raw material for producing sustainable biofuels and will not cause food shortage like

ethanol feedstock.

OIL PRODUCTION HITS A CEILING
Production followed demand until 2005, when it levelled off despite continued price increases. There seems to be a production 'cap' at about 75 million barrels per day.
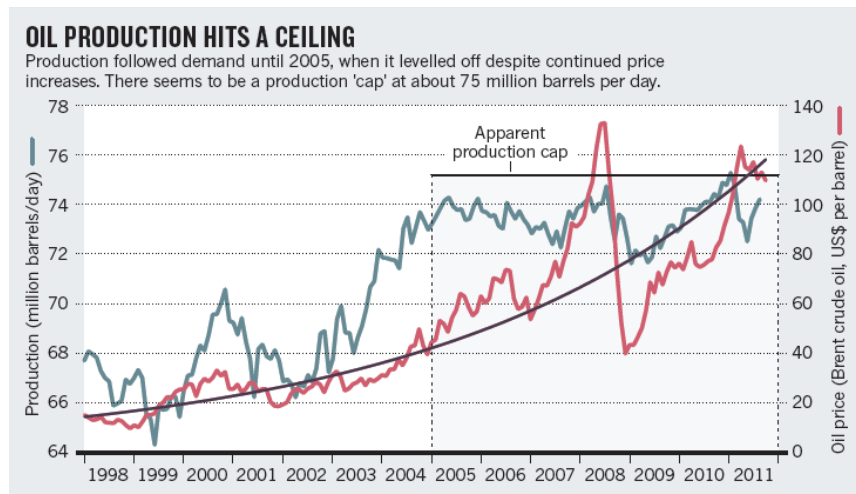
Figure 3-1. Global oil production from 1998 to 2011

Production of crude oil increased along with demand from 1988 to 2005. But after 2005 the production has roughly remained constant for seven years, despite an increase in price of around 15% per year. Adapted from J. Murray et al, 2012. [179]

Generally, bioethanol production from lignocellulosic plant biomass consists of three main

steps: (1) Cellulose pretreatment for enhancing the enzymatic degradation of polysaccharides, (2)

hydrolysis of cellulose to fermentable sugars by cellulases, and (3) ethanol fermentation by

microorganisms, such as yeast (Figure 3-2). [180, 182]

Although cellulosic biomass is a promising material for providing fermentable sugars, it

has a highly crystalline polymer structure in which cellulose chains are tightly packed by

multivalent inter- and intramolecular hydrogen bonding. This crystalline structure makes biomass

recalcitrant to enzymatic digestion, and limits release of cellulosic sugars for fermentation to

biofuels. As a result, several techniques have been developed to pretreat biomass and enhance

disrupting the highly ordered structure of lignocellulose and make the cellulose more accessible to

hydrolytic enzymes.
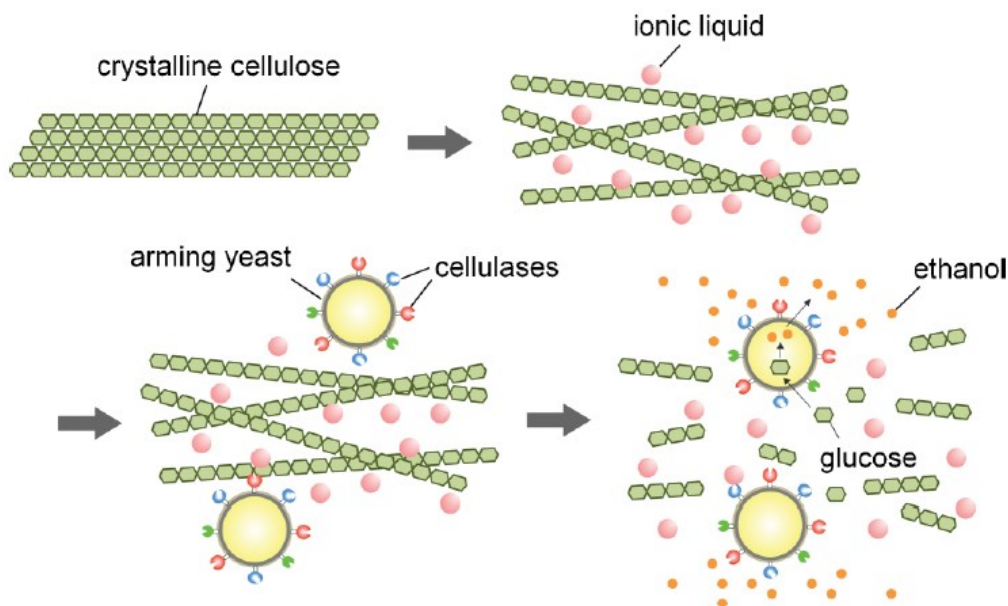
Figure 3-2. Bio-ethanol production yeast from cellulose pretreated with ionic liquid

The functionalized microorganism is called an "arming yeast" because the yeast cell is apparently armed with a number of cellulase enzymes via the cell-wall binding domain as an adhesion moiety. Adapted from K. Nakashima et al, 2011. [181]

Ionic liquids (IL) pretreatment is an emerging pretreatment technology that is found to be

able to dramatically enhance the cellulose degradation and ethanol productivity. Ionic liquids are

neutral salts that have a relatively low melting temperature and attain a liquid state at temperatures

mostly below 100 °C. These solvents have unique properties such as negligible volatility, thermal

stability, and tunable physicochemical properties. Ionic liquids are also reported to be effective in

dissolving various kinds of bio-polymers including cellulose. Cellulose can be easily dissolved in

ILs under moderate conditions (e.g. mostly under 100 °C, or in some cases at room temperature),

and then it can be highly accessible and degradable by cellulase enzymes that hydrolyze it into

monomeric glucose. Imidazolium ionic liquids (IILs) such as 1-ethyl-3-methylimidazolium chloride [C_2C_1im] Cl), 1-ethyl-3-methylimidazolium acetate ([C_2C_1im] [OAc]), and 1-butyl-3-methylimidazolium chloride ([C_4C_1im] Cl) are mostly used in renewable bioenergy applications.[180-182]

However, there are two disadvantages in using IL solvents for biofuel production. They are pretty expensive and they are also toxic to biofuel-producing microbes, including the yeast *Saccharomyces cerevisiae* which is the dominant fermentative yeast and is particularly sensitive to low levels of the most common ILs 30-60 mM [C_2C_1im] Cl).[183-185]

Although there is a washing step following IL pretreatment, but small quantities of residual IL can inhibit fermentative microorganisms downstream. It has been reported that after IL treatment, up to 270 mM IL may persist during fermentation and such concentrations of IILs can severely damage yeast growth and biofuel production.[183, 186]

In a study done by Ouellet et al (2011), it is shown that *S. cerevisiae* growth is highly inhibited by IL concentration of more than 50 mM (Figure 3-3). However, more concentrated IL in pretreatment results is in more ethanol titers.[183] Therefore, in order to achieve higher efficiency in biofuel production, genetically modified yeasts are required to remain viable in the inhibitory IIL concentrations used in cellulose pretreatment.

To generate strains capable of tolerating residual ILs present in treated feedstocks, various approaches have been implemented such as extensive screening library of yeasts to discover more IL-tolerant species or strain [187] and inserting gene sequences from IIL-tolerant microbes into biofuel-producing microbes. Using the latter strategy, Higgins et al (2018), introduced SGE1 mutations into the genome of BY strain by CRISPR/Cas9 and reported a fast growth ($OD_{600} \sim 1.2$ after 48 hr) in SC media containing 125 mM [C_2C_1im] Cl.[188] Dickinson et al, undertook chemical

genomic profiling using a panel of > 4000 yeast non-essential gene deletion strains and analyzed the sensitive mutant genome to find out which protein functionality is affected by $[C_2C_1im]$ Cl.[184]

As described above, several potential advanced techniques have been implemented to produce more resistant biofuel microorganisms. However, to attain the cost-effective commercial production of biofuels, further engineering of the production pathways and the microorganisms themselves is needed. To date, several researches has highlighted the low tolerance of *S. cerevisiae* to $[C_2C_1im]$ [OAc] compared to the other types of ILs. [187, 189]
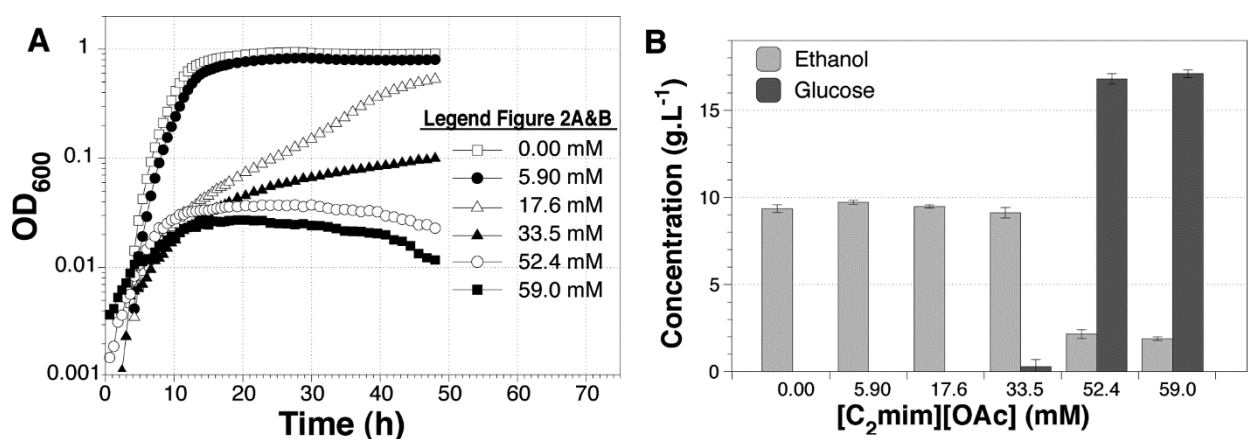
Figure 3-3. Impact of IL pretreated biomass on *S. cerevisiae* growth.

(a) S. cerevisiae growth in 20 g L^{-1} glucose in the presence of [C2mim][OAc] (b) Ethanol titers and final glucose concentration after 72 h of fermentation in 20 g L-1 glucose in presence of [C2mim][OAc]. Adopted from M. Ouellet et al, 2011. [183]

By taking advantage of advanced technologies such as microfluidic devices, it may be possible to screen much larger library of *S. cerevisiae* mutants and isolate the most tolerant ones. Moreover, following the isolation of most tolerant yeast, it will be possible to study the gene sequence responsible for IL-tolerance in yeast genome.

3.2 Droplet microfluidics for biofuel organism screening

Microdroplets (either in microchannels or on DMF) have been widely used for analyzing chemical reactions involving ionic liquids and screening biofuel organisms. [190-192]

Using droplet microfluidics has resolved the limitation of testing a miniscule fraction of biodiversity caused by low throughput screening systems. Najah et al (2014), described an ultra-high-throughput droplet-based microfluidic system that allowed the screening of over 100,000 bacteria without prior cultivation in less than 20 min. They were also able to sort droplets based on cellobiohydrolase activity using DEP. Their results showed ~ 240-fold increase in throughput and a ~250,000-fold decrease in reagent volume compared to state-of the art, robotic microtiter plate screening systems.[193] Kim et al (2015), represented a droplet microfluidics-based microalgae analysis platform capable of measuring both growth and oil content of various microalgal strains with single-cell resolution in a high throughput manner.[194] The same group, later, reported another microfluidics screening platform for selecting fast- growing and high lipid- producing microalgae from a mutant library.[195] In the same vein, Huang et al (2015), performed a high throughput screening of mutant yeast strain libraries, generated by UV mutagenesis using a microfluidic droplet-sorting method for improving protein secretion.[196]

All the above mentioned technologies, although benefit from their high throughput systems, they lack two important features. They do not have individual addressability over each microorganism under study to be able to do further manipulation on the same device and they are only able to do binary sorting. Here, we introduce a novel integrated droplet-digital microfluidics which encompass both above mentioned features.

3.3   Thesis Objectives

To address the challenges described above, we report here a new hybrid microfluidic device for on-demand n-ary sorting of library of microorganisms such as yeasts. We call this new platform an Integrated Droplet-Digital Microfluidics (ID2M) which enables individual control over all necessary functions for a biological assay including droplet generation, mixing, incubation, and sorting. Our ID2M platform is validated by constructing a fluorescein standard curve through n-ary sorting of fluorescein droplets with different concentration. In this study, EMS mutagenesis is accomplished to produce mutant of *Saccharomyces cerevisiae* that can tolerate and grow under high concentrations of a well know Imidazolium ionic liquid. Then, we report the application of ID2M to evaluate the effect of Ionic liquid on two of the most tolerant yeast mutants that can be potential candidates for biofuel production. The results of this work (to our knowledge) are the first to show automated and multiple sorting of droplets that have been applied to sorting mutant yeast libraries. We believe this will serve as a platform for other possibilities like directed evolution or protein engineering applications.

My research was segmented into five steps, described below in chronological order:

1.   ID2M design and fabrication: The device layout was established for on-demand droplet generation, mixing, incubation and sorting for screening the tolerance of the mutant yeast to IL.

2.   ID2M integration and optimization: ID2M was integrated to an optical detection system consisting of a flame spectrometer and optical fibers. Oil and water flow rates were optimized with the actuation voltage to be able to maintain control over droplets.

3.   Platform validation: A fluorescein calibration curve was constructed through making dilutions of fluorescein solution on chip and n-ary sorting of the diluted droplet based on their fluorescent signals into four groups.

4.   Proof-of-Concept: EMS mutagenesis was performed at macro scale on a wild-type yeast strain and different levels of tolerance to IL compared with the wild-type was observed.

5.   Application: To confirm the broad applicability of our platform, we proposed to study the effect of ionic liquid on two of the most tolerant mutants, by performing the whole assay including single cell encapsulation, mixing with IL, incubating droplets and sorting based on the number of cells after 2 days on our ID2M chip.

Chapter 4.   Methodology: Operating the N-ary Sorter System

In this chapter, the methodology for integrating the processes needed for n-ary sorting of biofuel organisms on the ID2M platform is described. Device fabrication, assembly, operation with the automation system, syringe pump and the flame spectroscopy is discussed before reviewing the method for generating an on-chip calibration curve for fluorescein. Finally, the macro-scale experiments that were done for generating ionic liquid tolerant yeast cells and the work flow for on-chip sorting of the generated mutants will be presented.

4.1   Reagents and Materials

1-ethyl-3-methylimidazolium acetate $\geq$ 95 % (HPLC grade), ethyl methanesulfonate, sodium thiosulfate, sodium hydroxide (lab grade), fluorescein (free acid) dye content 95 %, yeast nitrogen base without amino acids and with ammonium sulfate, bovine serum albumin (lyophilized powder) $\geq$ 96 % ,and α-D-Glucose anhydrous 96% were purchased from Sigma, unless specified otherwise. L-Leucine, L-Histidine, L-Methionine, and Uracil were purchased from Bio basic Canada Inc. Yeast BY4741 strains (genotype: MATa his3Δ1 leu2Δ0 met15Δ0 ura3Δ0) were generously donated from Dr. Vincent Martin. 3M Novec HFE7500 engineering fluid was purchased from M.G. Chemicals (Burlington, ON Canada). Aquapel^{TM} was purchased from Aquapel.ca (Lachute, QC Canada). 20 g of 5% wt of fluoro-surfactant dissolved in HFE7500 was purchased from Ran Biotechnologies (Beverly, MA). Sodium phosphate monobasic and sodium phosphate dibasic (Anhydrous, ASC grade) were purchased from BioShop (Burlington, ON).

Microfluidics device fabrication reagents and supplies include chromium coated glass slides with S1811 photoresist from Telic (Valencia, CA), MF-321 positive photoresist developer from Rohm and Haas (Marlborough, MA), CR-4 chromium etchant from OM Group (Cleveland,

OH), and AZ-300T photoresist stripper from AZ Electronic Materials (Somerville, NJ). Polylactic acid (PLA) material for 3D printing were purchased from 3Dshop (Mississauga, ON, Canada). Poly(dimethylsiloxane) (PDMS -- Sylgard 194) was purchased from Krayden Inc. (Westminster, CO). SU8 photoresist and developer were purchased from Microchem (Westborough, MA). Deionized (DI) water had a resistivity of 18 MΩ•cm at 25 °C.

A 100 mM phosphate buffer was prepared by mixing 5.77 mL of 1 M Na_2HPO_4 and 4.23 mL of 1 M NaH_2PO_4 solutions, and the pH was adjusted to 7.0. 5 g of sodium thiosulfate salt was added to deionized water to produce a 5 % (w/v) sodium thiosulfate solution. Fluorescein solutions (0.5 mM) was prepared by adding about 1.66 mg of fluorescein powder (332.3 g/mol) to 10 mL 1 M NaOH solution.

4.2 Device fabrication and operation

4.2.1 Photolithography

ID2M Devices were designed using AutoCAD 2016 and were fabricated in the Concordia cleanroom using a transparent photomask printed at high resolution by CAD/Art Services Inc. (Bandon, OR). The "hybrid" microfluidic chip consisted of three layers: a digital microfluidic, dielectric, and channel layer (Fig. 1). As described previously,[178, 197] the digital microfluidic layer consisted of a bottom glass substrate with chromium and coated with positive photoresist S1811. Electrodes were patterned by UV exposure (5 sec) on a Quintel Q-4000 mask aligner (Neutronix Quintel, Morgan Hill, CA). Exposed substrates were developed in Microposit MF-321 developer (2 min), rinsed with DI water, and post-baked on a hot plate (115°C, 1 min). After photolithography, substrates were etched in chromium (CR-4) etchant (2 min). Finally, the remaining photoresist was stripped in AZ300T (2 min). Next, DMF devices were rinsed by

acetone, isopropanol (IPA), and DI water before coating a SU-8 based dielectric. The device surface was treated with a plasma cleaner (Harrick Plasma PDC-001, Ithaca, NY) for 2 min and then immediately spin-coated (Laurell, North Wales, PA) with SU8-5 photoresist to achieve a thickness of 7 μm (10 s, 500 rpm, 30 s 2000 rpm). The dielectric layer was then soft-baked on hot plate (1. 65 °C, 2 min, 2. 95 °C, 5 min) and exposed to UV light for 5 sec. A post exposure bake (1. 65 °C, 1 min, 2. 95 °C, 1 min) followed by immersing in SU-8 developer (2 min) was performed. After rinsing with IPA and DI water, a hard bake was performed in three steps (1. 65 °C, 2 min, 2. 95 °C, 4 min, 3. 180 °C, 10 min). For the channel layer, devices were cleaned with IPA and DI water prior to plasma cleaning (2 min). Next, SU-8-2075 photoresist was immediately spin-coated (1. 10 s 500 rpm, 2. 30 s 2000 rpm) on the chip and soft-baked at 65°C and 95°C for 3 and 9 min respectively, based on the manufacturer's instructions for 110-120 μm thickness. Following UV exposure (15 sec), devices were post-baked (1. 65 °C, 2 min- 2. 95°C, 7 min) and developed in SU-8 developer for 7 min and rinsed with IPA and DI water. The devices were hard-baked using a three-step procedure (1. 65 °C, 2 min, 2. 95 °C, 4 min, 3. 180 °C, 10 min) to achieve a channel layer with depth ~110-120 μm.

4.2.2   Device sealing and channel treatment

After the layers, hybrid devices were largely completed, except for the final preparation step of PDMS bonding and channel treatment. The hybrid microfluidic chip was bonded to a slab (60 mm x 30 mm) of ~ 0.5 mm thick PDMS (1:10 weight ratio, w/w curing agent to prepolymer). Inlets and outlets that were 0.75 mm in diameter were created using a 0.75 mm puncher (Biopsy Punch, Sklar, West Chester, PA). Before bonding, the PDMS slab was plasma-treated for ~1 min and then it was exposed to (3-aminopropyl)triethoxysilane 99% in a desiccator for 30 min. After treatment, PDMS was immediately bonded to the device and baked at 160 °C for 20 min. Before

operation, channels were treated with Aquapel^TM for ~5 min and rinsed with HFE oil mixed with 0.75% fluoro-surfactant by pipetting. Syringes were prepared with the following fittings and tubing: 1/4-28 to 10-32 PEEK adapter, (10-32) peek union assembly, finger tight micro ferrule 10-32 coned for 1/32" OD, and PEEK tubing (1/32 inch diameter) from IDEX Health & Science, LLC (Oak Harbor, WA). Gastight glass 500 μL-syringes were purchased from Hamilton (Reno, NV) and installed on the neMESYS system (Cetoni, Korbussen, DE).
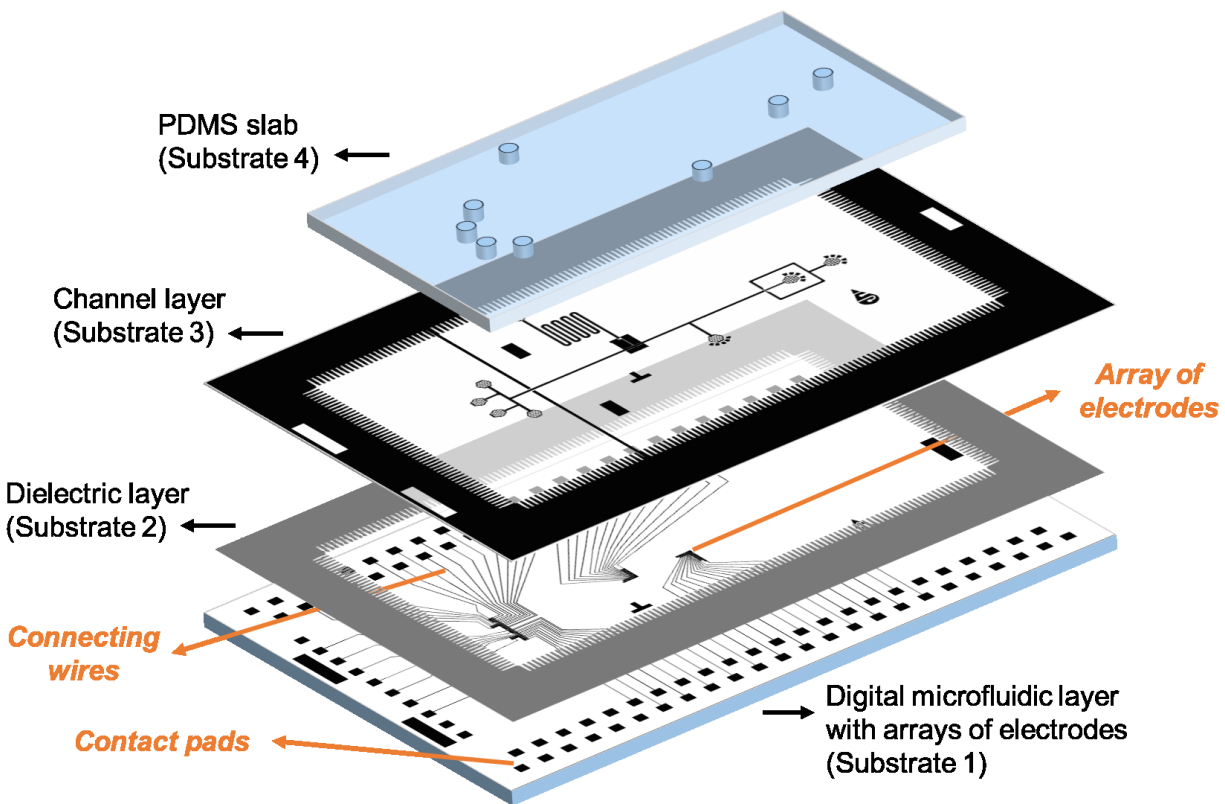
Figure 4-1. ID2M device fabrication.

4.2.3   Device operation

Device operation comprised of five stages: droplet generation by a flow-focusing or T-junction configuration followed by droplet mixing, incubation, detection, and sorting. In the first stage, droplet generation by flow-focusing was implemented by initializing the flow rates using the neMESYS for the aqueous and oil flow rates to 0.0005 [μL/s] and 0.01 [μL/s] respectively.

For the T-junction configuration, droplets were created on-demand through following steps Figure 4-2: (1) the aqueous flow of a second reagent such as water or fluorescein was initialized at 0.0005 [μL/s], (2) when the continuous flow reaches the sixth electrode, an AC voltage (15 kHz, ~200 V_{rms}) was used to drive the flow to the T-junction, (3) electrodes were actuated sequentially (i.e. electrodes are turned on one after another) to drag the fluid to the main channel and finally (4) a ~20 nL droplet is formed by both intersecting the oil phase with flow rate of 0.01 [μL/s] and actuation of electrodes in two different area as shown in Figure 4-2. After on-demand droplet generation, droplets were pressure-driven using the oil phase in the main channel and using actuation sequences to drive the droplet into the mixing region. After mixing the droplet with other droplet constituents, this mixed droplet was actuated to the main channel which followed an incubation step. After incubation, droplets were passed through a detection region which were further sorted by actuation using the optical fiber based sorting region.
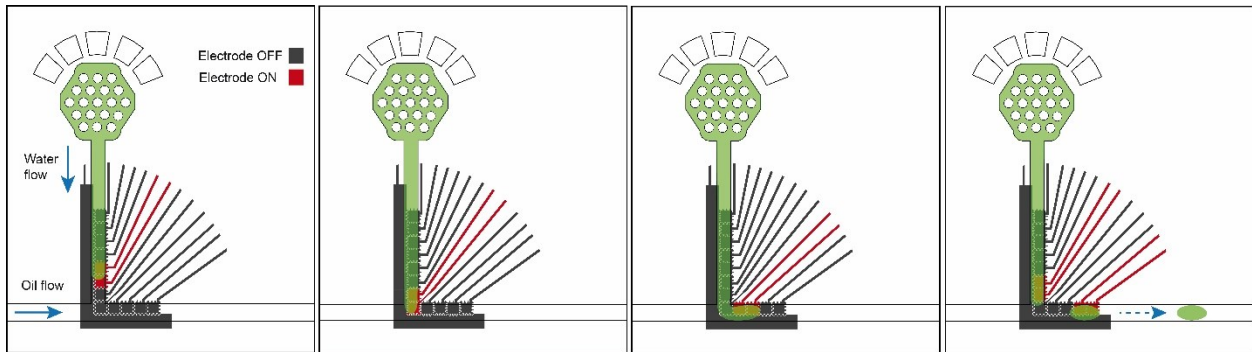

Figure 4-2. On-demand droplet generation with T-junction configuration

Droplet manipulation was controlled by an automated control system in a MATLAB base workspace (Mathworks, Natlick, MA) interfaced to an Arduino Uno for controlling the states of a network of high-voltage relays (AQW216 Panasonic, Digikey, Winnipeg, MB). A neMESYS software interfaced syringe pump software for fluid flow control, and Flame spectrometer (Ocean Optics, Largo, FL) data was collected with the Ocean View spectroscopy software. The 'hybrid' microfluidic chip is mounted on a pogo pin-control board (104 pins) with a 3D printed base platform as reported in our previous paper,[178, 197] and was placed on the stage of an inverted IX-73 Olympus microscope (Olympus Canada, Mississauga, ON). The whole system is imaged live through a CMOS camera. The control board delivered AC signals from a high-voltage amplifier (PZD-700A, Trek Inc., Lockport, NY) paired with a function generator (33201A Agilent, Allied Electronics, Ottawa, ON) to initiate actuation sequences on the device (Figure 4-3).
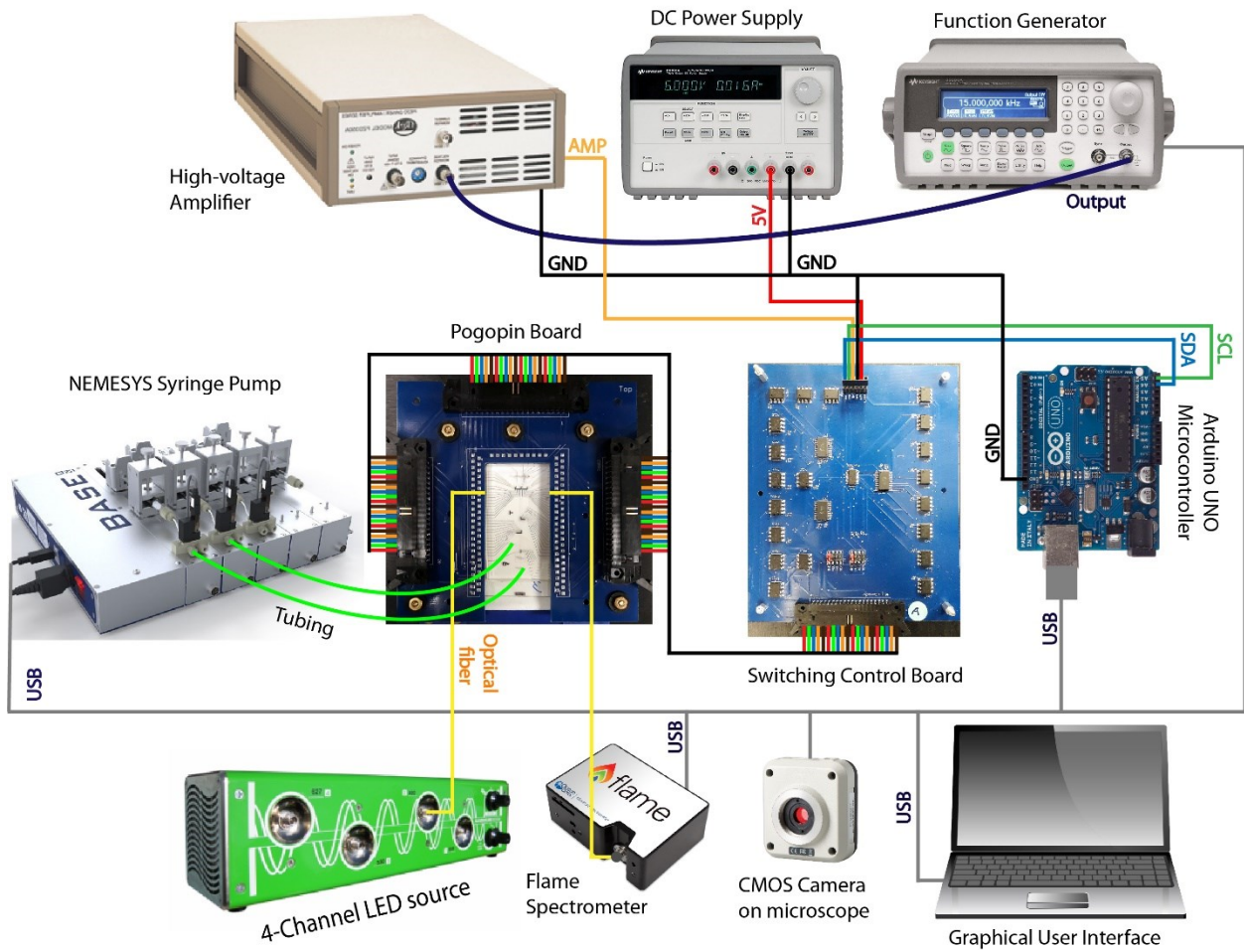
Figure 4-3. ID2M automation system for n-ary sorting.

4.3 ID2M microfluidic optical fiber detection interface

The optical fiber detection interface consists of a Flame spectrometer, two bare fiber (100 μm core) with numerical aperture of 0.22, and a multi-channel LED light sources that contains four high-power (1 mW) LED modules: 470, 530, 590, 627 nm. In each experiment, a hybrid microfluidic device was placed on the pogo-pin holder and two optical fibers were inserted into two fabricated 300 μm channels that was perpendicular to the direction of the fluid flow (see Figure 4-1). On the other ends of the fiber, one fiber was connected to the multi-channel LED source and the other was connected to the Flame spectrometer. These ends were polished carefully using the ocean optics termination kit and fitted with an SMA connector by the help of bare boots for guiding the bare fiber. The distance between the fiber and the channel is ~ 200 μm. All data were collected using the Ocean View spectroscopy software (Ocean Optics, Largo, FL) using the following settings: integration time was set to 100 ms, boxcar smoothing width = 3, number of scans = 5, update rate = 1, and strip chart was enabled to collect data from a single wavelength (530 nm) and executed without stopping.

4.4 On-chip calibration curves – Fluorescein measurement

To generate on-chip calibration curves, a droplet containing fluorescein (1 mM each in 1M NaOH buffer, pH 9) was generated using the flow-focusing configuration with a flow rate of 0.0005 μL/s for fluorescein and 0.01 μL for HFE oil. Next, a droplet of buffer or water (~ 13.5 nL) was generated using the T-junction configuration. These droplets were merged and mixed by moving them across several electrodes. Depending on the concentration, more buffer droplets were added to one fluorescein droplet to create four different concentrations: 1, 0.5, 0.25, and 0.125 mM. After

mixing of the droplets, these were detected by using our optical fiber setup and sorted using the four different on-demand sorting channels.

After collecting the time traces of the recorded signals from the optical fiber detection setup using Ocean View, the peak intensities were recorded for each concentration. The standard deviation was calculated from 20 replicates.

4.5   EMS Mutagenesis and Generating IL Resistant Yeast Strains

Before generating mutants, wild-type *S. cerevisiae* BY4741 yeast cells were stored on agar plates containing synthetic defined medium (6.8 yeast nitrogen base without amino acids, 20 g agar, 20 g 2% glucose, 20 g methionine, 20 g histidine, 20 g uracil, 120 g leucine) at 4 °C. To initiate mutagenesis, the cells were induced using ethyl methanesulfonate (EMS) according to Winston's protocol.[198] For mutagenesis, wild-type yeast was grown in 50 mL of synthetic defined medium in an Erlenmeyer flask at 30 °C with shaking at 200 rpm for 48 hours. Then, aliquots of 2×10^8 yeast cells measured on the basis of the optical density (O.D.) at 600 nm was transferred to four micro-centrifuge tubes corresponding to technical triplicate and one control sample. The cells were washed two times in 1 mL phosphate buffered saline (PBS) and a single time in 1 mL sodium phosphate buffer (SPB) (0.1 M- pH 7.0). After centrifugation, the pellets were re-suspended in 1.5 mL SPB. Four 15mL Falcon tubes (corresponding to three different EMS treatment time) were filled with 1 mL SPB and 0.7 mL cell solution of each micro-centrifuge tube. 50 µL of EMS was added to three of the 15 mL falcon tubes in a biological safety cabinet. One falcon tubes related to the control sample were kept without EMS addition. All tubes were incubated at 30 °C on a shaker (200 rpm) for 30 min. The EMS mutagenesis experiment was repeated for 40, 50, 60, 75, and 90 min. Mutagenesis was stopped by adding 8 mL of 5 % (w/v) sterile sodium thiosulfate

(STS) solution at each time point. 1 mL aliquots of each falcon tubes were added to a micro-centrifuge tube and were diluted 1000 times with SD media. 200 μL of the final dilution of the yeast cells suspensions was inoculated to solid SD plates at each time point. The plates were sealed with parafilm and incubated at 30 °C for colony formation for 48 h. Cell viability was measured by counting the number of colonies and at each EMS time point it was compared to the wild-type cells (Figure 4-4).

EMS Treatment time Vs. Viability

$y = 267.93e^{-0.058x}$

$R^2 = 0.9482$

Cell Viability (%)

EMS treatment time (min)
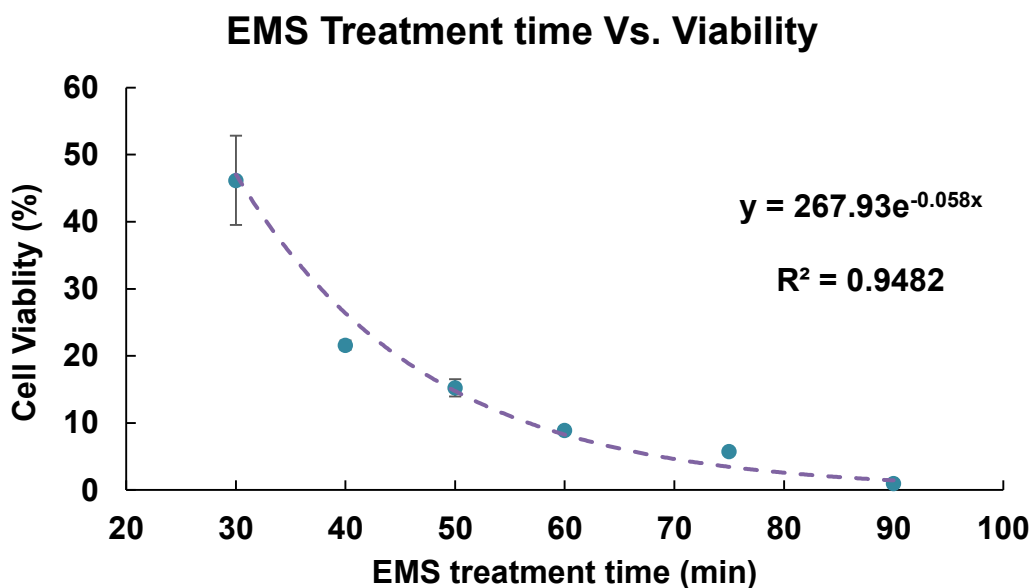
Figure 4-4. Cell viability measurement in different EMS treatment time

Yeast viability changes during mutagenesis induced by EMS shaker at 30°C and 200 rpm. Standard deviations are indicated in the graph by bars.

To increase the yeast tolerance to 1-ethyl-3-methylimidazolium acetate, successive cultures of BY4741 mutants were stored in SD media supplemented with increasing IL concentrations.

After mutagenesis, random colonies were picked from the plates of the mutants at different EMS time point (60, 75, 90 min) and were added to a sterile test tube containing 5 mL synthetic

defined medium and 50, 75, 100 mM 1-ethyl-3-methylimidazolium acetate IL. Test tubes were incubated for 24 h at 30 °C on a shaker with 200 rpm. Then, a 1 mL aliquots of each test tubes along with a wild-type sample were diluted 100 times with SD media and then were plated onto several solid SD plates containing 50, 75, 100 mM IL. These plates were sealed in sterile bags and incubated for 4-6 days at 30 °C. Colonies were randomly selected from the plates and cultured in 5 mL SD media at 30 °C. After 24 h, we measured the OD of the culture and if the OD was greater than 0.3, samples were diluted and cultured in different ionic liquid conditions otherwise they were discarded. An aliquot (depending on IL concentration) from the 5 mL was added to the wells of a microwell plate to make up a final volume of 200 μL. In each well, the OD was measured every 20 min at 30 °C with shaking at 200 rpm for 48 hours using a Tecan Sunrise microplate reader (Tecan, Salzburg, Austria). Three replicates were measured for each condition.

4.6   N-ary Sorting of Yeast Mutants library on ID2M Device

For analyzing the effect of IL on wild-type and mutant yeast on chip, two best performing IL tolerant mutant and wild-type yeast were selected and cultured them in regular SD (see EMS mutagenesis protocol in previous section) without IL for 48 hours. For single cell encapsulation, Poisson distribution (Equation 1-2 and Equation 1-3) was used to calculate the cell density that we must have in 1 ml of the primary cell suspension. Given that the average volume of droplets generated in our chip was 1.32×10^{-2} μL, and out of three droplets we wanted to have one that contains a single cell (i.e. $\lambda=3$), the primary cell culture (with 2×10^8 cells based on OD_{600} measurement) was diluted 1000 times with 1 mL SD media containing 1% bovine serum albumin (BSA) which is used as a surfactant. Using our neMESYS syringe pump, the diluted cell suspension with HFE oil containing 2 % fluorinated surfactant were pumped into the ID2M device.

Cell encapsulation was performed through the flow focusing droplet formation with flow rates of 0.0008 µL/sec and 0.01 µL/sec for cell media and oil, respectively. Using the other inlet on the device and the T-Junction droplet generator, droplets of 100mM IL were formed on demand.

Droplets containing a single cell actuated into the mixing channel by sequentially applying electric potential to the electrodes. After trapping the single cell-encapsulated droplet, a second droplet of IL was directed to the mixing channel and two droplets were merged and mixed. Upon mixing the droplet with a 100 mM IL, the droplet was trapped into incubation slot using actuation. This process was repeated for three other incubation regions. After trapping all four droplets, the ID2M device was removed from the automation system and droplets were incubated for 48 h on a hot plate at 30 °C using a humidified chamber. After incubation, droplets were pulled back to the main channel and passed through the optical detection area where the two optical fibers are placed perpendicular to the main channel. According to the absorbance peaks differences, droplets were sorted into three groups using the three sorting channels. Any excess droplets in this procedure was actuated to the waste channel.

4.7   COMSOL simulation

To investigate the flow velocity and the flow circulation of the filler media (i.e. oil in our system) in the mixing area with the sinking channels, we performed a simulation using COMSOL Multiphysics V5.3 (COMSOL Inc., Cambridge, MA, USA) with the following parameters (Table 4.1) and with the following assumptions for simplification: 1) fluid is Newtonian, 2) no-slip boundary condition, and 3) the flow in the microfluidic channel is incompressible. To generate a 2D model, a CAD file showing the mixing region of ID2M device was imported to COMSOL with the same geometry and feature size. A single phase laminar flow using Navier Stokes model

(equation 4-1) was selected as the physics of our stationary study with the assumption that our fluid is 3M™ Novec™ 7100 Engineered Fluid. We used quadratic meshes. Wall boundaries and inlet and outlet were defined as depicted in Figure 4-5. The inlet velocity of the fluid flow was initialized to 0.033 ms^{-1} and the channel fluid flow was computed and a velocity magnitude plot was generated for the main and sinking channels along with the filtering regions. A pressure contour plot was also generated.

Equation 4-1: Navier-Stokes with continuity equation

$$\rho \left(\frac{\partial u}{\partial t} + u.\nabla u\right) = -\nabla p + \mu\nabla^2 u + F$$

$$(\partial\rho/\partial t + \nabla.(\rho u) = 0)$$

where u is the fluid velocity, p is the fluid pressure, ρ is the fluid density, and μ is the fluid dynamic viscosity. These equations are always solved together with the continuity equation. The first term in the equation corresponds to the inertial forces. However, in microfluidics, the effects of the inertial forces are negligible compared to the viscous forces; thereby, it can be neglected in the previous equation. The second and the third term corresponds to the pressure gradient inside the channel and the viscous forces, respectively. Last term represents the external forces applied to the fluid.

Table 4.1. Simulation parameter

| Parameter	Value	unit
Oil density (ρ)	1614	Kg.m^{-3}
dynamic viscosity (μ)	0.00124	Pa.s
Inlet velocity (u_0)	0.033	m.s^{-1}
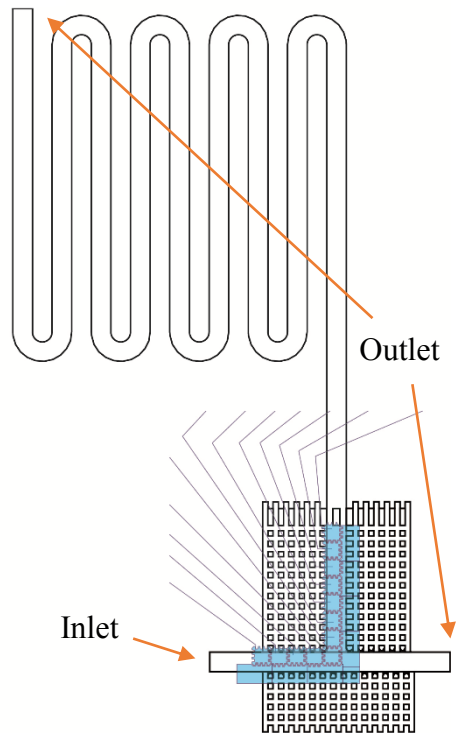
Figure 4-5. Imported CAD design with the boundary conditions.

Chapter 5.   Validation of the ID2M platform

This chapter consists of my results and discussion. Three steps were involved in developing the ID2M platform. First, device characterization and optimization was essential to produce the ID2M platform for n-ary sorting. Next, the ID2M platform was validated as a robust on-demand sorting system by multiple sorting of fluorescein droplets of different concentrations. Finally, the ID2M platform was demonstrated to hold promise in screening a library of yeast mutants with an ultimate goal of discovering the most tolerant mutant to IL.

5.1   ID2M Design: Device Characterization and Optimization

We have developed a new architecture mating droplet microfluidics (useful for generating and sorting droplets) to digital microfluidics (useful for on-demand droplet manipulation and individual control). The new ID2M device were formed by creating a single-plate DMF device (i.e. the ground and driving electrodes are on the same plane) and fabricating a network of channels consisting of inlets and outlets for generating and sorting droplets respectively and an area for droplet mixing. An exploded view is shown in Figure 4-1, as depicted, the digital microfluidic device is defined by the bottom substrates that consists of 104 patterned electrodes, the dielectric layer (substrate 1 and 2), the network of channels which is defined by a SU-8 fabricated layer, and a slab of PDMS with inlets and outlets (substrates 3 and 4). This new multilayer integrated architecture facilitates pressure-based and on-demand droplet generation using flow focusing and T-junction configurations, droplet mixing, and droplet incubation and sorting. This represents a significant advantage over other types of droplet-to-digital methods which relied on two separate design configurations (which can cause difficulties in moving the droplet from one platform to the other).[161-163, 168]

The new device was designed such that the two microfluidic paradigms are stacked together – pressure based oil flow to move the droplets in the main channel and electrostatic droplet movement to the mixing, incubation, and sorting regions (i.e. away from the main channel). As shown in Figure 5-1, the main channel is highlighted in red in which normal operation starts with droplet generation using flow-focusing techniques. Next, this droplet is actuated away from the main channel and moved to the mixing area to merge with other droplets. For example, a droplet containing dilution buffer is generated on-demand via actuation from the T-junction, actuated to the mixing area, and merged and mixed with the former droplet to create a droplet of different concentration. After generating the concentration of interest, these droplets can be actuated to the main channel and can be stored in the incubation pockets and eventually n-ary sorted in one of the channels using electrostatic actuation. Droplets containing analytes or proteins are manipulated without the addition of Pluronics or any other surfactant that is typically added to the droplets for digital microfluidic operation.[169, 199] Furthermore, the droplets are manipulated without pressure- or valve-based control (which is main driving force for manipulating droplets in droplet microfluidics), they are manipulated by application of electric potential allowing individual addressability of the droplets. There are groups who have demonstrated the addition of electrodes in devices containing microchannels. In these studies, the electrodes are used to direct bulk fluid flow [164] or to form liquid channels.[200, 201] In this work, the electrodes are used to provide direct droplet control for droplet generation, mixing, and sorting for droplet microfluidic systems that are usually dependent on tuning input flow rates.
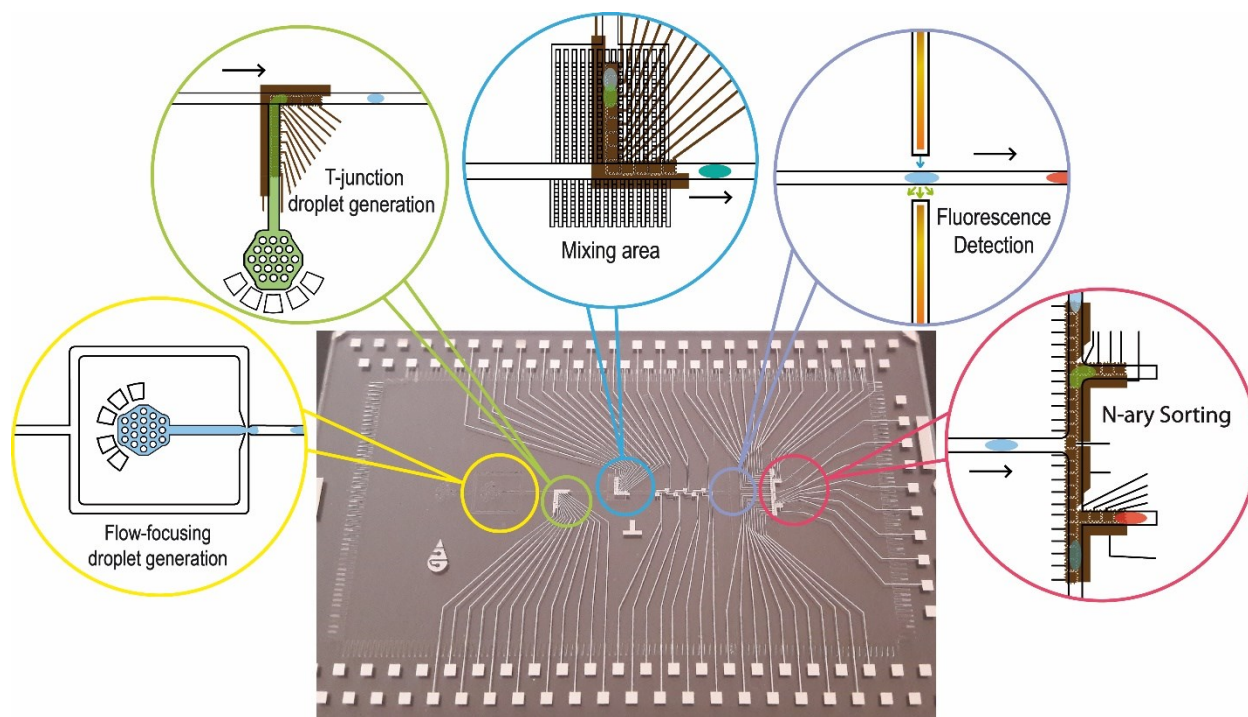
Figure 5-1. ID2M device operation.

A photo of the device with schematics depicting the operations of the device, namely droplet dispensing (using T-junction and flow focusing), droplet mixing, droplet incubation, droplet detection, and droplet n-ary sorting.

As shown in Figure 5-1, the central feature of this device is the incorporation of electrodes for droplet manipulation without the dependence of tuning input flow rates. Thus, in this scheme, droplets are manipulated on demand in the regions that require specific operations – i.e. generation, mixing, incubation, and sorting. In initial electrode designs, we followed the one-electrode design on the bottom plate with alternating ground and driving potentials. [166, 201] However, droplets in the main channel are not able to overcome the pressure generated from the oil flow rate and be actuated into the mixing, incubation, or sorting regions. The coplanar electrode configuration with overlapping regions, as shown by some groups, [202-204] showed optimal operation as droplets are easily actuated into the region of interest on the device. The introduction of a grounding electrode or to a grounding electrode line may not be able to generate the highest applied force as compared

to other electrode designs, [202] but the selected design is easiest to fabricate and is capable to overcome the applied pressure on the droplet (i.e. the oil flow rate) in our system (which are generally 0.0005 – 0.05 µL/s).

In initial work, the design and fabrication protocol for the ID2M devices was optimized to address two challenges: adhesion of the dielectric, channel, and PDMS layers during fabrication and to ensure droplets can be controlled by application of electric potentials in the in the mixing area. For the former challenge, we found that introducing finger-like structures on the boundary of the layer to prevent peeling from the substrate (Figure 5-2). In initial fabrication procedures, we found that if each layer did not have these finger-like structures, the layer will start to peel or crack and remove features from the layer below during the process of hard-baking. These cracks are mostly made by internal stresses. High evaporation and heating/cooling rate in addition to temperature difference in different layers of SU8-5 causes residual stresses in the layer.[205] Adding finger-like structures gives more flexibility to the layer to bear the temperature difference and also a bigger perimeter for evaporation and releasing the developer's vapor.
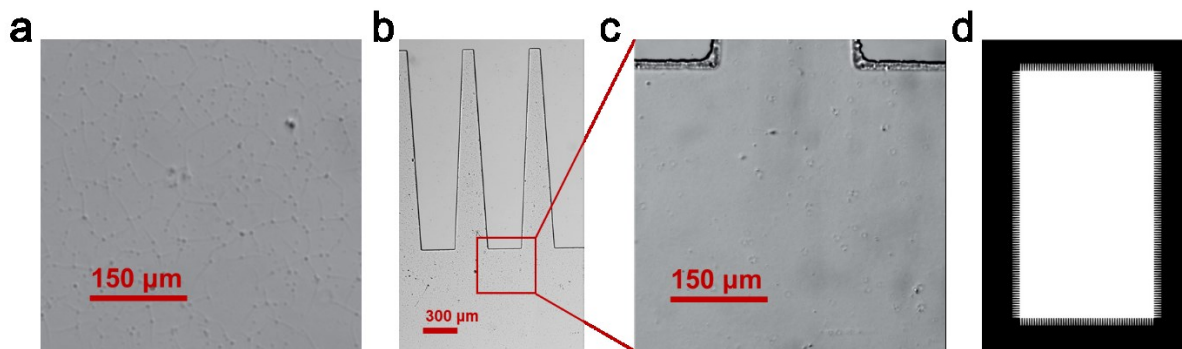

Figure 5-2. Finger-like structures on the boundary of the negative resist layer.

(a) Very small cracks distributed in the resist layer fabricated with the mask without fingers, (b) and (c) 10X and 20X image of the same layer fabricated with mask design with fingers d) Mask design with finger-like boundaries.

In the final design, each of the layers contained 300 μm repeated finger structures on the boundary to ensure stability of the layers during the hard bake process.

In addition, for increasing the adhesion of the PDMS slab to the SU-8 layer, we tried a previously established method using (3-aminopropyl)triethoxysilane (APTES). [206] After plasma treatment of the PDMS, the slab were exposed to the vapor of APTES in a desiccator for 30 min. So the -NH2 group from the APTES molecule on the plasma activated PDMS surface reacted with the epoxy group from the SU-8 surface. A strong bonding was achieved between PDMS and SU-8 layer. For the latter challenge, we found that adding sinking channels in the mixing area is necessary to slow down the flow rate and to enable droplets to be actuated from the main channel to the mixing area. In our initial designs, we created a side channel (i.e. a channel branching out of the main channel) with the co-planar electrodes; however, droplets were not capable to be moved by actuation from the main channel. We explored increasing the voltage [207]; however the higher voltage tend to cause dielectric breakdown in the oil phase.
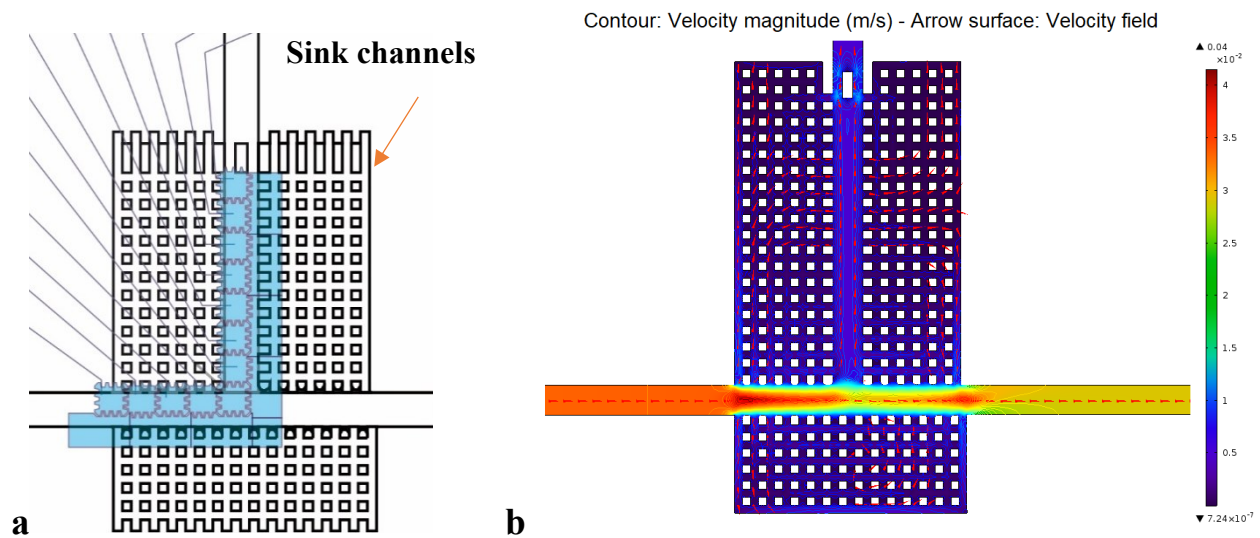

Figure 5-3. COMSOL simulation - Mixing channel design.

(a) Schematic of the multiple sink channels in mixing area (b) COMSOL Simulation of the oil flow velocity in the mixing area, indicating a visible decrease in its velocity.
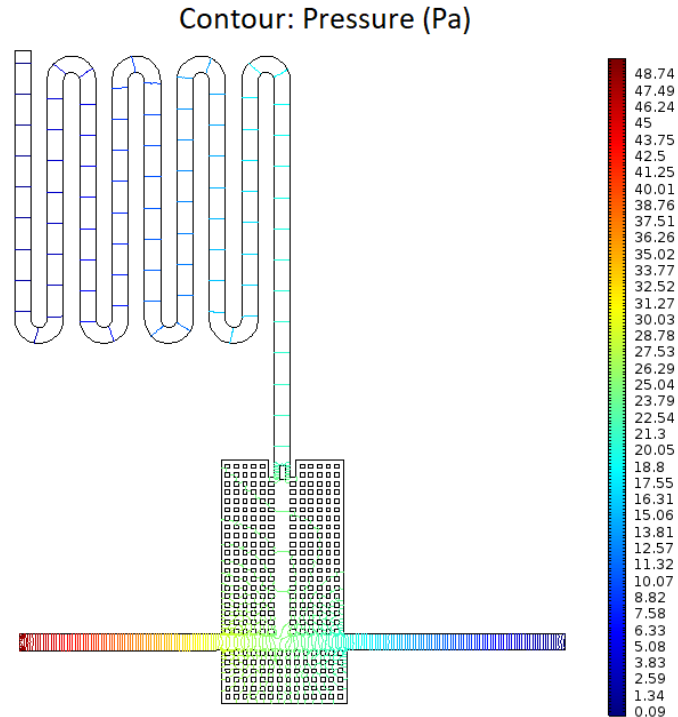
Figure 5-4. COMSOL simulation - Pressure contour in sinking channels.

We added multiple sink channels [208] to create flow eddies from the main flow channel which allow the oil phase to have multiple flow paths (Figure 5-3 and Figure 5-4). This reduction in oil flow rate enables droplets in the main channel to be actuated into the mixing channel. The sink channels are particularly important when a droplet is already in the mixing area since the droplet acts as a plug (i.e. increase the hydrodynamic resistance).[209] Since the hydrodynamic resistance in the mixing channel is higher than the main channel when a droplet is present, the generated droplets favour flow in the main channel. Alternatively, having multiple sink channels, this reduces the resistance in the mixing channel, leading to mixing of the droplets in this area.

An additional challenge for device operation was optimization of the configuration of the n-ary sorting channels. Sorting in droplet microfluidics typically follows a Y-shaped configuration,[60, 210] in which droplets are discriminated by two physical characteristics. There has

been interest in sorting droplets in additional states (i.e. more than two states) since this can expand the range of droplets being detected and analyzed. [123, 211, 212] However, Y-channels have a tendency to create a stagnation zone (i.e. an area where the droplet faces an uncontrolled choice for an outlet) and biases like asymmetric presence of drops (creating different resistances) when it is expanded to more than two channels. [213] In response to this challenge, we adapted a different strategy that enable multiple sorting (i.e. n-ary) possibilities. Instead of Y-shaped channels, we designed a symmetrical T-channel that consists of four different sorting areas. Pressure-driven droplets are detected using the optical interface and flow toward the sorting region which are actuated to their respective channel for collection. In the future, we may design rails [214] or linear electrodes [200] with the symmetric T-channels to reduce the footprint and to increase the number of sorting channels.

5.2   Proof-of-Concept: On-chip calibration

The unique system that we have reported here makes it straightforward to integrate sample processing with incubation and n-ary sorting. As shown in Figure 5-5, droplets can be generated through flow-focusing geometry or by on-demand generation using T-junction (frame 1 and 2), stored (frame 3-I), merged (frame 3-II), mixed (frame 3-III), incubated (frame 4), and sorted (frame 5). We investigated the relation between the droplet size and the oil flow rate at a constant flow rate of water (Figure 5-6). In the hydrodynamic mode, droplet size decreases with increasing the oil flow rate, as expected, due to a bigger shear force cause by the liquid flow. However, in the electrically controlled droplet generation, as we increase the oil flow rate, due to the presence of the electric field, droplet will be hold in the place and stretched instead of breaking at the corner point of the T-juntion channel, resulting in a larger droplet.

Mixing and sorting are particularly useful capabilities, as most droplet microfluidic systems are incapable of generating dilutions of droplets and sorting them into multiple channels. In the design reported here, after droplet generation, droplets can be actuated to the mixing area and merged with another droplet (Figure 5-5, frame 3) and transferred to the main channel area for sorting and analysis (Figure 5-5, frame 5). To illustrate this, we used this method to generate calibration standards on this platform with sorting analysis.
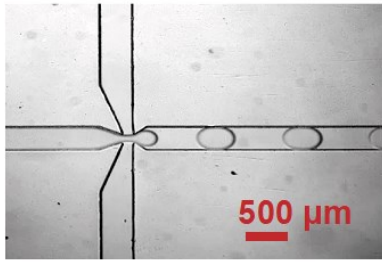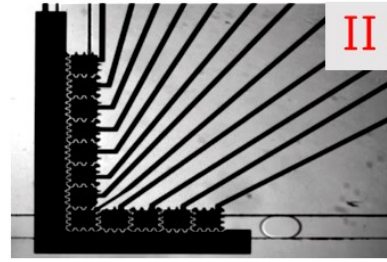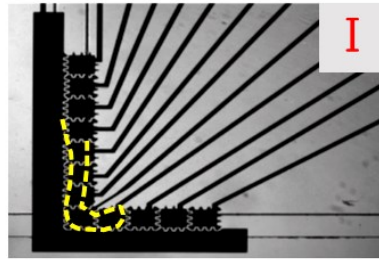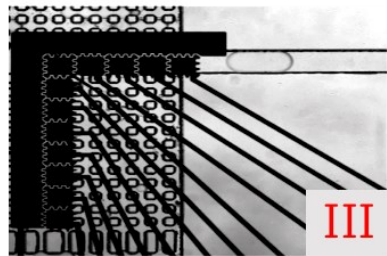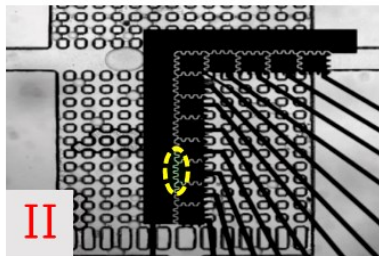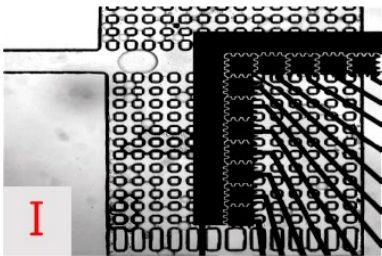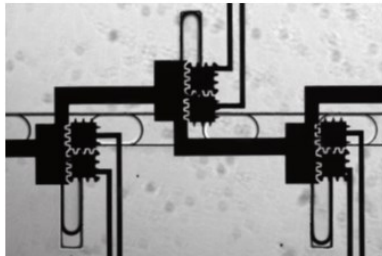
Figure 5-5. Device operation for sorting fluorescein droplets of different concentrations.

Frame (1) and (2) illustrates droplet formation in a hydrodynamic and on-demand fashion. Frame (3) shows the mixing process of two droplets in three steps. Frame (4) displays incubation station and Frame (5) shows two of the channels for n-ary sorting
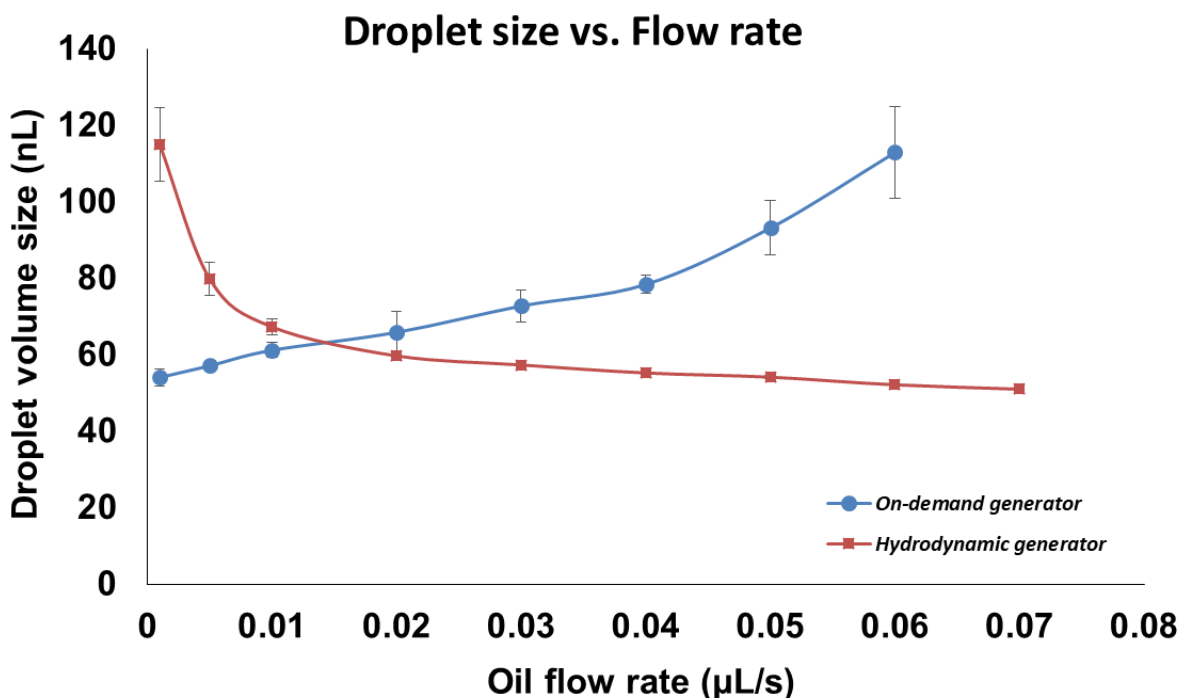
Figure 5-6. Droplet size versus oil flow rate at a constant water flow rate.

Droplet size varies with oil flow rate at both on-demand and hydrodynamic mode enabling generation of droplets with various sizes.

Dilutions were formed by merging a droplet containing analyte (fluorescein) with a droplet of diluent (buffer). This merged droplet was mixed (by moving the merged droplet in a linear pattern – up-and-down – for several seconds [215]) producing a droplet with a 2x dilution of analyte. This droplet was analyzed by optical detection (Figure 5-7) and sorted for further processing. Subsequent droplets of analyte with different concentrations (4x and 8x) followed the similar protocol except the droplet containing fluorescein was mixed with two, three, or four droplets of diluent respectively (Figure 5-8). Note that this type of process, which includes on-demand droplet generation and mixing to create different droplets of different concentration of analytes was only made possible with the integration of digital microfluidics. Such operations were not possible with typical droplet microfluidic platforms unless we increase the number of inlets and injectors or

reinject droplets into the device.[114] The devices used in this experiment were done in droplet-in-channels with minimal inlets, which allowed for a maximum 8x dilution of stock analyte. In the future, more dilutions could be implemented or mixing different types of analytes could be implemented by using these devices.
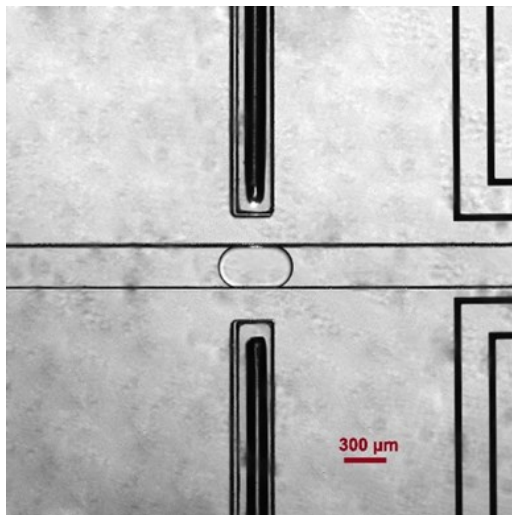
Figure 5-7. The integrated optical detection system.

Two optical fiber were place inside the same channel perpendicular to the main fluid channel.
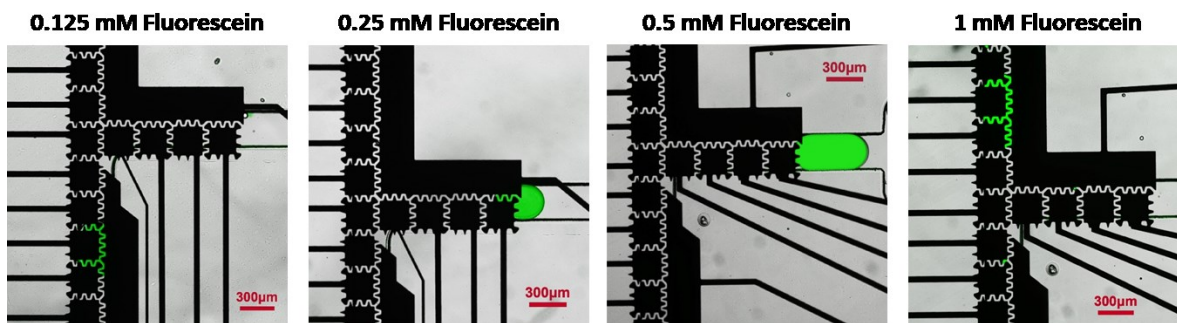
Figure 5-8. N-ary sorting of fluorescein droplets with different concentrations.

Figure 5-9 summarizes the results from this experiment with fluorescein. As the droplets pass the optical fiber setup, the emitted fluorescence from the droplet was detected by the

spectrometer which outputted arbitrary units proportional to the emitted fluorescence of the droplet. As shown in Figure 5-9, the yellow curve depicts droplets that have minimal emitted fluorescence (i.e. droplets of diluent without fluorescein). The blue curve shows the fluorescence intensity for different concentration of fluorescein.

As expected, the highest fluorescein concentration (1 mM) showed the highest signal with a sorting threshold ~1900 arbitrary units and the lower fluorescein concentration (0.125 mM) showed the lowest signal with a threshold of ~ 700.
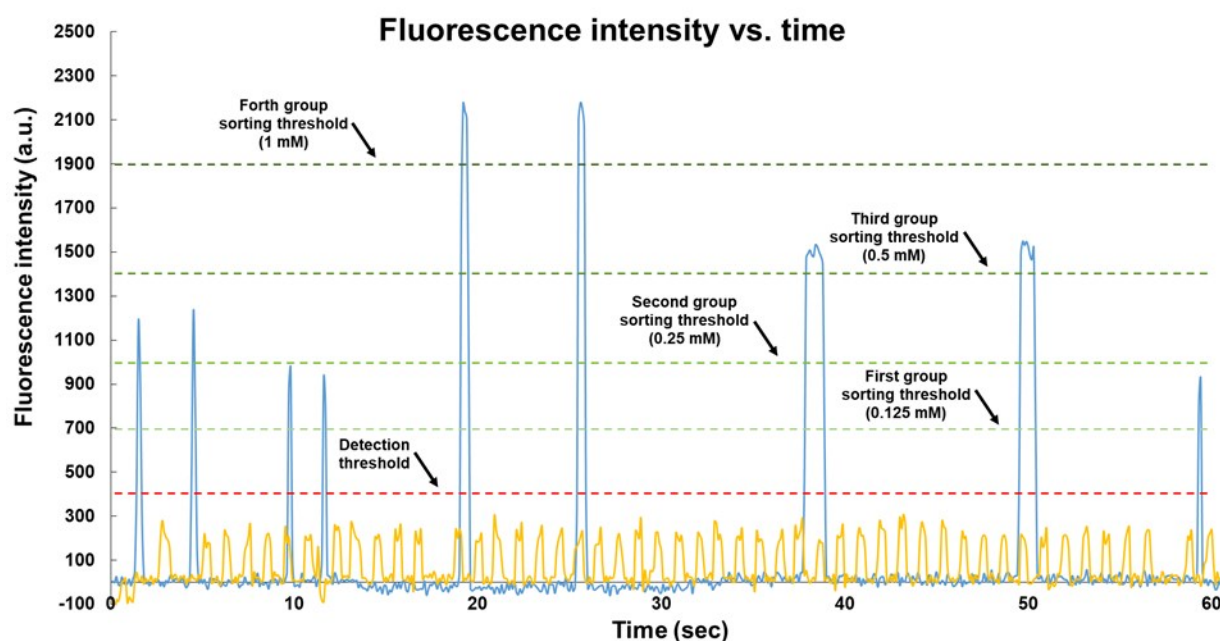
Figure 5-9. Fluorescence intensity of individual droplets during microfluidic sorting.

A calibration curve (N = 10) was generated by plotting the ratio of analyte peak intensity as a function of analyte concentration (Figure 5-10). The precision in each measurement (RSD = 3.2%, 4.6 %, 7.5%, and 10.7% for the stock, 2x, 4x, and 8x dilution, respectively) and the correlation coefficient (R^2 = 0.99) demonstrates that the method is reproducible and linear. Furthermore, we measured the sorting efficiency by sorting positive-fluorescein (1 mM) vs.

negative-fluorescein droplets and obtained ~96 % efficiency for positive bright which is similar to other reported sorting efficiencies. Errors in sorting mostly arised by droplet breakage in the entrance of two neighbor channels. In addition, manual actuation of the related sorting electrodes with delay, was another issue causing the false results, as the actuation was not automated and integrated with the detection system to be done precisely on time.
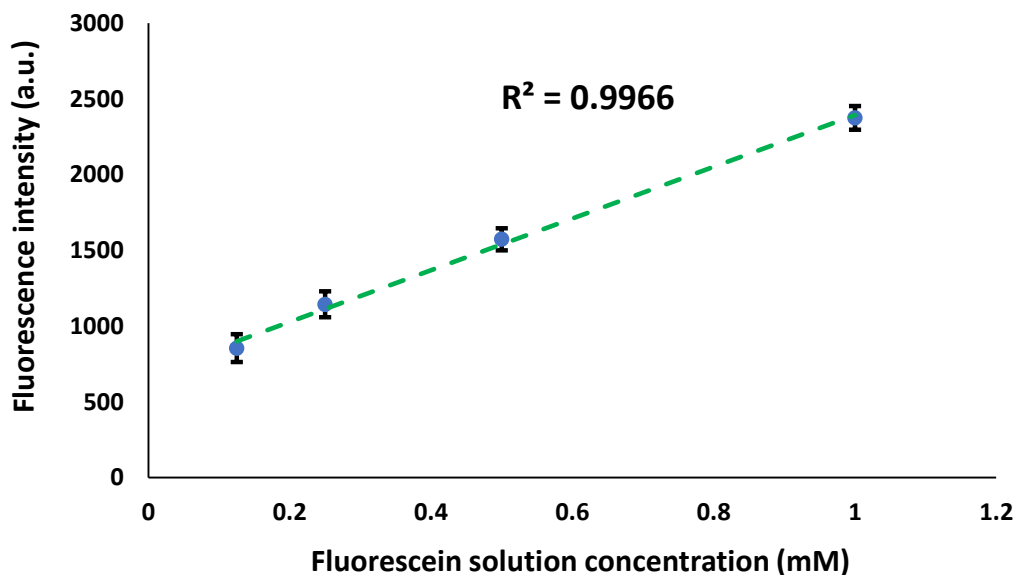
Figure 5-10. Fluorescein standard curve constructed on ID2M.

5.3   Application: Studying the Effect of IL on Two Yeast Mutants

As an application of this work, we examined the effects of ionic liquid (IL) on wild-type and mutant yeast cells. Ionic liquid has been used as a promising pretreatment method for breaking down polysaccharides from typical feedstocks (e.g., lignin). After this treatment, the polysaccharides are easier to be taken up by micro-organisms, for sustainable production of renewable biofuels. [216, 217] Typically, there has been a wide range of available ILs that are suitable for effectively breaking down the required biomass. [183, 218] However, a major disadvantage with current commonly used ILs (especially imidazolium ILs) is their inherent microbial toxicity which can either arrest growth of microbial cells, like *E.coli or S. cerevisiae*, or inhibit biofuel-related enzymes which can reduce the overall yield of biofuel production. [185, 219] Hence, there is much interest in investigating the mechanisms of tolerance for microbes to different levels of IL.

Here, we compare the effects of IL on wild-type and mutant yeast cells and show the ability to interrogate each cell type with different IL concentrations and to sort cells based on their growth differences. To our best knowledge, this is the first time that micro-organisms have been selected for ionic liquid resistance on-chip, by culturing, mixing with ionic liquid and sorting based on multiple conditions (i.e. not binary). As a first step, we performed a mutagenesis of *S. cerevisiae* BY4748 (via ethyl methylsulfonate treatment) and verified growth rates under different IL concentrations (Figure 5-11). Wild-type and the two mutants that have higher IL tolerance are chosen to be used for further on-chip testing. The strains were then cultured with and without 100 mM ionic liquid. As shown in Figure 5-12, both mutant cells showed higher growth rate (~1.7 and ~2.6 cells per hour for mutant #1 and mutant #2, respectively) compared to the wild-type yeast growth rate (very minimal) during the 48 hours incubation in 100 mM ionic liquid. In fact, the wild-type cells exhibited virtually no detectable growth in ionic liquid conditions. When the wild

type cells were cultured without ionic liquid, it showed faster rates than both mutant cells. We hypothesize that mutations related to this tolerance could be due to mutations in areas that are related to efflux pumps (i.e. to bring IL in-and-out of the cells) [220] and to transcriptional regulators that are related to stabilizing stress response.[221]
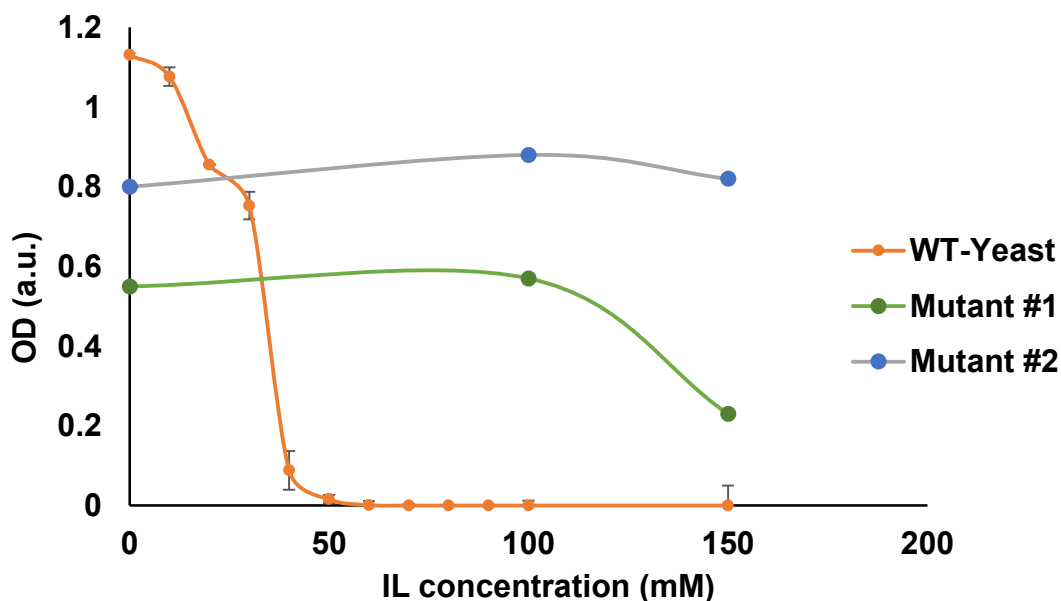
Figure 5-11. Wild-type and mutant yeast growth in SD media containing IL.

Wild-type and two mutant yeast growth based on OD_{600} measurement after 45 hours incubation at 30°C in SD media containing different concentrations of IL.

Clearly, more work is required to determine the location of the mutations using a whole-genome sequencing and a bioinformatics analysis comparing all mutants and wild-types, [196] but this experiment confirmed that we are capable of obtaining three different strains that will be used to show the utility of our device.
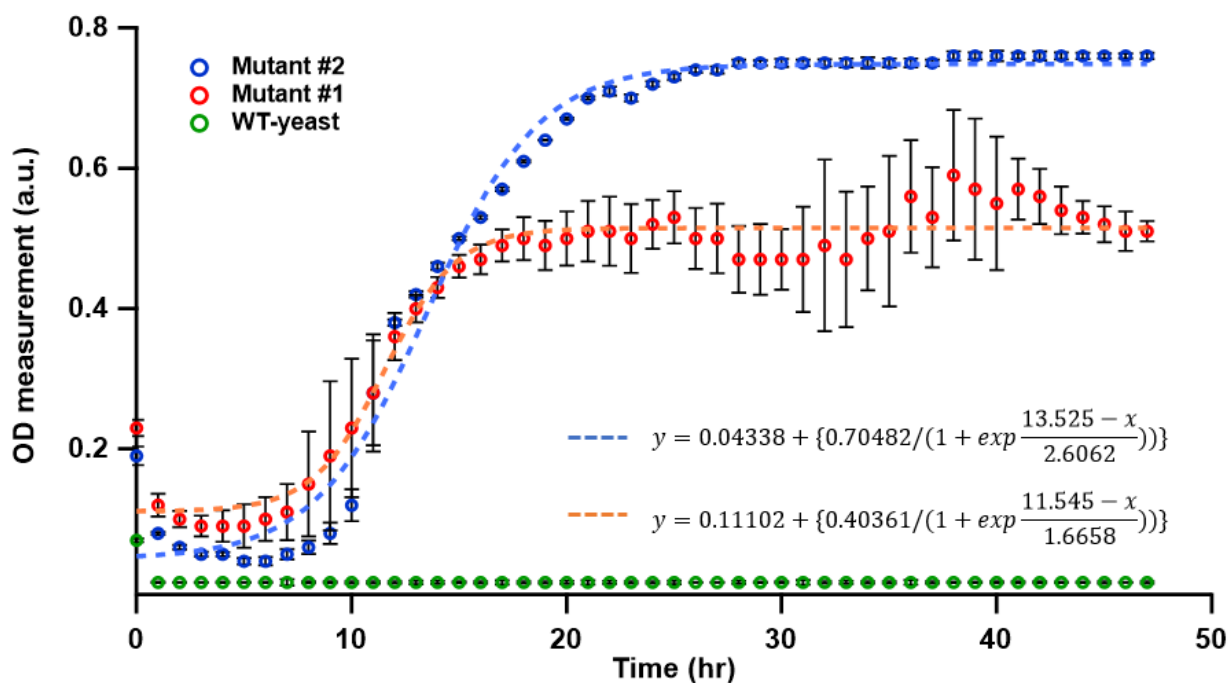
Figure 5-12. Growth curve for the two mutants and WT-Yeast

Average cell densities (OD600) are reported from 3 independent biological replicates after 48 hr of incubation at 30°C in SD media containing 100 mM IL.

After selecting the clones, we continue with the on-chip procedure. As shown in Figure 5-13, we first encapsulated droplets containing single cells and actuated them into the mixing channel. These droplets were mixed with a droplet of 100 mM IL which was generated from the on-demand T-channel configuration. The droplet was incubated in one of the four trapping regions (Figure 5-14). We have further planned to analyze the droplet after incubation for 2 days by absorbance and sort by their growth (i.e. cell number).

We expect mutant-type cells to show a significant difference in the cell density compared to wild-type cells matching with the growth rate results in macro scale. Similar to the fluorescein droplet detection protocol, the absorbance of these droplets will be measured as the droplets passed through the optical fiber region (aligned face-to-face) on the device. We anticipate droplets'

signals will be increased as the cell density increases while the signal for the oil phase remains constant as the background media.
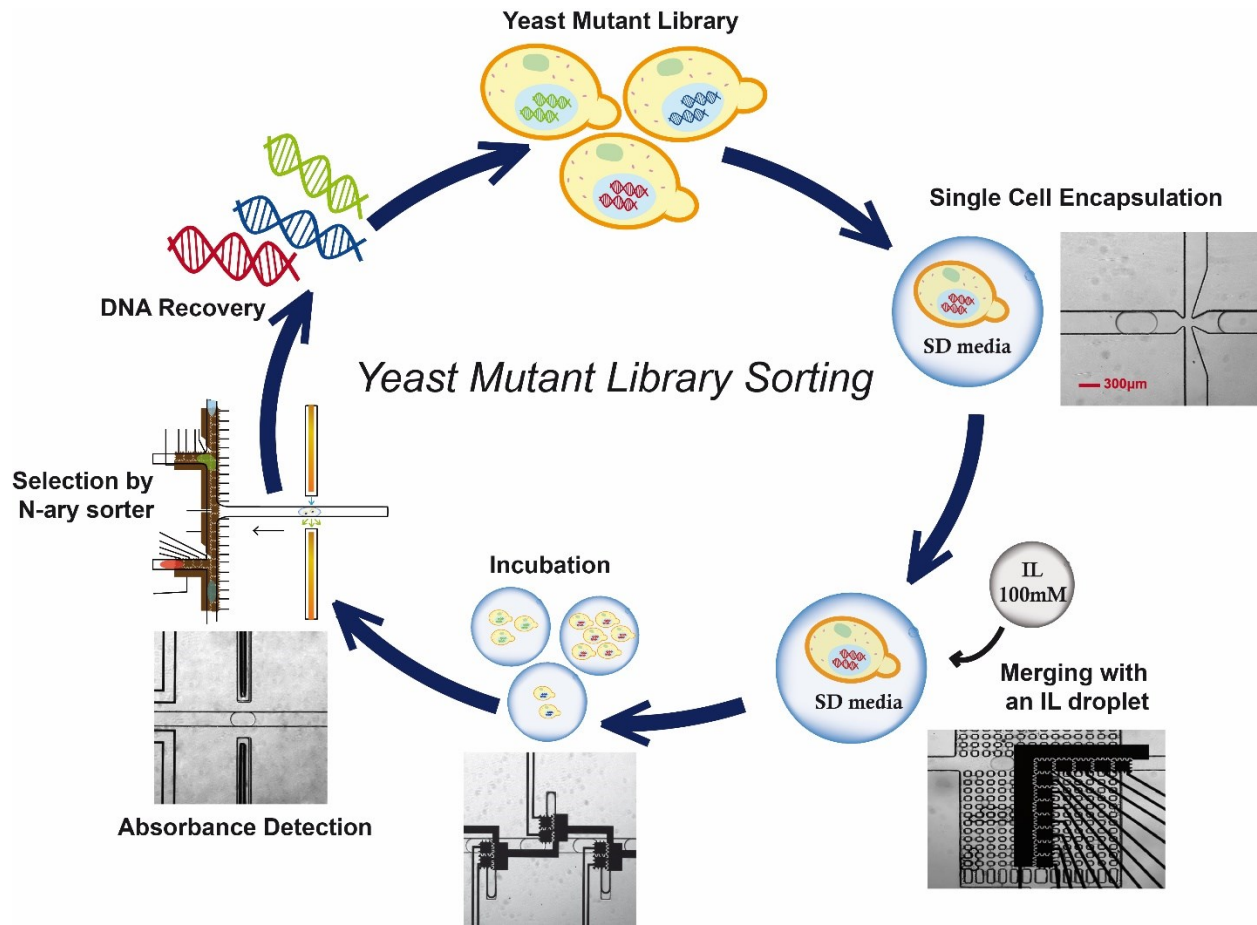
Figure 5-13. Schematic of the ID2M work flow for sorting the yeast mutant library.
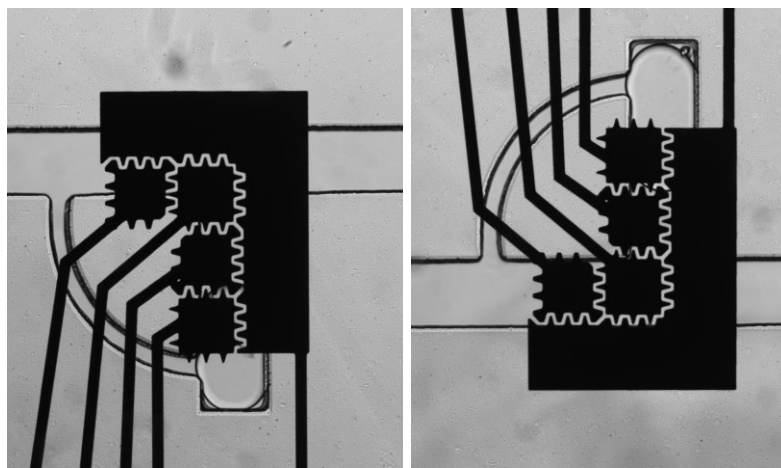
Figure 5-14. Trapping droplets containing yeast cell for incubation.

Indeed, sensitivity of the signals depend on fiber alignment and background. We propose that improvement on the optical setup [222] or device fabrication [223] can increase the sensitivity of our design and expanding the range of cell densities being observed.

Chapter 6.   Concluding Remarks and a Look to the Future

In this section, we recapitulate the hallmarks of the thesis and vent the merits of the ID2M platform as a versatile screening system. In addition, we assess the limitations of this work and evaluate the future work related to the ID2M platform.

6.1   Conclusion

In this thesis, we report the first integrated droplet-digital microfluidic platform enabling on-demand droplet generation, mixing, incubation, and n-ary sorting for screening clonal libraries of microorganism. First we optimized microfabrication procedures related to ID2M to accommodate cell encapsulation using flow focusing configuration, droplet dilution using sequential mixing with individual addressability, and droplet sorting into multiple level based on their fluorescent or absorbance signals. An optical detection system consisting of a flame spectrometer and optical fibers was integrated to the system and droplet manipulation was automated by an automated control system in a MATLAB base workspace. We optimized and validated our system for n-ary sorting by constructing a fluorescein standard curve through sequential dilutions on chip. After successful proof-of-concept n-ary sorting, we demonstrated an EMS mutagenesis at macro scale to produce mutants of *S. cerevisiae* BY4748 that are tolerant under high concentration of ionic liquid. Then, we selected two highly IL-tolerant mutants with WT yeasts for performing an n-ary sorting on our platform. We were able to demonstrate single cell encapsulation, mix them with 100 mM IL droplets, and incubate them on chip for 48 h. We plan to perform n-ary sorting of this clonal library on ID2M platform using their related cell density and absorbance peaks. The method reported here enables a wide variety of droplet operations that is typically not possible with droplet or digital microfluidic systems – encapsulation, mixing (to generate different ionic liquid

concentrations), culture and incubation, and n-ary sorting. Together the new methods described here may be particularly useful for high-throughput applications that require a creation of different drug concentrations or clonal libraries and sorting them at multiple levels.

6.2 Future Perspectives

Hybrid microfluidics has been used as a novel strategy to address some of the limitations in droplet and digital microfluidics. While hybrid microfluidics has a great potential to have the combination of high throughputs and individual controllability, there are still some drawback that requires optimization of the system.

Hybrid microfluidics has mostly been limited by their complex fabrication procedure. Performing microscale photolithography for multiple layers (in a separate mode or integrated as a single device), requires advanced cleanroom facilities and expertise, not to mention the cost of the whole process. Additionally, precise alignment of the microscale features on different layers is another concern. However, this limitation can be attributed to the immaturity of the fabrication technology today. There have been lots of researches on low-cost, rapid-prototyping of digital microfluidics devices in copper substrates without any conventional cleanroom equipment, but this technique is usually deficient in its resolutions (minimum feature size of 50 micron). Currently, our ID2M platform has a minimum feature size of ~ 10 microns, which could be seen as a limiting factor for switching from cleanroom to a rapid prototype fabrication technique. However, now that the platform has been functionally tested and validated, we can consider strategies for more efficient electrode designs and bigger features that also empowers the platform for tolerating higher voltages.

Another concerning issue is the low throughput of this primary ID2M platform which is a limiting factor in high throughput screening (HTS) applications. To address this issue, there are three main factors that needs to be optimized:

First, for a high-throughput droplet microfluidics (i.e. faster droplet generation and manipulations), higher flow rate of the fluids is required. However, increasing the flow rate will consequently result in larger hydrodynamic forces inside the channel, meaning that we must also apply higher electric potential to make electrostatic the dominant force in controlling droplets movement. As previously mentioned, our ID2M platform consists of small electrodes that limits the level of applied voltage, because increasing the voltage for small-area electrode, results in burning. So, changing the DMF layer design to accommodate larger electrodes would be one possible solution.

Another factor affecting the throughput of ID2M, is the integrated detection system which is presently optical fibers and a flame spectrometer. Integrating a photosensor along with a more focused light source such as lasers can provide a detection system with higher sensitivity and faster response time that is necessary for HTS.

Integrating the detection system and the syringe pump with the automation setup, is the other factor that can help increasing the throughput. Now, starting the liquid flow and actuation of the electrodes is manually performed, meaning that a good time distance is required between droplets to avoid delays or wrong actuation in operating the system. Therefore, integration will make full automation of the system possible, thus resulting in a higher throughput.

In the future, we envision a consolidated high throughput screening platform streamlining on-demand mixing, incubation, and n-ary sorting of microorganism enabling applications like directed evolutions to be fully done on a chip. To our knowledge, such a consolidated automated

screening platform has not yet been developed and would hold tremendous value in the directed evolution community.

References

1.	Castillo-León, J. & Svendsen, W.E. Lab-on-a-Chip Devices and Micro-Total Analysis Systems a Practical Guide. (Springer International Publishing Cham; 2015).

2.	Whitesides, G.M. The origins and the future of microfluidics. *Nature* **442**, 368-373 (2006).

3.	Klingenberg, M. When a common problem meets an ingenious mind. *EMBO Rep* **6**, 797-800 (2005).

4.	Kong, F., Yuan, L., Zheng, Y.F. & Chen, W. Automatic liquid handling for life science: a critical review of the current state of the art. *J Lab Autom* **17**, 169-185 (2012).

5.	 (Credence Research, Inc, Credence Research, Inc. website; 2017).

6.	Chiu, D.T. et al. Small but Perfectly Formed? Successes, Challenges, and Opportunities for Microfluidics in the Chemical and Biological Sciences. *Chem* **2**, 201-223 (2017).

7.	Choi, K., Ng, A.H., Fobel, R. & Wheeler, A.R. Digital microfluidics. *Annu Rev Anal Chem (Palo Alto Calif)* **5**, 413-440 (2012).

8.	Liu, P. & Mathies, R.A. Integrated microfluidic systems for high-performance genetic analysis. *Trends Biotechnol* **27**, 572-581 (2009).

9.	Reyes, D.R., Iossifidis, D., Auroux, P.-A. & Manz, A. Micro Total Analysis Systems. 1. Introduction, Theory, and Technology. *Analytical Chemistry* **74**, 2623-2636 (2002).

10.	Thorsen, T., Maerkl, S.J. & Quake, S.R. Microfluidic large-scale integration. *Science* **298**, 580-584 (2002).

11.	Wang, Y. et al. An integrated microfluidic device for large-scale in situ click chemistry screening. *Lab Chip* **9**, 2281-2285 (2009).

12.	Song, H., Chen, D.L. & Ismagilov, R.F. Reactions in droplets in microfluidic channels. *Angew Chem Int Ed Engl* **45**, 7336-7356 (2006).

13.	Xu, J. et al. Droplet-based microfluidic device for multiple-droplet clustering. *Lab Chip* **12**, 725-730 (2012).

14.	Jebrail, M.J., Bartsch, M.S. & Patel, K.D. Digital microfluidics: a versatile tool for applications in chemistry, biology and medicine. *Lab Chip* **12**, 2452-2463 (2012).

15.	Jebrail, M.J. & Wheeler, A.R. Let's get digital: digitizing chemical biology with microfluidics. *Curr Opin Chem Biol* **14**, 574-581 (2010).

16.	Wheeler, A.R. Putting electrowetting to work. *Science* **322**, 539-540 (2008).

17. Hattori, K., Sugiura, S. & Kanamori, T. Generation of arbitrary monotonic concentration profiles by a serial dilution microfluidic network composed of microchannels with a high fluidic-resistance ratio. *Lab Chip* **9**, 1763-1772 (2009).

18. Joanicot, M. & Ajdari, A. Applied physics. Droplet control for microfluidics. *Science* **309**, 887-888 (2005).

19. Bogojevic, D., Chamberlain, M.D., Barbulovic-Nad, I. & Wheeler, A.R. A digital microfluidic method for multiplexed cell-based apoptosis assays. *Lab Chip* **12**, 627-634 (2012).

20. Stone, H.A., Stroock, A.D. & Ajdari, A. Engineering Flows in Small Devices: Microfluidics Toward a Lab-on-a-Chip. *Annual Review of Fluid Mechanics* **36**, 381-411 (2004).

21. Shoji, S. & Esashi, M. Microflow Devices and Systems. *Micromechanics and Microengineering* **4**, 157-171 (1994).

22. Duffy, D.C., McDonald, J.C., Schueller, O.J. & Whitesides, G.M. Rapid Prototyping of Microfluidic Systems in Poly(dimethylsiloxane). *Anal Chem* **70**, 4974-4984 (1998).

23. Jacobson, S.C., Hergenroder, R., Koutny, L.B., Warmack, R.J. & Ramsey, J.M. Effects of Injection Schemes and Column Geometry on the Performance of Microchip Electrophoresis Devices. *Anal Chem* **66**, 1107-1113 (1994).

24. Takayama, S. et al. Subcellular positioning of small molecules. *Nature* **411**, 1016 (2001).

25. Liu, Y. et al. Multilayer-assembled microchip for enzyme immobilization as reactor toward low-level protein identification. *Anal Chem* **78**, 801-808 (2006).

26. Heyries, K.A. et al. Megapixel digital PCR. *Nat Methods* **8**, 649-651 (2011).

27. Araci, I.E. & Quake, S.R. Microfluidic very large scale integration (mVLSI) with integrated micromechanical valves. *Lab Chip* **12**, 2803-2806 (2012).

28. Unger, M.A., Chou, H.P., Thorsen, T., Scherer, A. & Quake, S.R. Monolithic microfabricated valves and pumps by multilayer soft lithography. *Science* **288**, 113-116 (2000).

29. Novotny, J. & Foret, F. Fluid manipulation on the micro-scale: Basics of fluid behavior in microfluidics. *J Sep Sci* **40**, 383-394 (2017).

30. Nguyen, N.-T., Hejazian, M., Ooi, H.C. & Kashaninejad, N. Recent Advances and Future Perspectives on Microfluidic Liquid Handling. *Micromachines* **8** (2017).

31. Lee, C.Y., Chang, C.L., Wang, Y.N. & Fu, L.M. Microfluidic mixing: a review. *Int J Mol Sci* **12**, 3263-3287 (2011).

32. Bertsch, A., Heimgartner, S., Cousseau, P. & Renaud, P. Static micromixers based on large-scale industrial mixer geometry. *Lab Chip* **1**, 56-60 (2001).

33. Vijayendran, R.A., Motsegood, K.M., Beebe, D.J. & Leckband, D.E. Evaluation of a Three-Dimensional Micromixer in a Surface-Based Biosensor. *Langmuir* **19**, 1824-1828 (2003).

34. Buchegger, W., Wagner, C., Lendl, B., Kraft, M. & Vellekoop, M.J. A highly uniform lamination micromixer with wedge shaped inlet channels for time resolved infrared spectroscopy. *Microfluidics and Nanofluidics* **10**, 889-897 (2011).

35. Mengeaud, V., Josserand, J. & Girault, H.H. Mixing processes in a zigzag microchannel: finite element simulations and optical study. *Anal Chem* **74**, 4279-4286 (2002).

36. Dong Sung, K., Seok Woo, L., Tai Hun, K. & Seung, S.L. A barrier embedded chaotic micromixer. *Journal of Micromechanics and Microengineering* **14**, 798 (2004).

37. Yang, J.T., Huang, K.J. & Lin, Y.C. Geometric effects on fluid mixing in passive grooved micromixers. *Lab Chip* **5**, 1140-1147 (2005).

38. Jen, C.P., Wu, C.Y., Lin, Y.C. & Wu, C.Y. Design and simulation of the micromixer with chaotic advection in twisted microchannels. *Lab Chip* **3**, 77-81 (2003).

39. He, B., Burke, B.J., Zhang, X., Zhang, R. & Regnier, F.E. A picoliter-volume mixer for microfluidic analytical systems. *Anal Chem* **73**, 1942-1947 (2001).

40. Stroock, A.D. et al. Chaotic mixer for microchannels. *Science* **295**, 647-651 (2002).

41. Singh, M.K., Anderson, P.D. & Meijer, H.E. Understanding and Optimizing the SMX Static Mixer. *Macromol Rapid Commun* **30**, 362-376 (2009).

42. Ahmed, D., Mao, X., Juluri, B.K. & Huang, T.J. A fast microfluidic mixer based on acoustically driven sidewall-trapped microbubbles. *Microfluidics and Nanofluidics* **7**, 727 (2009).

43. Luong, T.-D., Phan, V.-N. & Nguyen, N.-T. High-throughput micromixers based on acoustic streaming induced by surface acoustic wave. *Microfluidics and Nanofluidics* **10**, 619-625 (2011).

44. Yang, Z., Matsumoto, S., Goto, H., Matsumoto, M. & Maeda, R. Ultrasonic micromixer for microfluidic systems. *Sensors and Actuators A: Physical* **93**, 266-272 (2001).

45. Chen, C.o.-K. & Cho, C.-C. Electrokinetically driven flow mixing utilizing chaotic electric fields. *Microfluidics and Nanofluidics* **5**, 785-793 (2008).

46. Lim, C.Y., Lam, Y.C. & Yang, C. Mixing enhancement in microfluidic channel with a constriction under periodic electro-osmotic flow. *Biomicrofluidics* **4**, 14101 (2010).

47. Fu, L.M., Yang Rj Fau - Lin, C.-H., Lin Ch Fau - Chien, Y.-S. & Chien, Y.S. A novel microfluidic mixer utilizing electrokinetic driving forces under low switching frequency.

48. Campisi, M., Accoto, D., Damiani, F. & Dario, P. A soft-lithographed chaotic electrokinetic micromixer for efficient chemical reactions in lab-on-chips. *Journal of Micro-Nano Mechatronics* **5**, 69-76 (2009).

49. Eunpyo, C., Byungkyu, K. & Jungyul, P. High-throughput microparticle separation using gradient traveling wave dielectrophoresis. *Journal of Micromechanics and Microengineering* **19**, 125014 (2009).

50. Zhao, C. & Yang, C. AC field induced-charge electroosmosis over leaky dielectric blocks embedded in a microchannel. *Electrophoresis* **32**, 629-637 (2011).

51. Du, Y., Zhang, Z., Yim, C., Lin, M. & Cao, X. A simplified design of the staggered herringbone micromixer for practical applications. *Biomicrofluidics* **4** (2010).

52. Wang, Y., Zhe, J., Chung, B.T.F. & Dutta, P. A rapid magnetic particle driven micromixer. *Microfluidics and Nanofluidics* **4**, 375-389 (2008).

53. Wen, C.Y., Yeh, C.P., Tsai, C.H. & Fu, L.M. Rapid magnetic microfluidic mixer utilizing AC electromagnetic field. *Electrophoresis* **30**, 4179-4186 (2009).

54. Bau, H., Zhong, J. & Yi, M. A minute magneto hydro dynamic (MHD) mixer, Vol. 79. (2001).

55. Xu, B., Wong, T.N., Nguyen, N.T., Che, Z. & Chai, J.C. Thermal mixing of two miscible fluids in a T-shaped microchannel. *Biomicrofluidics* **4**, 44102 (2010).

56. Tsai, J.-H. & Lin, L. Active microfluidic mixer and gas bubble filter driven by thermal bubble micropump. *Sensors and Actuators A: Physical* **97-98**, 665-671 (2002).

57. Tice, J.D., Song, H., Lyon, A.D. & Ismagilov, R.F. Formation of Droplets and Mixing in Multiphase Microfluidics at Low Values of the Reynolds and the Capillary Numbers. *Langmuir* **19**, 9127-9133 (2003).

58. Ahn, K. et al. Dielectrophoretic manipulation of drops for high-speed microfluidic sorting devices. *Appl Phys Lett* **88** (2006).

59. Ahn, B., Lee, K., Louge, R. & Oh, K.W. Concurrent droplet charging and sorting by electrostatic actuation. *Biomicrofluidics* **3**, 44102 (2009).

60. Baret, J.C. et al. Fluorescence-activated droplet sorting (FADS): efficient microfluidic cell sorting based on enzymatic activity. *Lab Chip* **9**, 1850-1858 (2009).

61. Teh, S.Y., Lin, R., Hung, L.H. & Lee, A.P. Droplet microfluidics. *Lab Chip* **8**, 198-220 (2008).

62. Niu, X., Gulati, S., Edel, J.B. & deMello, A.J. Pillar-induced droplet merging in microfluidic circuits. *Lab Chip* **8**, 1837-1841 (2008).

63. Chabert, M., Dorfman, K.D. & Viovy, J.L. Droplet fusion by alternating current (AC) field electrocoalescence in microchannels. *Electrophoresis* **26**, 3706-3715 (2005).

64. Song, H., Tice, J.D. & Ismagilov, R.F. A microfluidic system for controlling reaction networks in time. *Angew Chem Int Ed Engl* **42**, 768-772 (2003).

65. Yadav, M.K. et al. In situ data collection and structure refinement from microcapillary protein crystallization. *J Appl Crystallogr* **38**, 900-905 (2005).

66. Tekin, H.C. & Gijs, M.A. Ultrasensitive protein detection: a case for microfluidic magnetic bead-based assays. *Lab Chip* **13**, 4711-4739 (2013).

67. Gerdts, C.J., Sharoyan, D.E. & Ismagilov, R.F. A synthetic reaction network: chemical amplification using nonequilibrium autocatalytic reactions coupled in time. *J Am Chem Soc* **126**, 6327-6331 (2004).

68. Brouzes, E. et al. Droplet microfluidic technology for single-cell high-throughput screening. *Proc Natl Acad Sci U S A* **106**, 14195-14200 (2009).

69. Macosko, E.Z. et al. Highly Parallel Genome-wide Expression Profiling of Individual Cells Using Nanoliter Droplets. *Cell* **161**, 1202-1214 (2015).

70. Klein, A.M. et al. Droplet barcoding for single-cell transcriptomics applied to embryonic stem cells. *Cell* **161**, 1187-1201 (2015).

71. Bui, M.P.N. et al. Enzyme Kinetic Measurements Using a Droplet-Based Microfluidic System with a Concentration Gradient. *Analytical Chemistry* **83**, 1603-1608 (2011).

72. Sjostrom, S.L., Joensson, H.N. & Svahn, H.A. Multiplex analysis of enzyme kinetics and inhibition by droplet microfluidics using picoinjectors. *Lab Chip* **13**, 1754-1761 (2013).

73. Hassan, S.U., Nightingale, A.M. & Niu, X.Z. Continuous measurement of enzymatic kinetics in droplet flow for point-of-care monitoring. *Analyst* **141**, 3266-3273 (2016).

74. Zagnoni, M. & Cooper, J.M. Droplet microfluidics for high-throughput analysis of cells and particles. *Methods Cell Biol* **102**, 25-48 (2011).

75. Guo, M.T., Rotem, A., Heyman, J.A. & Weitz, D.A. Droplet microfluidics for high-throughput biological assays. *Lab Chip* **12**, 2146-2155 (2012).

76. Rahman, T.M. & Rebrov, V.E. Microreactors for Gold Nanoparticles Synthesis: From Faraday to Flow. *Processes* **2** (2014).

77. Wan, J.D. Microfluidic-Based Synthesis of Hydrogel Particles for Cell Microencapsulation and Cell-Based Drug Delivery. *Polymers-Basel* **4**, 1084-1108 (2012).

78.   Mancera-Andrade, E.I., Parsaeimehr, A., Arevalo-Gallegos, A., Ascencio-Favela, G. & Parra Saldivar, R. Microfluidics technology for drug delivery: A review. *Front Biosci (Elite Ed)* **10**, 74-91 (2018).

79.   Abbyad, P., Dangla, R., Alexandrou, A. & Baroud, C.N. Rails and anchors: guiding and trapping droplet microreactors in two dimensions. *Lab Chip* **11**, 813-821 (2011).

80.   Ahn, B. et al. Guiding, distribution, and storage of trains of shape-dependent droplets. *Lab Chip* **11**, 3915-3918 (2011).

81.   Xu, L., Lee, H., Panchapakesan, R. & Oh, K.W. Fusion and sorting of two parallel trains of droplets using a railroad-like channel network and guiding tracks. *Lab Chip* **12**, 3936-3942 (2012).

82.   Fradet, E. et al. Combining rails and anchors with laser forcing for selective manipulation within 2D droplet arrays. *Lab Chip* **11**, 4228-4234 (2011).

83.   Link, D.R. et al. Electric control of droplets in microfluidic devices. *Angew Chem Int Ed Engl* **45**, 2556-2560 (2006).

84.   Park, S.Y., Kalim, S., Callahan, C., Teitell, M.A. & Chiou, E.P. A light-induced dielectrophoretic droplet manipulation platform. *Lab Chip* **9**, 3228-3235 (2009).

85.   Ahn, B., Lee, K., Panchapakesan, R. & Oh, K.W. On-demand electrostatic droplet charging and sorting. *Biomicrofluidics* **5**, 24113 (2011).

86.   Joensson, H.N. & Andersson Svahn, H. Droplet Microfluidics—A Tool for Single-Cell Analysis. *Angewandte Chemie International Edition* **51**, 12176-12192 (2012).

87.   Beer, N.R. et al. On-chip single-copy real-time reverse-transcription PCR in isolated picoliter droplets. *Anal Chem* **80**, 1854-1858 (2008).

88.   Hung, L.H., Lin, R. & Lee, A.P. Rapid microfabrication of solvent-resistant biocompatible microfluidic devices. *Lab Chip* **8**, 983-987 (2008).

89.   Nguyen, N.-T., Lassemono, S. & Chollet, F.A. Optical detection for droplet size control in microfluidic droplet-based analysis systems. *Sensors and Actuators B: Chemical* **117**, 431-436 (2006).

90.   Xu, J.H., Li, S.W., Tan, J., Wang, Y.J. & Luo, G.S. Controllable preparation of monodisperse O/W and W/O emulsions in the same microfluidic device. *Langmuir* **22**, 7943-7946 (2006).

91.   Li, H., Fan, Y., Kodzius, R. & Foulds, I.G. Fabrication of polystyrene microfluidic devices using a pulsed CO2 laser system. *Microsystem Technologies* **18**, 373-379 (2012).

92.   Begolo, S., Colas, G., Viovy, J.L. & Malaquin, L. New family of fluorinated polymer chips for droplet and organic solvent microfluidics. *Lab Chip* **11**, 508-512 (2011).

93. Ma, Y., Thiele, J., Abdelmohsen, L., Xu, J. & Huck, W.T.S. Biocompatible macro-initiators controlling radical retention in microfluidic on-chip photo-polymerization of water-in-oil emulsions. *Chem Commun* **50**, 112-114 (2014).

94. Zhu, P. & Wang, L. Passive and active droplet generation with microfluidics: a review. *Lab Chip* **17**, 34-75 (2016).

95. Christopher, G.F. & Anna, S.L. Microfluidic methods for generating continuous droplet streams. *Journal of Physics D: Applied Physics* **40**, R319 (2007).

96. Holtze, C. et al. Biocompatible surfactants for water-in-fluorocarbon emulsions. *Lab Chip* **8**, 1632-1639 (2008).

97. Baret, J.C. Surfactants in droplet-based microfluidics. *Lab Chip* **12**, 422-433 (2012).

98. Shang, L., Cheng, Y. & Zhao, Y. Emerging Droplet Microfluidics. *Chem Rev* **117**, 7964-8040 (2017).

99. Simon, M.G. & Lee, A.P. in Microdroplet Technology: Principles and Emerging Applications in Biology and Chemistry. (eds. P. Day, A. Manz & Y. Zhang) 23-50 (Springer New York, New York, NY; 2012).

100. Bremond, N., Thiam, A.R. & Bibette, J. Decompressing emulsion droplets favors coalescence. *Phys Rev Lett* **100**, 024501 (2008).

101. Chen, C. et al. Passive Mixing inside Microdroplets. *Micromachines* **9** (2018).

102. Yang, C.-G., Xu, Z.-R. & Wang, J.-H. Manipulation of droplets in microfluidic systems. *TrAC Trends in Analytical Chemistry* **29**, 141-157 (2010).

103. Priest, C., Herminghaus, S. & Seemann, R. Controlled electrocoalescence in microfluidics: Targeting a single lamella. *Appl Phys Lett* **89**, 134101 (2006).

104. Ahn, K., Agresti, J., Chong, H., Marquez, M. & Weitz, D.A. Electrocoalescence of drops synchronized by size-dependent flow in microfluidic channels. *Appl Phys Lett* **88**, 264105 (2006).

105. Wang, W., Yang, C. & Li, C.M. On-demand microfluidic droplet trapping and fusion for on-chip static droplet assays. *Lab on a Chip* **9**, 1504-1506 (2009).

106. Wang, W., Yang, C. & Li, C.M. Efficient On-Demand Compound Droplet Formation: From Microfluidics to Microdroplets as Miniaturized Laboratories. *Small* **5**, 1149-1152 (2009).

107. Atten, P., Lundgaard, L. & Berg, G. A simplified model of electrocoalescence of two close water droplets in oil. *Journal of Electrostatics* **64**, 550-554 (2006).

108. Tan, W.H. & Takeuchi, S. Timing controllable electrofusion device for aqueous droplet-based microreactors. *Lab Chip* **6**, 757-763 (2006).

109. Gallaire, F., Baroud, C., N. & Delville, J.-P. Thermocapillary manipulation of microfluidic droplets: Theory and applications. *International Journal of Heat and Technology* **26**, 161-166 (2008).

110. Cordero, M.L., Burnham, D.R., Baroud, C.N. & McGloin, D. Thermocapillary manipulation of droplets using holographic beam shaping: Microfluidic pin ball. *Appl Phys Lett* **93**, 034107 (2008).

111. Long, Z., Shetty, A.M., Solomon, M.J. & Larson, R.G. Fundamentals of magnet-actuated droplet manipulation on an open hydrophobic surface. *Lab on a Chip* **9**, 1567-1575 (2009).

112. Wixforth, A. et al. Acoustic manipulation of small droplets. *Anal Bioanal Chem* **379**, 982-991 (2004).

113. Li, L., Boedicker, J.Q. & Ismagilov, R.F. Using a Multijunction Microfluidic Device To Inject Substrate into an Array of Preformed Plugs without Cross-Contamination: Comparing Theory and Experiments. *Analytical Chemistry* **79**, 2756-2761 (2007).

114. Abate, A.R., Hung, T., Mary, P., Agresti, J.J. & Weitz, D.A. High-throughput injection with microfluidics using picoinjectors. *Proc Natl Acad Sci U S A* **107**, 19163-19166 (2010).

115. Joensson, H.N. & Svahn, H.A. Droplet Microfluidics-A Tool for Single-Cell Analysis. *Angew Chem Int Edit* **51**, 12176-12192 (2012).

116. Mazutis, L. & Griffiths, A.D. Preparation of monodisperse emulsions by hydrodynamic size fractionation. *Appl Phys Lett* **95**, 204103 (2009).

117. Huh, D. et al. Gravity-Driven Microfluidic Particle Sorting Device with Hydrodynamic Separation Amplification. *Analytical Chemistry* **79**, 1369-1376 (2007).

118. Sciambi, A. & Abate, A.R. Accurate microfluidic sorting of droplets at 30 kHz. *Lab Chip* **15**, 47-51 (2015).

119. Gielen, F. et al. Ultrahigh-throughput-directed enzyme evolution by absorbance-activated droplet sorting (AADS). *Proc Natl Acad Sci U S A* **113**, E7383-E7389 (2016).

120. Franke, T., Abate, A.R., Weitz, D.A. & Wixforth, A. Surface acoustic wave (SAW) directed droplet flow in microfluidics for PDMS devices. *Lab Chip* **9**, 2625-2627 (2009).

121. Wakui, D., Takahashi, S., Sekiguchi, T. & Shoji, S. in 2010 IEEE 23rd International Conference on Micro Electro Mechanical Systems (MEMS) 144-147 (2010).

122. Cao, Z. et al. Droplet sorting based on the number of encapsulated particles using a solenoid valve. *Lab Chip* **13**, 171-178 (2013).

123. Zhang, K. et al. On-chip manipulation of continuous picoliter-volume superparamagnetic droplets using a magnetic force. *Lab on a Chip* **9**, 2992-2999 (2009).

124. Wong, A.H. et al. Drug screening of cancer cell lines and human primary tumors using droplet microfluidics. *Sci Rep* **7**, 9109 (2017).

125. Agresti, J.J. et al. Ultrahigh-throughput screening in drop-based microfluidics for directed evolution. *Proc Natl Acad Sci U S A* **107**, 4004-4009 (2010).

126. Mary, P. et al. Analysis of gene expression at the single-cell level using microdroplet-based microfluidic technology. *Biomicrofluidics* **5**, 024109 (2011).

127. Collins, D.J., Neild, A., deMello, A., Liu, A.Q. & Ai, Y. The Poisson distribution and beyond: methods for microfluidic droplet production and single cell encapsulation. *Lab Chip* **15**, 3439-3459 (2015).

128. He, M. et al. Selective encapsulation of single cells and subcellular organelles into picoliter- and femtoliter-volume droplets. *Anal Chem* **77**, 1539-1544 (2005).

129. Hong, J., deMello, A.J. & Jayasinghe, S.N. Bio-electrospraying and droplet-based microfluidics: control of cell numbers within living residues. *Biomed Mater* **5**, 21001 (2010).

130. Edd, J.F. et al. Controlled encapsulation of single-cells into monodisperse picolitre drops. *Lab Chip* **8**, 1262-1264 (2008).

131. Freire, S.L.S. Perspectives on digital microfluidics. *Sensors and Actuators A: Physical* **250**, 15-28 (2016).

132. Fair, R.B. Digital microfluidics: is a true lab-on-a-chip possible? *Microfluidics and Nanofluidics* **3**, 245-281 (2007).

133. Abdelgawad, M. & Wheeler Aaron, R. The Digital Revolution: A New Paradigm for Microfluidics. *Advanced Materials* **21**, 920-925 (2008).

134. Choi, K., Ng, A.H.C., Fobel, R. & Wheeler, A.R. Digital Microfluidics. *Annual Review of Analytical Chemistry, Vol 5* **5**, 413-440 (2012).

135. Wheeler, A.R. Chemistry. Putting electrowetting to work. *Science* **322**, 539-540 (2008).

136. Li, X.M., Reinhoudt, D. & Crego-Calama, M. What do we need for a superhydrophobic surface? A review on the recent progress in the preparation of superhydrophobic surfaces. *Chem Soc Rev* **36**, 1350-1368 (2007).

137. Pollack, M.G., Fair, R.B. & Shenderov, A.D. Electrowetting-based actuation of liquid droplets for microfluidic applications. *Appl Phys Lett* **77**, 1725-1726 (2000).

138.	Lee, J., Moon, H., Fowler, J., Schoellhammer, T. & Kim, C.-J. Electrowetting and electrowetting-on-dielectric for microscale liquid handling. *Sensors and Actuators A: Physical* **95**, 259-268 (2002).

139.	Chatterjee, D., Hetayothin, B., Wheeler, A.R., King, D.J. & Garrell, R.L. Droplet-based microfluidics with nonaqueous solvents and solutions. *Lab Chip* **6**, 199-206 (2006).

140.	Jones, T.B. On the Relationship of Dielectrophoresis and Electrowetting. *Langmuir* **18**, 4437-4443 (2002).

141.	Hsieh, T. & Fan, S. in 2008 IEEE 21st International Conference on Micro Electro Mechanical Systems 641-644 (2008).

142.	Chatterjee, D., Shepherd, H. & Garrell, R.L. Electromechanical model for actuating liquids in a two-plate droplet microfluidic device. *Lab Chip* **9**, 1219-1229 (2009).

143.	Gao, J. et al. Adhesion promoter for a multi-dielectric-layer on a digital microfluidic chip. *Rsc Adv* **5**, 48626-48630 (2015).

144.	Song, J.H., Evans, R., Lin, Y.Y., Hsu, B.N. & Fair, R.B. A scaling model for electrowetting-on-dielectric microfluidic actuators. *Microfluid Nanofluid* **7**, 75-89 (2009).

145.	Ding, H. et al. Accurate dispensing of volatile reagents on demand for chemical reactions in EWOD chips. *Lab Chip* **12**, 3331-3340 (2012).

146.	Jebrail, M.J. et al. Synchronized synthesis of peptide-based macrocycles by digital microfluidics. *Angew Chem Int Ed Engl* **49**, 8625-8629 (2010).

147.	Miller, E.M. & Wheeler, A.R. A digital microfluidic approach to homogeneous enzyme assays. *Anal Chem* **80**, 1614-1619 (2008).

148.	Nichols, K.P. & Gardeniers, H.J. A digital microfluidic system for the investigation of pre-steady-state enzyme kinetics using rapid quenching with MALDI-TOF mass spectrometry. *Anal Chem* **79**, 8699-8704 (2007).

149.	Sista, R.S. et al. Heterogeneous immunoassays using magnetic beads on a digital microfluidic platform. *Lab Chip* **8**, 2188-2196 (2008).

150.	Miller, E.M., Ng, A.H., Uddayasankar, U. & Wheeler, A.R. A digital microfluidic approach to heterogeneous immunoassays. *Anal Bioanal Chem* **399**, 337-345 (2011).

151.	Abdelgawad, M., Freire, S.L., Yang, H. & Wheeler, A.R. All-terrain droplet actuation. *Lab Chip* **8**, 672-677 (2008).

152.	Aijian, A.P., Chatterjee, D. & Garrell, R.L. Fluorinated liquid-enabled protein handling and surfactant-aided crystallization for fully in situ digital microfluidic MALDI-MS analysis. *Lab Chip* **12**, 2552-2559 (2012).

153. Wheeler, A.R., Moon, H., Kim, C.J., Loo, J.A. & Garrell, R.L. Electrowetting-based microfluidics for analysis of peptides and proteins by matrix-assisted laser desorption/ionization mass spectrometry. *Anal Chem* **76**, 4833-4838 (2004).

154. Barbulovic-Nad, I., Yang, H., Park, P.S. & Wheeler, A.R. Digital microfluidics for cell-based assays. *Lab Chip* **8**, 519-526 (2008).

155. Barbulovic-Nad, I., Au, S.H. & Wheeler, A.R. A microfluidic platform for complete mammalian cell culture. *Lab Chip* **10**, 1536-1542 (2010).

156. Sista, R.S. et al. Digital microfluidic platform for multiplexing enzyme assays: implications for lysosomal storage disease screening in newborns. *Clin Chem* **57**, 1444-1451 (2011).

157. Pollack, M.G., Pamula, V.K., Srinivasan, V. & Eckhardt, A.E. Applications of electrowetting-based digital microfluidics in clinical diagnostics. *Expert Review of Molecular Diagnostics* **11**, 393-407 (2011).

158. Son, S.U. & Garrell, R.L. Transport of live yeast and zebrafish embryo on a droplet digital microfluidic platform. *Lab Chip* **9**, 2398-2401 (2009).

159. Pyne, D.G., Liu, J., Abdelgawad, M. & Sun, Y. Digital microfluidic processing of mammalian embryos for vitrification. *PLoS One* **9**, e108128 (2014).

160. Shah, G.J. et al. Specific binding and magnetic concentration of CD8+ T-lymphocytes on electrowetting-on-dielectric platform. *Biomicrofluidics* **4**, 44106 (2010).

161. Abdelgawad, M., Watson, M.W. & Wheeler, A.R. Hybrid microfluidics: a digital-to-channel interface for in-line sample processing and chemical separations. *Lab Chip* **9**, 1046-1051 (2009).

162. Watson, M.W., Jebrail, M.J. & Wheeler, A.R. Multilayer hybrid microfluidics: a digital-to-channel interface for sample processing and separations. *Anal Chem* **82**, 6680-6686 (2010).

163. Shih, S.C. et al. A droplet-to-digital (D2D) microfluidic device for single cell assays. *Lab Chip* **15**, 225-236 (2015).

164. Huh, D. et al. Reversible switching of high-speed air-liquid two-phase flows using electrowetting-assisted flow-pattern change. *Journal of the American Chemical Society* **125**, 14678-14679 (2003).

165. Gu, H., Malloggi, F., Vanapalli, S.A. & Mugele, F. Electrowetting-enhanced microfluidic device for drop generation. *Appl Phys Lett* **93** (2008).

166. Malloggi, F., Gu, H., Banpurkar, A.G., Vanapalli, S.A. & Mugele, F. Electrowetting - A versatile tool for controlling microdrop generation. *Eur Phys J E* **26**, 91-96 (2008).

167.   de Ruiter, R. et al. Electrostatic potential wells for on-demand drop manipulation in microchannels. *Lab on a Chip* **14**, 883-891 (2014).

168.   Shih, S.C.C. et al. A Versatile Microfluidic Device for Automating Synthetic Biology. *Acs Synthetic Biology* **4**, 1151-1164 (2015).

169.   Au, S.H., Kumar, P. & Wheeler, A.R. A new angle on pluronic additives: advancing droplets and understanding in digital microfluidics. *Langmuir* **27**, 8586-8594 (2011).

170.   Freire, S.L. & Tanner, B. Additive-free digital microfluidics. *Langmuir* **29**, 9024-9030 (2013).

171.   O'Donovan, B., Eastburn, D.J. & Abate, A.R. Electrode-free picoinjection of microfluidic drops. *Lab Chip* **12**, 4029-4032 (2012).

172.   Dryden, M.D.M., Fobel, R., Fobel, C. & Wheeler, A.R. Upon the Shoulders of Giants: Open-Source Hardware and Software in Analytical Chemistry. *Anal Chem* **89**, 4330-4338 (2017).

173.   Shih, S.C.C., Barbulovic-Nad, I., Yang, X., Fobel, R. & Wheeler, A.R. Digital microfluidics with impedance sensing for integrated cell culture and analysis. *Biosens. Bioelectron.* **42**, 314-320 (2013).

174.   Zeng, X. et al. Chemiluminescence detector based on a single planar transparent digital microfluidic device. *Lab Chip* **13**, 2714-2720 (2013).

175.   Lin, L., Evans, R.D., Jokerst, N.M. & Fair, R.B. Integrated optical sensor in a digital microfluidic platform. *IEEE Sens. J.* **8**, 628-635 (2008).

176.   Malic, L., Veres, T. & Tabrizian, M. Two-dimensional droplet-based surface plasmon resonance imaging using electrowetting-on-dielectric microfluidics. *Lab Chip* **9**, 473-475 (2009).

177.   Au, S.H., Shih, S.C.C. & Wheeler, A.R. Integrated microbioreactor for culture and analysis of bacteria, algae and yeast. *Biomed. Microdevices* **13**, 41-50 (2011).

178.   Vo, P.Q.N., Husser, M.C., Ahmadi, F., Sinha, H. & Shih, S.C.C. Image-based feedback and analysis system for digital microfluidics. *Lab on a Chip* **17**, 3437-3446 (2017).

179.   Murray, J. & King, D. Oil's tipping point has passed. *Nature* **481**, 433 (2012).

180.   Buijs, N.A., Siewers, V. & Nielsen, J. Advanced biofuel production by the yeast Saccharomyces cerevisiae. *Current Opinion in Chemical Biology* **17**, 480-488 (2013).

181.   Nakashima, K. et al. Direct bioethanol production from cellulose by the combination of cellulase-displaying yeast and ionic liquid pretreatment. *Green Chemistry* **13**, 2948-2953 (2011).

182. Peralta-Yahya, P.P. & Keasling, J.D. Advanced biofuel production in microbes. *Biotechnology Journal* **5**, 147-162 (2010).

183. Ouellet, M. et al. Impact of ionic liquid pretreated plant biomass on Saccharomyces cerevisiae growth and biofuel production. *Green Chemistry* **13**, 2743-2749 (2011).

184. Dickinson, Q. et al. Mechanism of imidazolium ionic liquids toxicity in Saccharomyces cerevisiae and rational engineering of a tolerant, xylose-fermenting strain. *Microbial Cell Factories* **15**, 17 (2016).

185. Docherty, K.M. & Kulpa, J.C.F. Toxicity and antimicrobial activity of imidazolium and pyridinium ionic liquids. *Green Chemistry* **7**, 185-189 (2005).

186. Datta, S. et al. Ionic liquid tolerant hyperthermophilic cellulases for biomass pretreatment and hydrolysis. *Green Chemistry* **12**, 338-345 (2010).

187. Sitepu, I.R. et al. Yeast tolerance to the ionic liquid 1-ethyl-3-methylimidazolium acetate. *FEMS Yeast Res* **14**, 1286-1294 (2014).

188. Higgins, D.A. et al. Natural Variation in the Multidrug Efflux Pump SGE1 Underlies Ionic Liquid Tolerance in Yeast. *Genetics* (2018).

189. Mehmood, N. et al. Impact of two ionic liquids, 1-ethyl-3-methylimidazolium acetate and 1-ethyl-3-methylimidazolium methylphosphonate, on Saccharomyces cerevisiae: metabolic, physiologic, and morphological investigations. *Biotechnol Biofuels* **8**, 17 (2015).

190. Dubois, P. et al. Ionic liquid droplet as e-microreactor. *Anal Chem* **78**, 4909-4917 (2006).

191. Pan, J. et al. Quantitative tracking of the growth of individual algal cells in microdroplet compartments. *Integr Biol (Camb)* **3**, 1043-1051 (2011).

192. Sjostrom, S.L. et al. High-throughput screening for industrial enzyme production hosts by droplet microfluidics. *Lab Chip* **14**, 806-813 (2014).

193. Najah, M. et al. Droplet-based microfluidics platform for ultra-high-throughput bioprospecting of cellulolytic microorganisms. *Chem Biol* **21**, 1722-1732 (2014).

194. Kim, H.S., Guzman, A.R., Thapa, H.R., Devarenne, T.P. & Han, A. A droplet microfluidics platform for rapid microalgal growth and oil production analysis. *Biotechnol Bioeng* **113**, 1691-1701 (2016).

195. Kim, H.S. et al. High-throughput droplet microfluidics screening platform for selecting fast-growing and high lipid-producing microalgae from a mutant library. *Plant Direct* **1**, e00011 (2017).

196.   Huang, M. et al. Microfluidic screening and whole-genome sequencing identifies mutations associated with improved protein secretion by yeast. *Proc Natl Acad Sci U S A* **112**, E4689-4696 (2015).

197.   Husser, M.C., Vo, P.Q.N., Sinha, H., Ahmadi, F. & Shih, S.C.C. An Automated Induction Microfluidics System for Synthetic Biology. *ACS Synthetic Biology* **7**, 933-944 (2018).

198.   Winston, F. EMS and UV Mutagenesis in Yeast. *Current Protocols in Molecular Biology* **82**, 13.13B.11-13.13B.15 (2008).

199.   Luk, V.N., Mo, G. & Wheeler, A.R. Pluronic additives: a solution to sticky problems in digital microfluidics. *Langmuir* **24**, 6382-6389 (2008).

200.   Liu, Y.G., Banerjee, A. & Papautsky, I. Precise droplet volume measurement and electrode-based volume metering in digital microfluidics. *Microfluidics and Nanofluidics* **17**, 295-303 (2014).

201.   Banerjee, A., Kreit, E., Liu, Y.G., Heikenfeld, J. & Papautsky, I. Reconfigurable virtual electrowetting channels. *Lab on a Chip* **12**, 758-764 (2012).

202.   Abdelgawad, M., Park, P. & Wheeler, A.R. Optimization of device geometry in single-plate digital microfluidics. *J Appl Phys* **105** (2009).

203.   Paik, P.Y., Pamula, V.K. & Chakrabarty, K. Adaptive cooling of integrated circuits using digital microfluidics. *Ieee T Vlsi Syst* **16**, 432-443 (2008).

204.   Yi, U.C. & Kim, C.J. Characterization of electrowetting actuation on addressable single-side coplanar electrodes. *Journal of Micromechanics and Microengineering* **16**, 2053-2059 (2006).

205.   Yang, R., Soper, S.A. & Wang, W. A new UV lithography photoresist based on composite of EPON resins 165 and 154 for fabrication of high-aspect-ratio microstructures. *Sensors and Actuators A: Physical* **135**, 625-636 (2007).

206.   Ren, Y. et al. A Simple and Reliable PDMS and SU-8 Irreversible Bonding Method and Its Application on a Microfluidic-MEA Device for Neuroscience Research. *Micromachines* **6** (2015).

207.   Cui, W.W. et al. Dynamics of Electrowetting Droplet Motion in Digital Microfluidics Systems: From Dynamic Saturation to Device Physics. *Micromachines* **6**, 778-789 (2015).

208.   Yanagisawa, N. & Higashiyama, T. Quantitative assessment of chemotropism in pollen tubes using microslit channel filters. *Biomicrofluidics* **12** (2018).

209.   Bithi, S.S. & Vanapalli, S.A. Behavior of a train of droplets in a fluidic network with hydrodynamic traps. *Biomicrofluidics* **4**, 044110 (2010).

210. Mazutis, L. et al. Single-cell analysis and sorting using droplet-based microfluidics. *Nat Protoc* **8**, 870-891 (2013).

211. Li, S.X. et al. An On-Chip, Multichannel Droplet Sorter Using Standing Surface Acoustic Waves. *Analytical Chemistry* **85**, 5468-5474 (2013).

212. Yoon, D.H., Ito, J., Sekiguchi, T. & Shoji, S. Active and Precise Control of Microdroplet Division Using Horizontal Pneumatic Valves in Bifurcating Microchannel. *Micromachines* **4**, 197-205 (2013).

213. Pit, A.M. et al. High-throughput sorting of drops in microfluidic chips using electric capacitance. *Biomicrofluidics* **9** (2015).

214. Fradet, E. et al. Combining rails and anchors with laser forcing for selective manipulation within 2D droplet arrays. *Lab on a Chip* **11**, 4228-4234 (2011).

215. Paik, P., Pamula, V.K. & Fair, R.B. Rapid droplet mixers for digital microfluidic systems. *Lab on a Chip* **3**, 253-259 (2003).

216. Liu, C.-Z., Wang, F., Stiles, A.R. & Guo, C. Ionic liquids for biofuel production: Opportunities and challenges. *Applied Energy* **92**, 406-414 (2012).

217. Blanch, H.W., Simmons, B.A. & Klein-Marcuschamer, D. Biomass deconstruction to sugars. *Biotechnol J* **6**, 1086-1102 (2011).

218. Sun, J. et al. Solubilization and Upgrading of High Polyethylene Terephthalate Loadings in a Low-Costing Bifunctional Ionic Liquid. *ChemSusChem* **11**, 781-792 (2018).

219. Park, J.I. et al. A thermophilic ionic liquid-tolerant cellulase cocktail for the production of cellulosic biofuels. *PLoS One* **7**, e37010 (2012).

220. Ruegg, T.L. et al. An auto-inducible mechanism for ionic liquid resistance in microbial biofuel production. *Nat Commun* **5**, 3490 (2014).

221. Frederix, M. et al. Development of an E. coli strain for one-pot biofuel production from ionic liquid pretreated cellulose and switchgrass. *Green Chemistry* **18**, 4189-4197 (2016).

222. Cole, R.H., de Lange, N., Gartner, Z.J. & Abate, A.R. Compact and modular multicolour fluorescence detector for droplet microfluidics. *Lab Chip* **15**, 2754-2758 (2015).

223. Blue, R. & Uttamchandani, D. Recent advances in optical fiber devices for microfluidics integration. *J Biophotonics* **9**, 13-25 (2016).